DISS. ETH NO. 23151

The Impact of PGC-1α on Engineered Muscle Tissue and the Use of PET-Scan for Cell Tracking and Functional Analyses

A thesis submitted to attain the degree of

DOCTOR OF SCIENCES of ETH ZURICH

(Dr. sc. ETH Zurich)

presented by

DEANA G. HARALAMPIEVA

M.Sc., University of Konstanz

born on 20.02.1986

citizen of Bulgaria and Germany

accepted on the recommendation of

Prof. Dr. Simon M. Ametamey, examiner

Prof. Dr. Roger Schibli, co-examiner

PD Dr. Dr. Daniel Eberli, co-examiner

Prof. Dr. Christoph Handschin, co-examiner

Prof. Dr. Tullio Sulser, co-examiner

2016

"If your plan is for 1 year, plant rice;
If your plan is for 10 years, plant trees;
If your plan is for 100 years, educate children."
Confucius

Acknowledgements

I would like to express my deep gratitude to a number of people who supported, encouraged and motivated me during my PhD studies. First of all I would like to thank Prof. Simon M. Ametamey and Prof. Roger Schibli for giving me the opportunity to enrol my multicentre project using the high-end technologies their lab could offer. Simon, my doctoral thesis supervisor, has proven continually his role as an academic advisor and always managed to find time for fruitful discussions and brainstorming, looking for an optimal solution for every hurdle on the way. Thank you, Simon, for the relaxed and friendly atmosphere at all our meetings and for the efforts you put into managing the PET team for this project. Although, at first sight, radiopharmaceutical sciences seemed to me like a very deep ocean, I am glad I was encouraged by Roger and Simon to learn some of the secrets of molecular imaging, thereby allowing me to paddle at the surface of the ocean, widening my scientific view.

Next, I want to express my appreciation to PD Dr. Dr. Daniel Eberli, my direct supervisor from University Hospital of Zurich (USZ). He assisted me throughout all stages of my studies, guided me, but also granted me a lot of independence for developing and accomplishing my own ideas. Thanks to Daniel I learned the whole process of a scientific project: from writing grants, through management of people, resources and administration, accomplishment of experiments, publishing, and last but not least, improvement of my negotiation and networking skills. I was given the great opportunity to attend and present my projects at above-average number of national and international conferences during my doctoral studies. Thank you, Daniel, for pushing me forward, when I was getting cold feet. I was fortunate to be able to execute a part of my studies at his Laboratory for Tissue Engineering and Stem Cell Therapy, widening my knowledge about the bench-to-bedside translation of different approaches. At this point, I would like to thank Prof. Tullio Sulser for providing the opportunity to work within the Urology department of USZ.

I owe Prof. Chistoph Handschin from the Biozentrum in Basel my deepest gratitude for the initiation of this exciting multicentre project. Particularly, I appreciated his intellectual support and kind attitude during all our meetings. As an established expert in the role of PGC-1α in muscle physiology, he had many helpful inputs and ideas for the ongoing experiments. Here, I have to express my thankfulness to Dr. Ivana Dinulovic for the design and successful production of the adenoviral particles used in this collaborative project.

There are no words to describe my appreciation to the whole Tissue Engineering team at USZ, Dr. Souzan Salemi, Dr. Markus Rottmar, Sarah Nötzli, Ria Tauscher, Jakub Smolar, Daniel Keller, Dr. Regina Grossmann, Dr. Oliver Gross, Dr. Ashkan Mortezavi, who

supported me in good and bad times, motivated me and were always there. A special thanks goes to my mentor (not just in research), Souzan, for her kindness, for her positive attitude, for her help with the experiments, for her patience in explaining to me how to properly handle proteins and genes, for her care, and last but not least, for her addictive laugh. Furthermore, I wish to express my huge appreciation to Damina Balmer, who reviewed all my manuscripts showing great professionalism at an unbeatable pace. Next, I want to express my gratitude to Dr. Selman Sakar for the countless, inspiring discussions. Thank you, TE team, for being great colleagues and friends, and for all the shared moments in science and beyond!

I greatly appreciate the challenging discussions and scientific exchange I shared during my collaborations with Dr. Thomas Betzel at the ETH. Thomas, herewith, I would like to acknowledge your indispensable help with the synthesis of the various radioligands used in this project. Moreover, I thank you for being patient while explaining sophisticated chemical reactions and procedures and for always finding time to talk about life over a piece of your rhubarb cake. Further, I wish to express my appreciation to PD Dr. Stefanie Krämer for the vital inputs regarding the PET experiments, for patiently teaching me how to handle Π-mod and to analyze the huge amounts of data, for letting me supervise her biopharmacy students during the practical courses, and for her kindness and friendly attitude. At this point, I would like to thank Claudia Keller not only for the countless hours at the PET scanner, but also for her interesting surfing stories. Thanks for always being on time and performing the measurements with such accuracy. Last, I want to thank Alain Blanc and Dr. Martin Béhé for the radiosynthesis of the [^{64}Cu]NODAGA-RGD radioligand at PSI.

My work has been financed by the Swiss National Science Foundation (SNSF) Sinergia Project (CRSI33_136197). Further financial support was granted by Novartis and Promedica Foundations, for which I am very thankful.

Last but not least, I would like to thank my fiancé Nicolas for dealing with my moody spirit through the various struggles involved in a PhD thesis and for always making me continue with a smile. Finally, I want to express my deep appreciation to my family and friends who encouraged and supported me limitlessly, and were there for me throughout these years until the successful completion of my PhD student life.

Thank you ALL!

Summary of the PhD thesis

Regeneration of skeletal muscles is a highly-orchestrated process that involves tight regulation of multiple cellular and molecular responses. Extensive studies have examined this process in detail and have shown that muscle precursor cells (MPCs) are an ideal cellular model to study muscle tissue regeneration. As quiescent satellite cells, they have a sub-laminar location in the healthy muscle. External stimuli such as injuries trigger their re-entry into the cell cycle. The MPCs as their progeny proliferate, differentiate and fuse to form new myofibers. In the field of tissue engineering and regenerative medicine MPC-based therapies have been proposed as a novel treatment option for various muscle diseases, including urinary incontinence. Despite the immense progress towards the successful implementation of this cell-therapy, several key aspects still need more investigations: (1) to enhance the survival and metabolism of the injected cells, in order to improve the quality of the bioengineered tissues, (2) to provide tools for non-invasive long-term read-outs of the implanted cells, thereby bypassing multiple harmful biopsies. In this respect, this thesis aimed to find possible solutions to these critical issues, in order to get one step closer towards the successful clinical application of this MPC therapy.

Chapter one of this thesis provides an overview about available non-invasive technologies for imaging applications in tissue engineering and regenerative medicine, focusing on their advantages and drawbacks, recent developments and future implementations. This is followed by a short description of MPCs, their characterisation and therapeutic utility. Furthermore, this section explains the key role of the peroxisome proliferator-activated receptor-γ coactivator α (PGC-1α) in the coordination of skeletal muscle metabolism and homeostasis. Finally, this chapter closes with a representation of the aims of the project, which are described in detail in the subsequent chapters.

The second chapter describes the first successfully achieved milestones towards the qualitative improvement of bioengineered constructs. The goal was to genetically modify human MPCs (hMPCs) to overexpress PGC-1α, which is the key regulator of exercise-mediated adaptation, and thereby to enhance early skeletal muscle formation. For this, adenoviral constructs were generated to support the robust and constitutive PGC-1α expression in the primary cells, which were isolated from patient biopsies and cultured until passage three. The sustained myogenic phenotype of the genetically modified hMPCs was confirmed by immunocytological analysis and flow cytometry. While maintaining their viability and proliferation potential, PGC-1α modified hMPCs showed an enhanced fiber formation capacity *in vitro.* Only 9 hours after the induction of cell differentiation, an increase in metabolic activity was detected in the genetically modified cells compared to controls as measured by intracellular creatine kinase levels. In nude mice subcutaneously injected with

cell-collagen suspension, earlier myotube formation in PGC-1α modified hMPCs could be demonstrated as revealed by histological analysis after 1, 2 and 4 weeks. Increased contractile proteins (Desmin, MyHC, MyHC1) levels were detected by Western Blot, suggesting the initial formation of mainly slow twitch oxidative fibers. This enhancement was further corroborated after RTPCR analysis of Desmin and MyHC1 gene expression levels. These results showed that modification of hMPCs to overexpress PGC-1α stimulated earlier muscle fiber formation *in vitro* and *in vivo*, with an initial switch to oxidative type fibers at 1 week. Thus, we considered overexpression of PGC-1α as a novel strategy for enhancement of skeletal muscle tissue engineering.

A method to non-invasively monitor hMPCs supplemented with PGC-1α longitudinally is of high interest therefore, an adenoviral system for the ectopic expression of a signaling-deficient form of a human dopamine 2 receptor (hD2R) was designed. For the non-invasive tracking of the engineered cells positron emission tomography (PET) being the most sensitive clinical imaging modality was used, and hD2R served as a reporter gene. Chapter three of this thesis describes the safety of the adenoviral delivery system, the successful tracking of the genetically modified cells *in vivo* and *in vitro*, and the effective monitoring of their hypoxic environment. First, the gene expression levels of the receptor in hMPCs were evaluated by RTPCR and infection efficiency was visualized by fluorescent microscopy. Then, the non-toxic effect of the viral gene-delivery was visualized by CaAM (cell viability assay), measured by WST-1 (cell proliferation assay) and, finally evaluated by a fiber formation assay. The results of these studies showed no impairment of cell viability, proliferation and differentiation capacities of the infected primary human cells. In addition, their sustained myogenic phenotype was confirmed by flow cytometry and fluorescent microscopy. Specificity of radioligand binding to hD2R-hMPCs was demonstrated *in vitro* with [^{18}F]Fallypride, a well-established D2R ligand, using PET imaging and autoradiography of the harvested tissues, and *in vivo* using biodistribution and PET imaging applying haloperidol as a D2R blocking agent. Additionally, [^{18}F]FMISO uptake for detecting hypoxic environment in the cells was evaluated at 1, 2 and 4 weeks after cell implantation *in vivo*. We detected a significant decrease of [^{18}F]FMISO uptake after the first week, corresponding to the formation of new blood vessels in the bioengineered muscle tissues as suggested by Western blot analysis of vWf protein levels and by RTPCR analysis of VEGF-A gene expression levels. Lastly, the sustained survival of the transplanted cells at 1, 2 and 4 weeks with formation of muscle tissue at the site of injection was confirmed by histological assessment of the harvested tissues. Taken together, these data show that indeed the non-invasive PET tracking of hMPC_hD2R cells and bioengineered muscle tissues is feasible. Moreover, vital information about the exact location and the hypoxic state of the forming tissues over time could be gathered.

As detailed in chapter four, we combined the expertise from the abovementioned studies to image the enhanced cell-driven regeneration in a *Tibilais anterior* (TA) muscle crush injury model. This model for skeletal muscle regeneration leads to a significant loss of muscle functionality, thereby mimicking the situation in patients with stress urinary incontinence (SUI). Addressing the limited long-term capacity of MPCs to heal muscle damages, we utilized the previously established genetically modified hMPC_PGC-1α to monitor the functional regenerative potential of the proposed cell-therapy and compared it to control hMPC_GFP. The regenerating muscles overexpressing PGC-1α demonstrated enhanced expression of markers associated with myogenesis (α-actinin, myosin heavy chain 1 and 2, Desmin), vascularization (VEGF), as well as with neuronal (ACHE) and mitochondrial (COXIV) activity. Concomitantly, muscle force measurements by myography revealed a significantly improved contractile force in muscles injected with hPGC-1α_hMPCs 1-3 weeks after injury, when compared to hMPC_GFP controls. Applying the previously established PET imaging conditions for hMPCs_hD2R using [^{18}F]Fallypride and [^{11}C]Raclopride for D2R, and [^{64}Cu]NODAGA-RGD for neo-vascularization, distinct differences between hMPCs_hD2R_hPGC-1α and GFP-infected control hMPCs injected in the TA crush injury were observed as reflected in the different signals of the used radiotracers. While tracking the hMPC_hD2R_hPGC-1α using the high-affinity D2R ligand [^{11}C]Raclopride, an unspecific tracer accumulation in the hMPC_GFP control injuries was observed leading to the assumption that this signal was most likely due to inflammation. This hypothesis was further confirmed in the regenerating muscles using [^{64}Cu]NODAGA-RGD, a specific $\alpha_V ß_{III}$ integrin PET radiotracer. Given that macrophages also express this integrin, we assumed that the recorded signal represented inflammation rather than neovascularization. Immunohistological assessment and gene analysis of harvested regenerating muscles at different time points confirmed the distinct inflammation levels (macrophage accumulation and TNF-α secretion), correlating with the PET signal.

In summary, we were able to facilitate early functional muscle tissue regeneration, thereby introducing a novel approach to further improve cell-based therapies for skeletal muscle tissue engineering. Besides successful tracking of the injected cells in muscle crush injuries, we were able to demonstrate that the specificities of the radioligands are significantly altered in areas with high inflammation, thus addressing a possible bottle-neck of PET imaging of neo-vascularization. Further research is necessary to fully understand the role of PGC-1α in regeneration enhancement and to validate further radiotracers which are suitable for non-invasive imaging of the cell-based tissue engineering process.

Zusammenfassung des PhD Projektes

Regenerative Medizin mit autologen Zellen wird zukünftig eine Alternative für den Organen- und Gewebeersatz darstellen. Die Nutzung von Muskelvorläuferzellen (Muscle Precursor Cells – MPCs) in autologen Stammzellentherapien für Krankheiten der Skelettmuskulatur scheint vielversprechend. MPCs haben die Fähigkeit, funktionelle Muskelfasern zu bilden. Im intakten, gesunden Muskel befinden sie sich im inaktiven Stadium als Satellitenzellen sublaminar in der Peripherie der Fasern. Durch äussere Einwirkung werden sie erneut aktiviert proliferieren und differenzieren sich zu neuen Muskelfasern. Die Funktionalität von Muskelfasern und –zellen nimmt mit zunehmendem Alter und eingeschränkter Regenerationsfähigkeit kontinuierlich ab. Dies äussert sich auch in einer höheren Stressinkontinenzrate (SUI) bei älteren Menschen. Die Implantation autologer MPCs in den Schliessmuskel der Blase ist eine vielversprechende Therapieoption für diese Erkrankung. Trotz des grossen Fortschrittes der Zelltherapie sind zwei entscheidende Aspekte noch näher zu untersuchen: (1) wie kann die Qualität der zu injizierenden Zellen verbessert werden, um die Regeneration zu fördern? Und (2) wie können Langzeitergebnisse der Stammzelltherapie nicht-invasiv dargestellt werden und somit wiederholte Biopsieentnahmen verhindert werden? Ziel dieses PhD Projekts war die Erstellung eines Lösungskonzepts um der klinischen Umsetzung der MPC-Therapie einen Schritt näher zu kommen.

Das erste Kapitel dieser Arbeit gibt eine Übersicht über verfügbare nicht-invasive Technologien zur Visualisierung von Zelltherapien in der regenerativen Medizin und Gewebezüchtung. Detailliert wird auf Vor- und Nachteile, neue Entwicklungen und zukünftige Realisierungen näher eingegangen. Es folgt eine Beschreibung und Charakteriseirung der MPCs mit möglichen therapeutischen Einsatzmöglichkeiten. Zusätzlich wird in diesem Kapitel die Schlüsselrolle des Peroxisom Proliferator-aktivierten Rezeptor-γ Co-Aktivator α (PGC-1α) in der Koordination des Skelettmuskelmetabolismus und der Homöostase erläutert. Abschliessend werden die Ziele der Doktorarbeit definiert, auf welche in den nachfolgenden Kapiteln eingegangen wird.

Das zweite Kapitel beschreibt die ersten Meilensteine zur qualitativen Verbesserung biotechnisch erzeugter Muskelkonstrukte. Die Idee ist, menschliche MPCs (hMPCs) dahingehend gentechnisch zu verändern, dass PGC-1α überexprimiert wird. Durch seine Schlüsselrolle im Muskelmetabolismus soll dadurch die Skelettmuskelbildung verbessert werden. Dafür wurden adenovirale Konstrukte (mit PGC-1α und GFP) erzeugt und hMPCs aus Patientenbiopsien isoliert und vermehrt. Der unveränderte Skelettmuskelzellphänotyp der genetisch modifizierten MPCs wurde mittels Durchflusszytometrie und Immunozytochemie bestätigt. Die Viabilität und Proliferationsraten der PGC-1α

überexprimierenden hMPC wurden nicht beeinträchtigt und entsprachen dem Wildtyp und den GFP-infizierten Kontrollzellen. Jedoch bewirkte die Überexprimierung von PGC-1α eine signifikante Erhöhung der Faserbildungskapazität *in vitro.* Schon 9 Stunden nach der Induktion der Differenzierung wurde eine Steigerung der metabolischen Aktivität in den genetisch veränderten Zellen gemessen. Dies wurde durch erhöhten Spiegel der intrazellulären Creatinkinase (CK) angezeigt. Für die *in vivo* Experimente wurden die Zell-Kollagen-Suspensionen subkutan in Nacktmäuse injiziert, die daraus biotechnisch erzeugten Gewebe wurden nach 1, 2 und 4 Wochen wieder entnommen. Histologische Analysen zeigten eine schnellere Muskelfaserbildung bei PGC-1α infizierten Muskelvorläuferzellen. Dies wurde auch in Proteinanalyse mittels Western Blot ersichtlich, bei welcher erhöhte Desmin, MyHC und MyHC1 Spiegel festgestellt wurden, was zusätzlich auf eine primäre Umschaltung auf oxidative Muskelfasertypen hinwies. Diese Erhöhung von Desmin und MyHC1 wurde zusätzlich mittels RTPCR Genanalyse nachgewiesen. Durch die frühere Muskelfaserbildung *in vitro* und *in vivo* mit einer primären Umschaltung zu oxidativen Fasern kann die Überexpression von PGC-1α in hMPCs als eine neuartige Strategie zur Verbesserung der Muskelgewebezucht betrachtet werden.

Im Kapitel drei dieser Arbeit wurde eine nicht-invasive Methode zur Verfolgung von hMPCs nach Implantation entwickelt. Dazu wurde ein adenovirales Konstrukt hergestellt, welches die Expression eines mutierten Dopamin D2 Rezeptor (D2R) mit mangelnder intrazellulärer Signalwirkung in hMPCs erlaubt. Nach der Gewinnung und Vermehrung der Patientenzellen wurden diese infiziert, sodass sie den hD2R exprimieren, welcher mit einem bereits klinisch erprobten Positronen Emissions Tomographie (PET) Tracer dargestellt werden kann. Zuerst wurde die erfolgreiche Zelltransduktion durch RTPCR und Fluoreszenzmikroskopie geprüft. Weiter wurde untersucht, ob die genetisch veränderten Muskelvorläuferzellen ihren Phänotyp verändert haben und ob sie weiterhin normale Muskelfasern bilden können. Dies wurde mittels Viabilitäts- (CaAM), Proliferations- (WST-1), Immunozytochemische-Untersuchungen und Durchflusszytometrie, sowie Faserbildungsassay (FFA) experimentell nachgewiesen. Die anschliessende Anwendung eines nicht-invasiven „PET-imagings“ lieferte weitere Erkenntnisse bezüglich Überlebensrate der Zellen und Bindungsspezifität des etablierten hD2R Radioliganden [^{18}F]Fallypride. Die Spezifität wurde *in vitro* mittels PET Visualisierung der infizierten Zellen und Autoradiographie der geernteten Gewebekonstrukten und *in vivo* mittels Biodistribution und PET mit Haloperidol-induzierte hD2R Blockierung, nachgewiesen. Die exakte Lokalisation des neu entwickelten Muskelgewebes *in vivo* konnte mit [^{18}F]Fallypride erfolgreich veranschaulicht werden. Zusätzlich wurde das [^{18}F]FMISO Signal via PET detektiert, um die Veränderungen des hypoxischen Zellmilieus *in vivo* 1, 2 und 4 Wochen nach der Implantation darzustellen. Dabei wurde nach der ersten Woche eine signifikante Signalabnahme von [^{18}F]FMISO detektiert,

welche der Neoangiogenese im biotechnologisch entwickelten Muskelgewebe entspricht. Die Entstehung von Blutgefässen wurde durch Western Blot Analyse der vWf Proteinmenge und durch RTPCR Analyse von VEGF-A in den entnommenen Geweben über vier Wochen nachgewiesen. Zum Schluss wurde die erfolgreiche Muskelfaserbildung nach subkutaner Zellinjektion histologisch nachgewiesen. Zusammenfassend hat dieser Teil des Projektes neuartige Einblicke in das Gebiet der Muskelregeneration und des Zellmetabolismus erlaubt und einen Beitrag zur nicht-invasiven Visualisierung biotechnologisch entwickelter Muskelgewebe geleistet, welcher für die zukünftigen klinischen Anwendungen entscheidend sein kann.

Im Kapitel vier wurden die oben beschriebenen Methoden kombiniert, um die verbesserte, durch Zellinjektionen unterstützte Muskelregeneration in einem Druckverletzungsmodell des *Tibialis anterior* (TA) nicht-invasiv darzustellen. Dieses Modell imitiert mit einem bedeutenden Verlust der Muskelfunktionalität die Situation in stressinkontinenten Patienten. In diesem Teil des Projektes wurde die Nachhaltigkeit der Behebung von Muskelschäden mittels hMPCs untersucht. Dafür wurden die genetisch veränderten hMPC_PGC-1α verwendet um eine funktionelle Verbesserung der vorgeschlagenen Zelltherapie zu stimulieren. Als Kontrolle wurden hMPC_GFP verwendet. Die Analyse der PGC-1α überexprimierenden Muskeln deutete auf eine erhöhte Myogenese (α-actinin, MyHC1und2, Desmin), Vaskularisation (VEGF), sowie neuronale (ACHE) und mitochondriale (COXIV) Aktivität hin. Gleichzeitig zeigte die mittels Myographie gemessene Muskelkontraktion der mit hPGC-1α injizierten Muskeln eine, im Vergleich zu den mit hMPC_GFP injizierten Kontrollen, signifikant verbesserte Kontraktionskraft in den Wochen 1-3 nach der Verletzung. Mit den etablierten PET Bildgebungsverfahren für hMPCs_hD2R mittels [^{18}F]Fallypride und [^{11}C]Raclopride (für D2R) und [^{64}Cu]NODAGA-RGD (für Neovaskularisation) konnten klare Unterschiede zwischen hMPCs_hD2R_hPGC-1α und hMPC_GFP injizierten Zellen nachgewiesen werden. Dies spiegelte sich in den unterschiedlichen Signalen der benutzen radioaktiven Tracer wieder. Die unspezifische Ansammlung des D2R Linganden [^{11}C]Raclopride in den Kontrollverletzungen führte zur Annahme, dass das Signal durch eine Entzündung verursacht wurde. Diese Hypothese wurde während des Imagings der Neovaskularisation im regenerierenden Muskel mittels [^{64}Cu]NODAGA-RGD, einem spezifischen $\alpha_v\beta_{III}$ Integrin PET Radiotracer, bestätigt. Da Makrophagen das Integrin ebenfalls exprimieren, folgerten wir, dass das Signal eher auf eine Entzündung als auf Neovaskularisation zurückzuführen ist. Immunohistologische und genetische Untersuchungen der regenerierenden Muskeln zu verschiedenen Zeitpunkten haben Entzündungen (Ansammlung an Makrophagen und TNF-α Sekretion), in Übereinstimmung mit dem PET Signal, bestätigt.

Zusammengefasst konnten wir die funktionelle Regeneration von Muskelgewebe ermöglichen und somit einen neuen Ansatz zur Verbesserung zellbasierter Therapien für die

Skelettmuskelgewebezucht entwickeln. Neben einem erfolgreichen Tracking der injizierten Zellen in den regenerierenden Muskeln konnten wir aufzeigen, dass die Spezifitäten der Radioliganden in entzündetem Gewebe signifikant verändert werden, wodurch ein mögliche Beeinträchtigung der PET Bildgebung der Neovaskularisation hervorgeht. Um die Rolle von PGC-1α in der Verbesserung der Regeneration vollständig zu verstehen, sowie zur Validierung weiterer Radiotracer für nicht-invasives Monitoring zellbasierter Therapien ist weitere Forschung nötig.

Abberviations

µ	micro
µm	micrometer
^{0}C	degrees Celsius
^{11}C	carbon-11 isotope
^{13}N	nitrogen-13 isotope
^{15}O	oxygen-15 isotope
^{18}F	fluorine-18 isotope
^{64}Cu	copper- 64 isotope
^{67}Ga	gallium-67 isotope
^{99m}Tc	technetium-99m isotope
^{111}In	indium-111 isotope
^{123}I	iodine-123 isotope
^{131}I	iodine-131 isotope
ACHE	acetylcholine esterase
AD	Alzheimer's disease
AD MSCs	adipose tissue derived mesenchymal stem cells
ANOVA	analysis of variance
AV	adenovirus
BCA	bovine carbonic anhydrase
BLI	bioluminiscence
BSA	bovine serum albumine
CaAM	calcein AM
CD34/36	cluster of differentiation 34/36
cDNA	complementary deoxyribonucleic acid
CH_3I	methyliodide
CH_4	methane
cm	centimeter

CMV	cytomegalovirus
CNS	central nervous system
CO_2	carbon dioxide
COXIV	cytochrome c oxidase subunit IV
CRISPR	clustered regularly interspaced short palindromic repeats
CT	computed tomogrpahy
$CuCl_2$	copper di-chloride
Cy3	cyanine 3
D2DR	dopamine D2 receptor
DAPI	4',6-diamidino-2-phenylindole
DMEM	dulbecco's modified eagle medium
DTPA	diethylene triamine pentaacetic acid
ECL	enhanced chemiluminescence
EF5	2-(2-nitro-1H-imidazol-1-yl)-N-(2,2,3,3,3-pentafluoropropyl)-acetamide
EFS	electrical field stimulation
ERRα	Estrogen-related *receptor* alpha
EtOH	ethanol
FACS	fluorescent activated cell sorting
FBS	fetal bovine serum
FDG	fluorodeoxyglucose
Fl	fluorescence
FFA	fiber formation assay
Fig	figure
FITC	fluorescein isothiocyanate
FLT	fluorothymidine
FMISO	fluoromisonidazole
GAPDH	glyceraldehyde-3-phosphate dehydrogenase
GBq	gigabequerel

GFP	green fluorescent protein
h	hour/s
H&E	haematoxilin and eosin
H_2O	water
H_3PO_4	phosphoric acid
HA tag	human influenza hemagglutinin tag
hbFGF	human basic fibroblast growth factor
HCl	hydrogen choride
hD2R	human dopamine 2 receptor
hEGF	human epidermal growth factor
HMPAO	hexamethylpropylenamineoxine
hMPCs	human muscle precursor cells
HPF	high power field
hPGC-1α=PPARGC1	human peroxisome proliferator-activated receptor gamma coactivator alpha
HPLC	high-performance liquid chromatography
HRP	horseradish peroxidase
HSV1-tk	Herpes Simplex Virus type 1 thymidine kinase
Hz	hertz
i.v.	intravenous
KO	knock-out
IgG	immunoglobulin M
IgM	immunoglobulin G
IL-6	interleukin-6
LSD	least significant difference
M	molar
MBq	megabequerel
MCAD	medium-chain acyl-CoA dehydrogenase

MIBI	methoxyisobutylisonitrile
min	minute/s
mm	milimeter
MOI	multiplicity of infection
MRI	magnetic resonance imaging
mRNA	messenger ribonucleic acid
MSC	mesenchymal stem cells
MyH1=MyHC1	myosin heavy chain 1
MyH2=MyHC2	myosin heavy chain 2
MyHC	myosin heavy chain
MyoD	myogenic regulatory factor
N	normal
$NaHCO_3$	sodium bicarbonate
NIS	sodium-iodide symporter
NITTP	3-(2-Nitroimidazol-1-yl)-2-*O*-tetrahydropyranyl-1-*O*-toluenesulfonylpropanediol
O_2	oxygen
OCT	optimal cutting temparature
p.i.	post injection
Pax7	paired box 7
PBS	phosphate-buffered saline
PET	positron emission tomography
PFA	paraformaldehyde
PMT	photmultiplier tube
pO_2	patial oxygen pressure
PSI	Paul Scherrer Institute
PVDF	polyvinylidene fluoride
RF	radiofrequency

RFP	red fluorescent protein
RGD	arginylglycylaspartic acid
RNA	ribonucleic acid
ROS	reactive oxygen species
rRNA	ribosomal ribonucleic acid
RTPCR	reverse transcription polymerase chain reaction
s.c.	subcutaneous
SEM	standard error of the mean
SN	striatum nigra
SNF	swiss national foundation
SPE	solid phase extraction
SPECT	single-photon emission computed tomography
SPIO	superparamagnetic iron-oxide
SUI	stress urinary incontinence
SUV	standardized uptake value
TA	tibialis anterior
TAcr	tibialis anterior crushed
TAnat	tibialis anterior native
TBS	tris-buffered saline
TNF-α	tumor necrosis factor alpha
V	volts
VEGF	vascular endothelial growth factor
VOI	volume of interest
vWf	Von Willebrand factor
w/v	weight/volume
WB	Wester Blot
WST-1	cell proliferation reagent
WT	wildtype

Table of Contents

1 Introduction

1.1 Non-Invasive Imaging Modalities For Clinical Investigation In Regenerative Medicine

Deana Haralampieva [1,2,3], Simon M. Ametamey [2,3], Tullio Sulser [1], Daniel Eberli [1,3]

[1] Laboratory for Tissue Engineering and Stem Cell Therapy, Division of Urology, University Hospital, Zurich, Switzerland

[2] Institute of Pharmaceutical Sciences, ETHZ, Zurich, Switzerland

[3] Zurich Center for Integrative Human Physiology (ZIHP), Switzerland

This chapter has been published in Cells and Biomaterials in Regenerative Medicine

D. Haralampieva wrote the manuscript. S. M. Ametamey, T. Sulser and D. Eberli read, reviewed and approved the different parts of the presented book chapter for submission.

1.1.1 Abstract

Recent developments in the field of regenerative medicine highlighted the emerging need for cellular therapies. This novel approach is at the doorstep to its clinical application. Nevertheless, there is still a lack of consistent and unbiased data on the survival, distribution and safety of implanted cells. The tight collaboration between pharmacology, chemistry, biology and physics expanded the collection of methods for *in vivo* imaging and allowed for real time assessment of functional read-outs, localization and viability of the implants. The successful implementation of stem cell visualization will provide for improvements in many healthcare fields. Of key importance is the identification of the most valuable method for non-invasive monitoring of cells and affected tissue. In this chapter we will assess the advantages and drawbacks of different imaging techniques, focusing specifically on cell therapy and methods utilized for tissue engineering and regenerative medicine.

1.1.2 Introduction

Organ transplantation still remains the gold standard for the treatment of terminally damaged organs. This method brings along a collection of drawbacks like the shortage of available donor organs and the high morbidity of immunosuppressive therapy. Regenerative medicine offers an alternative for the replacement of organs and tissues overcoming pitfalls and proposing a therapy with patient's own cells. The discovery of the self-renewal and differentiation capacities of stem cells accelerated the development of regenerative medicine and inspired researchers and clinicians to search for novel treatment options for the improvement of the quality of life of patients (1). The tremendous success in medical sciences and biotechnology allowed the development of many ideas, some of which are now being approved by clinical trials. Nearly 26'000 studies utilizing cell therapy are currently ongoing (2) trying to establish the safety and effectiveness of this new method for applications in neurology, cardiology or oncology. Autologous stem cell therapy is a novel promising approach with increasing impact on regenerative medicine. Preliminary data of many preclinical studies on different human disorders showed a beneficial effect of this treatment (3). The usage of the patient's own cells to rebuild tissues and regain functionality after trauma is currently investigated, as it may have a profound influence on many human diseases once its application is approved. Several hurdles are yet to be overcome before the safety of this method is guaranteed. One possibility to avoid the post mortem read-out of a study or the invasiveness of a biopsy is the use of *in vivo* imaging. Succeeding in this would also significantly reduce the number of animal experiments to be performed. The emerging need for "real time" visualization of cells

and tissue gives rise to many questions in the field of regenerative medicine. Many different cellular therapies are on the door step into clinics and a method for non-invasive tracking of transplanted cells and defining their fate, functionality and differentiation is of great importance. Of high interest is also the visualization of their effect on the damaged tissue or organ.

In the past two decades many researchers concentrated on developing new modalities for better visualization on the cellular and molecular level. As none of the available imaging systems fulfils all needs, many efforts have been put into expanding the potential of the available methods by testing the application of a variety of vectors, genes, proteins and cells for precise read-outs. The visualization techniques relevant to clinical cell tracking include positron emission tomography (PET), single-photon emission computed tomography (SPECT) and magnetic resonance imaging (MRI) (4). Hybridizations of computed tomography (CT) and MRI with PET and SPECT allow simultaneous acquisition of anatomical information and reveal new state-of-the-art modalities for successful molecular imaging (SPECT/CT, PET/CT, PET/MRI) (5). Generally, the utilization of radioactive tracers provides high sensitivity and requires short image acquisition time. Nevertheless, the production of the radioactive isotopes is very expensive and its application comes along with radiation exposure for the patient. Therefore, MRI seems to be an attractive alternative devoid of harmful radiation. This modality has spectacular image resolution and anatomical read-out capabilities (6). However, it is more time-consuming and lacks the high sensitivity of PET and SPECT (7) (see Table 1.1-1). There are also a few optical imaging modalities using bioluminescence (BLI) or fluorescence (FI), which have been widely utilized in small animal models (8). These are cost-saving methods (using fluorescent proteins or luciferase activity) which allow for very rapid result obtainment. Nevertheless, their spatial resolution is low and decreases with depth, which is the main reason why they are not applicable for life cell imaging in humans.

Imaging Modality	Spatial Resolution	Temporal Resolution	Sensitivity	Safety	Clinically Applied	Cost
CT	50-200 µm (preclinical) 0.5-1 mm (clinical)	minutes	not defined	Ionizing radiation	Yes	$$
MRI	25-100 µm (preclinical) ~1 mm (clinical)	minutes-hours	10^{-3} – 10^{-5}M poor	No ionizing radiation	Yes	$$$
PET	1-2 mm (preclinical) 5-7mm (clinical)	seconds-minutes	10^{-11} – 10^{-12}M excellent	Ionizing radiation	Yes	$$$
SPECT	1-2 mm (preclinical) 8-10 mm (clinical)	minutes	10^{-10} – 10^{-11}M excellent	Ionizing radiation	Yes	$$

Table 1.1-1 Characterizations of clinical imaging modalities (adapted from (9)).

Many cells are potentially accessible by imaging and developments in this field already support the diagnosis and therapy of several human diseases. However, a feasible technique for non-invasive monitoring of the tissue engineering process is still missing. A variety of cells was shown to be applicable for tissue and organ restoration, but yet little is known about the safety, viability, functionality and migration of these cells *in vivo* and their direct or indirect involvement in the healing process. Despite the abundance of new techniques for non-invasive visualization of cells, their translation into the clinic is challenging. Hence, here we will discuss the advantages and drawbacks of different imaging modalities applicable for humans and their implementation in the diagnostics and monitoring of the treatment of various diseases located in the hot spot of current clinical trials. Moreover, we will consider potential strategies for expansion of the available techniques, in particular for successful tissue engineering and regenerative medicine.

1.1.3 MR Imaging

1.1.3.1 MRI Basics

The phenomenon of Magnetic Resonance Imaging (MRI) was discovered observing the reaction of certain nuclei, mostly ^{1}H in the body, when placed in a strong magnetic field (B0) (9). Within a magnetic field, the sum of spins is a net magnetization aligned with the applied field. The macroscopic magnetization is an effect of a slight excess of spins in “low energy” state, in parallel to the B0 direction. The precession frequency of each atom with magnetic moment is directly proportional to the strength of the magnetic field. After applying a radiofrequency (RF) pulse which matches the precession frequency, some of the “excess” atoms absorb energy and flip, thereby changing the direction of the net magnetization vector. The flip angle depends on the intensity, waveform and duration of the RF pulse (10). These atoms then re-emit the energy during transition to their original orientation (relaxation) (Figure 1.1-1).

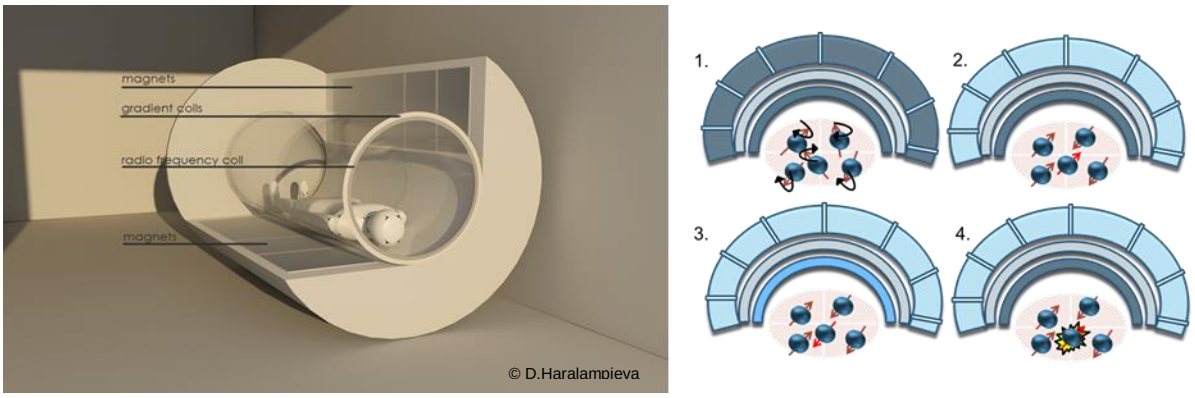

Figure 1.1-1. **MRI scanner** uses radiowaves and strong magnetic fields to obtain anatomical and functional body images. 1) Atoms spin in random directions. 2) Applying a magnetic field makes atoms line up either in the direction of B0, or in the opposite direction. The distribution is not exactly equal, as more atoms prefer to turn in “low energy” state, thereby creating a net magnetization parallel to B0. 3) Introducing a RF pulse makes half of the “excess” atoms change the direction of their magnetization moment - to the “high energy” state. 4) Turning the RF off makes these atoms turn back to their “low energy” position (relaxation), thereby emitting energy.

As already shown, MRI is based on a unique combination of radio waves and strong magnetic fields, which allows the generation of cross-sectional images of the body in any plane. Depending on the relaxation time after the RF pulse, one can distinguish between T1- and T2-weighted images.

MRI is an imaging modality, which uses non-ionizing electromagnetic radiation and is thus not harmful for patients. This is one of the strongest advantages of this technology over the other methods described in this chapter.

1.1.3.2 MRI Applications

One of the biggest advantages of MRI is its high soft tissue contrast. This allows for very precise images and simultaneous detection of functional, molecular and anatomical data. The tight collaboration of science and medicine led to the clinical implementation of the MRI modality for various diseases. Nevertheless, most of its potential remains at the pre-clinical state, as the application safety of many methods is still under investigation. Cerebral perfusion imaging, MR angiography flow imaging, cardiac MRI, functional MRI and MR spectroscopy are just a few of the MRI sub-groups. However, up-to-date, MR is clinically mainly used for the imaging of soft tissues.

A clinical trial study with patients suffering from acute myocardial infarction showed successful implementation of MRI. Intracoronary infusions of bone marrow-derived stem cells at different time points helped with cardio regeneration, which could be visualized by this technique (11). Another study is on its doorstep to clinics, gathering breast cancer patients for breast restoration. The aim is to use MRI of autologous adipose-derived stem cells to visualize the engraftment into the host tissue. The outcome of this study may have a great impact on the utilization of MRI for cell tracking as a novel tool for breast tissue regeneration (12). A further example for the implementation of MRI for cell therapy studies was the evaluation in a multiple sclerosis clinical trial. In this case, adult bone marrow derived stromal cells were intravenously administered to the patients and MRI scans were performed to follow the occurring changes. The main objective was to evaluate the effect of mesenchymal stem cell transplantation on the number of Gadolinium (Gd) -positive lesions (13). Another way of addressing the safety and efficacy of using autologous mesenchymal stem cells as a possible therapy for multiple sclerosis is being proposed by a group, using MR imaging for the assessment of the therapeutic effect of the cell treatment (14). All in all, MRI seems to be a promising tool for monitoring therapy and diagnostic outcomes. Nevertheless, most of the clinical studies using stem cell therapy in combination with MRI are focused on the visualization of the regenerating soft tissue, rather than on the transplanted stem cells, their localization, viability and safety.

Further efforts have been put into the development of strategies for bone and cartilage regeneration. Recent studies are concentrating on developing a MRI-based method for visualization of knee osteoarthritis by assessing the number and location of lesions, cartilage

thickness, and subchondral bone alteration at different time points (15). Others went further by using autologous adipose tissue derived mesenchymal stem cells (AD MSCs) as the most hopeful candidate progenitor cell source for cartilage tissue engineering in patients with degenerative arthritis. Promising results showed improved knee functions and reduced pain without any adverse events. The cartilage regeneration process was captured by MRI at different time points, showing decreased size of cartilage defect, while the volume of cartilage increased over time in the high-dose patients (Figure 1.1-2) (16). This depicts an excellent example of the gradual morphologic regeneration process, visualized by means of MRI.

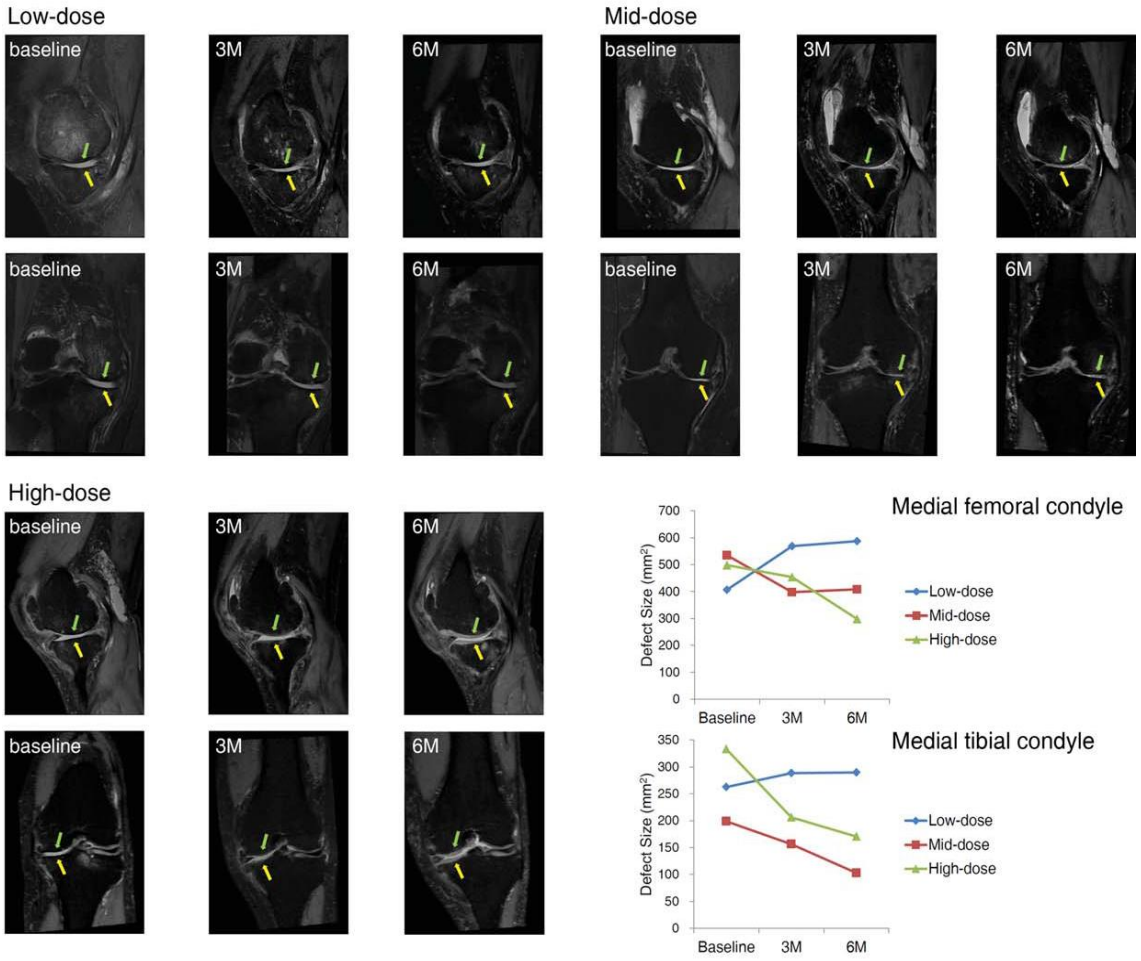

Figure 1.1-2. **MRI evaluation of articular cartilage regeneration in the medial and femoral condyles after intra-articular injection of autologous AD MSCs**. Sagittal and coronal MRIs before, 3, and 6 months after AD MSCs injection depicted the beneficial effect of the high-dose stem cell therapy upon cartilage regeneration by visualizing increase in thickness, and significantly decreased defect size. (Reprinted from (16), Copyright (2014), with permission from “John Wiley and sons” and Kang Sup Yoon, M.D., Ph.D.)

Besides its tremendous spatial resolution for visualization of soft tissues, MRI has proven successful in the imaging of the spinal cord and column. There are several clinical studies concentrating on the regeneration of this region using mesenchymal stem cell (MSC) transplants after injury. One group is trying to evaluate the change of MSC- treated spinal cord injury using MRI. Scans will be performed at 3 and 6 months after transplantation in order to track the effects of the possible cell treatment and the different ways of application (intravenous, intrathecal, into the spinal cord) (17). The outcome of this trial will allow suggesting the most beneficial cell delivery method for further studies. Another project was concentrating on the visualization of spinal cord lesions inducing limb paralysis. The proposed treatment strategy included injections of bone marrow derived stem cells. Again, the preferred non-invasive imaging method for localization of the injuries was MRI (18). It seems that MRI is a suitable imaging tool to assess spinal cord lesions and their repair by stem cells. One group addressed the safety and efficacy of autologous MSC injections in patients with chronic spinal cord injury. The outcome of this study revealed changes in MRI such as decreased cavity size and the appearance of fiber-like low signal intensity streaks (19). An increasing amount of research is concentrating on the transplantation of stem cells as a therapeutic tool, but still, most of the data derives from pre-clinical models. Nevertheless, promising studies in humans reveal new possible solutions for many disorders.

The implementation of contrast agents for enhancement of MRI offers higher contrast and resolution. Gadolinium (Gd) and superparamagnetic iron-oxide (SPIO) are most commonly used for direct stem cell labeling in clinical and preclinical trials, with SPIO particles offering the highest sensitivity amongst all MR contrast agents. Despite initial reports that SPIO labeling of stem cells is safe and does not affect cell biology, recent studies indicate certain metabolic and functional changes. Therefore, some essential issues need to be considered before accepting such agents for clinical trials. A recent study (20) used Gd- or SPIO-labeled mesenchymal stem cells, transduced with a luciferase vector to monitor their viability via BLI. The outcome showed a distinction between viable and non-viable Gd cells, correlating with the luciferase signal. However, dead SPIO-cells indicated a persistent signal void *in vivo*, with simultaneous decrease of luciferase activity. This demonstrates that the absence or presence of a contrast agent signal alone does not prove for cell viability. Often, dead cells are being phagocytized by macrophages and the labeling persists in the new “host cells”. Although Gd-labeling of stem cells seems feasible (21), its main disadvantages are the large amounts of Gd chelates needed to produce a signal, the toxic effect of Gd if released from the complex (affects kidneys) and the lower sensitivity compared to SPIO. These issues should be taken into consideration, as they might lead to false quantification of the imaging data. Recently, a new Gd-based contrast agent (Dotarem®) was approved by the FDA for Phase III clinical studies for MRI in brain, spine and associated tissues in adult and pediatric

patients to detect areas with disruption of the blood-brain barrier and/or abnormal vascularity (22). These clinical studies showed superiority of the enhanced over the unenhanced images of the CNS lesions. All in all, contrast agents improve the quality of the images, but their side effects have to be taken into consideration.

Safety and efficacy of autologous stem cell therapies remains a big issue and a non-invasive visualization tool like MRI is facilitating the refinement of the procedures. Since MRI provides more biological and functional data than CT - without radiation - the system provides a huge advantage for pediatric patients as well as patients needing multiple scans. This makes it a superior imaging modality in many clinical studies and encourages more patients to sign up for the trials, as the risk for unwanted complications is decreased. However, MRI does not come with excellent sensitivity and abundant molecular probes compared to other techniques, following in this chapter.

1.1.4 PET Imaging

1.1.4.1 PET Basics

Radionuclide-based positron emission tomography (PET) is one of the most sensitive molecular imaging techniques. Contrary to MRI, this technique uses radiation. The agents used for the visualization are labeled with a positron emitting radionuclide (^{11}C, ^{13}N, ^{15}O, ^{18}F etc.) which decays by emitting a positively charged particle (β^+). A positron is a particle with the same mass as an electron, but with an opposite charge. Every positron-emitting radionuclide has its own positron range (traveling distance), depending on the energy of its β^+-particle. The higher the energy, the longer the distance and, therefore, the larger the loss of spatial resolution. Once most of its energy is lost, the positron eventually annihilates with an electron from the surrounding tissue, whereby their mass is converted into electromagnetic energy in the form of high-energy photons (23). The PET Imaging technique is based on the coincidence detection of two 511 keV photons emitted simultaneously in opposite directions (180^o apart). They are collected by a ring system of photon-sensitive detectors (scintillation crystals), surrounding the object of interest (Figure 1.1-3). Although the exact location of a single annihilation is unknown, the acquisition of a large number of coincidence events over many angles can provide enough information to reconstruct an image of the spatial distribution of radioactivity as a function of time (5).

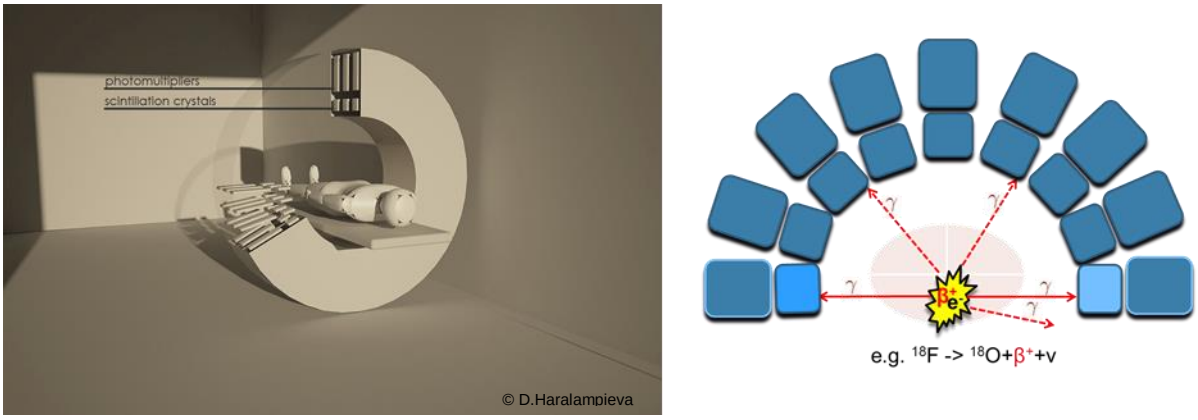

Figure 1.1-3. **PET scanner** detects coincidence of two 511 keV photons emitted in opposite directions after annihilation of a positron (β^+) with an electron (e^-) in the surrounding media. The signals are captured by scintillation crystals and amplified by photomultipliers. These events are then collected to construct images depicting the activity distribution

The idea for the development of the PET technique was developed in the 1950s and was introduced only a few decades later (24) as a clinical device for neurology and cardiology.

Later, the need of precise anatomic localization and metabolic readout led to the invention of new imaging strategies. Combining two complementary modalities can add anatomical and/or physiological information to molecular imaging studies using software fusion of data. This technology is most successful for studies of organs and tissues that do not move with time, e.g. the brain (25). Another approach allowing for simultaneous and/or sequential obtainment of data by a single device is the fusion of PET with CT or MRI. The immense value of combining the benefits of two imaging modalities in one instrument in order to assess molecular as well as morphologic information is of major interest nowadays. These devices allow for more exact attribution of the radioactivity to a specific anatomic site within the patient. Another great impact on the expansion of possible PET applications is the increasing availability of PET radiopharmaceuticals. Many researchers are working towards the development of novel radiotracers for diagnosis and/or therapy of various diseases. Combinations of new technologies and radioligands have already been applied in diverse studies and thus provided many insights for the further development of personalized medicine.

1.1.4.2 PET Applications

Great improvements have been made towards the diagnosis and the therapy monitoring of cancer, brain and heart diseases, as well as for a variety of malignancies and organ/tissue restorations. [^{18}F]fluorodeoxyglucose ([^{18}F]FDG) is the most widely used PET radiopharmaceutical. It is a metabolic tracer and the mechanism of uptake is based on phosphorylation to [^{18}F]FDG-6-phosphate, which is not further metabolized. [^{18}F]FDG has a wide range of applications in oncology, neurology, cardiology and inflammation imaging.

In the past few years many researchers concentrated on cell-based therapies for the restoration of damaged myocardium showing the involvement of different cell types in this process such as: skeletal myoblasts, embryonic stem cells, bone-marrow derived stem cells, cardiac resident cells, mesenchymal stem cells, and circulating progenitor cells. (26). The introduction of cells into the damaged myocardium seems to be a promising technique and therefore several tools for assessing the viability, localization and metabolism of the injected cells have been evaluated (27). The implanted cells should be suitably labeled for detection via imaging, in order to be distinguishable from the surrounding cells and structures. This can be achieved by PET imaging using [^{18}F]FDG. It was already shown to be feasible for dynamic tracking of [^{18}F]FDG-labeled progenitor cells during intracoronary injection after acute myocardial infarction (28). One of the main glucose uptake sites in the body are skeletal muscles. Using PET imaging of this glucose derivate allows for longitudinal assessment of

skeletal muscle regeneration and degeneration (29). This allows for easy visualization by [^{18}F]FDG uptake in response to physical exercise, thus making muscle cells a good diagnostic tool for therapy of muscle disorders (30). Whether this technology is suitable for regenerative medicine purposes has to be further evaluated.

Another application of this tracer was shown in a clinical study using bone marrow cells for autologous stem cell therapy after myocardial infarction. They included the PET modality in their experimental design and investigated the myocardial flow ([^{13}N]NH_3) and perfusion/metabolism mismatch ([^{18}F]FDG) (31). The usage of PET for tracking *in vivo* cell retention of adipose tissue-derived stem cells for myocardial regeneration also showed promising results (32). It seems that these cells support the cardiomyocyte regeneration and angiogenesis in the implanted area. The PET/CT modality appears to be a promising technique for effective cell-tracking *in vivo*, which is vital for a more in-depth investigation into future clinical applications.

Another possibility for PET application is the utilization of reporter-gene systems (e.g. Herpes Simplex Virus type 1 thymidine kinase (HSV1-tk)) (33). The main advantage of this method is that the obtained signal is specific only to viable cells, as they are able to express the reporters. This allows not only for visualization of acute cell retention, but also for viability read-outs (7). HSV1-tk is currently the most investigated enzyme reporter gene for long term *in vivo* visualization of cells applied in the treatment of various cardiovascular diseases (34-36). Recent studies also investigated the use of reporter gene tracking via PET imaging to track viable stem cells in large animal models (37-39). These studies confirm the potential of this novel method to allow for a better understanding of the cell fate after implantation. Using cell-based therapies for tissue engineering with stem and/or progenitor cells for boosting regeneration seems to offer great possibilities in regenerative medicine. Therefore, the development of novel methods for non-invasive imaging of implants *in vivo* is of high priority.

PET/CT has also become an essential tool for assessing prognosis and establishing treatment decisions in oncology. This system found broad application, mainly in defining different stages/locations of metastatic cancer. In this case PET is used for visualizing the increased metabolic activity of the tumor and the addition of CT provides anatomical information on its exact location in the body (40). This helped immensely in the management of a broad spectrum of malignancies, their diagnosis, staging and therapy-response-assessment. The most commonly used radiopharmaceutical in clinics [^{18}F]FDG was shown to be essential to the treatment of a great range of pathologies. This can significantly contribute to precise therapy response assessment possibly influencing the therapeutic management and treatment planning (41). Another study revealed a promising application of fluorine-18 labeled amino acid-based radiotracers for small cell lung cancer detection via

PET imaging (42). Furthermore, a recently developed categorization method for differentiation of osteosarcoma phenotypes by comparing SUV values of PET radioligands for glucose metabolism ([^{18}F]FDG), hypoxia ([^{18}F]FMISO) and bone remodelling ([^{18}F]fluoride) showed promising results. These findings can improve the future evaluation of the treatment strategy depending on the specificity of the malignancy (43). These tracers can be applicable also for regenerative purposes, studying the healing process of e.g. bones. A current clinical study for bone reconstruction of the skull is examining the regeneration after introducing an implant using PET/CT via [^{18}F]fluoride. Succeeding in this would help out many patients with cranial defects and significantly improve their quality of life (44).

Cardiology also gained immense benefits from the development of the hybrid imaging systems (e.g. correction of attenuation and evaluation of coronary classifications), CT for coronary angiography, and acquisition of 3-D hybrid images for the definition of heart viability and diagnosis of cardiac inflammations and infections (45). Recent advances in stem cell therapy show promising results for myocardium restoration, neovascularization and enhancement of perfusion (46-49).

Research on the central nervous system (CNS) mainly emphasized on mapping different aspects of neurotransmitter activity, e.g. dopaminergic, cholinergic, serotonergic and glutamatergic systems as well as beta-amyloid visualization for Alzheimer's disease (AD) (5, 50, 51). PET Imaging has been applied widely to detect and quantify subtle abnormalities in CNS diseases. Therefore, this technology is also immensely popular as a modeling tool in CNS drug discovery and development. It is used for evaluation of drug deposition, as well as for studying disease biomarkers to monitor drug effects on brain pathologies (23). Another CNS utilization of this modality was shown in a promising study regarding spinal cord injury (52). The combined efforts of stem cell and neuroscience researchers made it possible to visualize the spinal cord regeneration process on the cellular and molecular level. In order to explore the effect of *in vivo* PET on tracking dopamine receptor positive stem cells transplanted into the spinal cord, [^{11}C]Raclopride was injected intravenously, followed by a scan. The accumulation of signal in the site of injury showed successful tracking and localization of the injected cells. These results suggest that PET with a radiotracer is a useful technique for functional studies in developing cell-based therapies (53). Similar experimental setups allowed for more rapid progression of many pre-clinical and clinical studies of various CNS pathologies (e.g. [^{11}C]Methionine PET/CT in patients with cancer; [^{18}F]FLT in pediatric patients with CNS tumors (54)).

After the successful introduction of the PET/CT system to the clinics, the integration of PET with MRI was the next step. This new hybrid technique allows for simultaneous functional PET imaging combined with soft tissue morphological MR images. The novel approach

brings better contrast among soft tissues as well as functional imaging capabilities, when compared to PET/CT. Nevertheless, this technology is still not clinically mature at this point. Technically, the implementation of PET/MR faces three major issues: 1. The photomultiplier-based PET scanners do not work in the proximity of the magnetic field of the MR scanner; 2. Metallic objects (e.g. surface coils used to get the best MR quality images) interfere with gamma rays from PET, resulting in unwanted attenuation; 3. MR data cannot be used for attenuation correction, as CT data, which is a limiting factor for the use of PET in therapy response monitoring (55).

As PET signal processing might disturb the high-frequency signals of MRI, and conventional PET electronics fail in an even weak magnetic field, it soon became clear that new solutions had to be found to circumvent the joint interferences. One possibility would be to leave just the PET crystals in the MR field, whereas the PMTs are positioned outside and connected to the crystals by optical fibres. Another approach to avoid the disturbance would be to place the PET and MR scanners remote to each other, but still linked by a common bed, so that the patient does not move between the two scans. Last, but not least, the PMTs could be replaced by solid state electronics which are not disturbed by the MR field (56). Hence, various approaches were developed during the last fifteen years for application in small animal studies, where the usage of more PET tracers is allowed and where use is not as legally restricted, as in human studies. For a review, see Herzog, 2012 (56). Improvements in pre-clinical study design enable smooth transfer of knowledge and molecular measurements between species thereby facilitating clinical translation. Recently, PET/MRI for human imaging became available as well, towing to support form the industry. Siemens Healthcare first designed prototypes of a BrainPET/MRI device and the first reports of patients have been communicated (57, 58). This opened new possibilities in the field of molecular imaging and prepared the development of an integrated whole-body PET/MRI scanner. A recent study compared the performance of whole-body PET/MRI to PET/CT of breast cancer patients and claimed that PET/MRI is a feasible technique for usage in clinics, forgoing gamma radiation for high quality imaging with short examination time (59). Another example for implementation of this new technique was shown in a sarcoma patient, who underwent chemotherapy and autologous stem cell injection. MRI showed lesions in the upper and lower leg, whereas PET revealed high [^{18}F]FDG uptake only in one of the lesions (Figure 1.1-4). This case illustrates the benefit of combining different imaging modalities in order to get more precise outcomes, thereby improving the application fields of personalized medicine. This methodology might also be useful for the investigation of regenerative processes in damaged organs or tissues, for example after autologous stem cell therapy for boosting the healing progression.

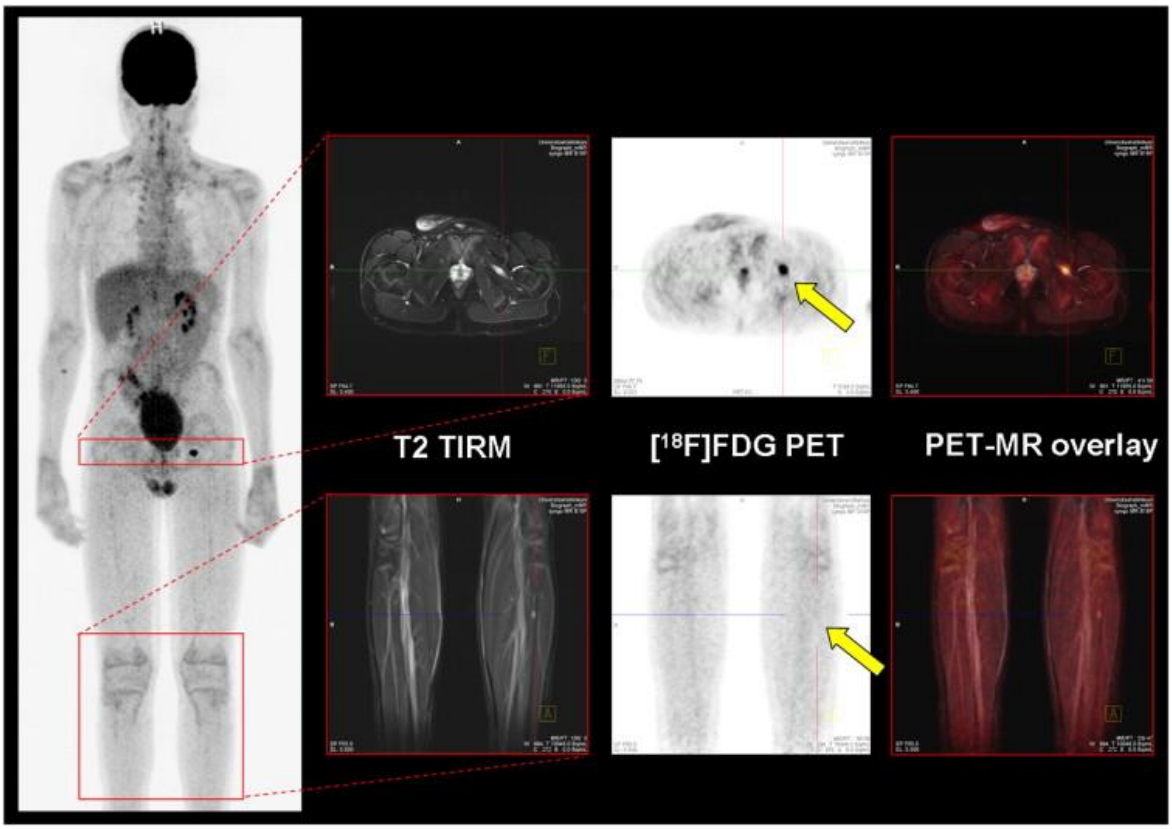

Figure 1.1-4. **Simultaneous whole-body PET/MRI acquired with a molecular MR (mMR) scanner in a 13-year old boy with a Ewing sarcoma known for six years.** The patient underwent standard chemotherapy together with autologous stem cell transplantation. After *i.v*. injection of [^{18}F]FDG whole body PET-MRI was carried out. MR resulted in two suspicious lesions: One in the left upper leg muscle region, and one in the left lower leg. While the lesion in the left upper leg muscles showed intense [^{18}F]FDG uptake, the other one was PET-negative (arrows). Follow-up confirmed a Ewing sarcoma relapse in the left upper leg muscle region. (Reprinted from (59), Copyright (2014), with permission from "Elsevier" and Prof. Dr. med. O. Sabri).

The clinical application of the PET/MRI technique has to be further established. Nevertheless, if MRI can replace CT for anatomical screening, it adds value as well as decreases radiation exposure, which would be of great benefit for the patients. However, the ongoing question of choosing the best suitable visualization method remains unanswered, as there is still insufficient knowledge about which PET/MRI applications are superior to the well-known PET/CT for a variety of clinical cases.

1.1.5 SPECT Imaging

1.1.5.1 SPECT Basics

Unlike PET, single photon emission computer tomography (SPECT) uses radiopharmaceuticals labeled with gamma emitters instead of positron emitters. The concept of transmission and emission tomography, later developed into SPECT, was first introduced in the late 1950s. This period is associated with phenomenal growth of Nuclear Medicine, when some of the most prominent gamma-radiation emitting radionuclides (^{131}I and ^{99m}Tc) were produced (60). While the primary use of ^{131}I was dedicated to thyroid cancer treatment, its use was later expanded for imaging of the thyroid gland itself, its function and the therapy of hyperthyroidism. The development of a generator system for ^{99m}Tc (1960s) was an important breakthrough and today it is the most utilized element in the field of Nuclear medicine. Other typical gamma emitting radionuclides utilized in SPECT are ^{123}I, ^{67}Ga and ^{111}In. The most common SPECT systems consist of a gamma camera with rotating NaI(Tl) detector modules located between the photomultipliers and collimators (Pb) (Figure 1.1-5), an on-line computer for acquisition and processing of data and a display system (61). Generally, a target-specific SPECT radiopharmaceutical consists of two parts: a gamma-emitting radionuclide and a targeting biomolecule (e.g. peptide, antibody fragment) (62). Similar to PET, SPECT also enables 3-D imaging and hybrid systems (SPECT/CT) are available as well.

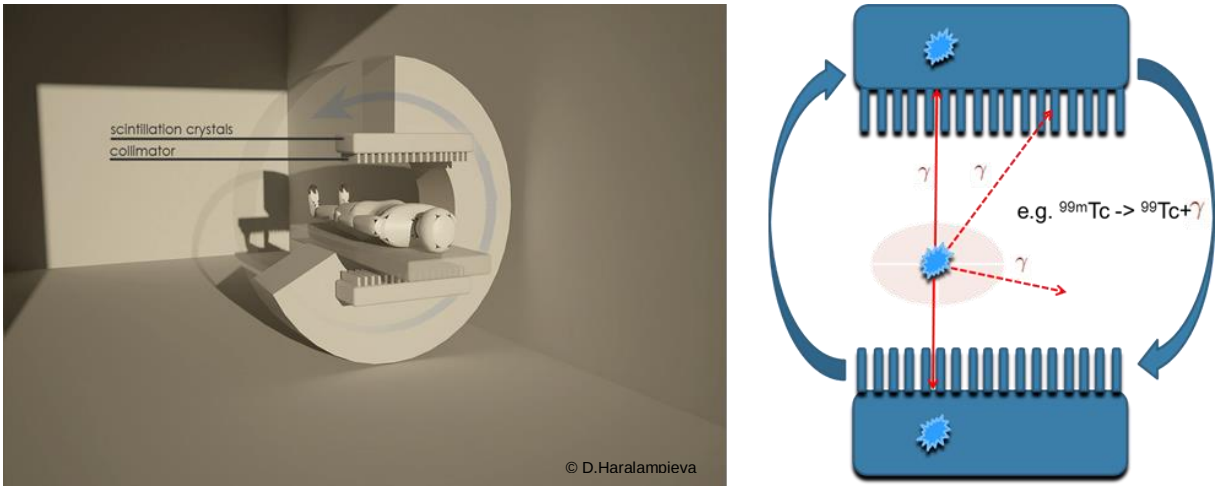

Figure 1.1-5. **Underlying principle of SPECT**: (1) A radioisotope decays by emitting gamma rays. (2) A rotating gamma-sensitive detector with a collimator in front indicates the scintillation site where gamma rays are parallel to the collimator pinholes. (3) The collected data is then transferred to photo-multipliers and finally to a computer for analysis.

1.1.5.2 SPECT Applications

Various stem cells hold promise for the treatment of many human diseases. However, little is known about the exact function, location and survival of the transplanted cells. The usage of the SPECT imaging modality to answer these questions revealed promising results. Clinical studies with SPECT indicated evidence for efficacious imaging of transplanted radiolabeled cells in cardiac disease. Encouraging results were obtained from studies using [^{99m}Tc]hexamethylpropylenamineoxine (HMPAO)-labeled stem cells. Comparison of intracoronary (IC) and transendocardial (TE) delivery of the cells to the heart showed more intense retention signal 18h after cell injection in the TE patients (63). Another study could illustrate homing of bone marrow mononuclear cells TE injection after acute myocardial infarction. Cell retention was successfully visualized in the damaged heart tissue (64). Similar results were obtained by a group showing homing of bone marrow progenitor cells after intracoronary transfer using the same radiotracer (65). Controversially, further experiments investigating the homing of the same cells after myocardial infarction indicated very heterogeneous uptake of the ^{99m}Tc-labeled cells, but for all patients there was lack of or decreased uptake of cells in walls with perfusion defects. The perfusion imaging was performed with thallium (^{201}Tl) (66). Although the safety of autologous stem cell transplantation to the heart after infarction has been shown, it is still not known how many of these cells actually remain in the damaged site, or in near proximity to it. To address their homing and apoptotic rate, autologous bone marrow cells were labeled with [^{111}In]oxine and injected *via* intracoronary route. SPECT imaging was performed 24h after the transplantation and showed homogenous tracer accumulation in liver and spleen, while uptake in the heart was focal. Up to 10% of the injected cells were retained in the myocardium (67). Similar results regarding cell retention were obtained by [^{18}F]FDG labeling of the cells and detection by PET (68). Further insights in this field were obtained from a trial using ^{111}In-oxine-labelled pro-angiogenic cells after intracoronary injection in patients at different time points after myocardial infarction. SPECT imaging was utilized to monitor the cell retention, showing highest values in patients with recent onset of the disease, progressively decreasing in patients treated in an intermediate phase or at chronic stage (69). The substantial amount of radioactivity in the myocardium suggests correct homing of these cells. Nevertheless, most of the injected cells still remain locked in other locations. One possibility for cell homing improvement might be by significantly reducing their entrapment in filter organs.

Further investigations were made to detect angiogenesis after myocardial infarction utilizing SPECT. This was assessed using a novel radiolabelled peptide ([^{99m}Tc]NC100692, Maraciclatide), which has high affinity to an angiogenesis-related integrin ($\alpha_v\beta_{III}$) (70) (Figure 1.1-6). The successful implementation of this tracer led to a follow-up study, addressing the

effect of bone marrow stem cells transplantation on angiogenesis in chronic ischaemic heart failure patients (71). The patients underwent SPECT imaging using the same [^{99m}Tc]RGD imaging peptide. This new imaging tracer was shown to be feasible in patients with heart failure. However, the changes with stem cell therapy did not reach statistical significance.

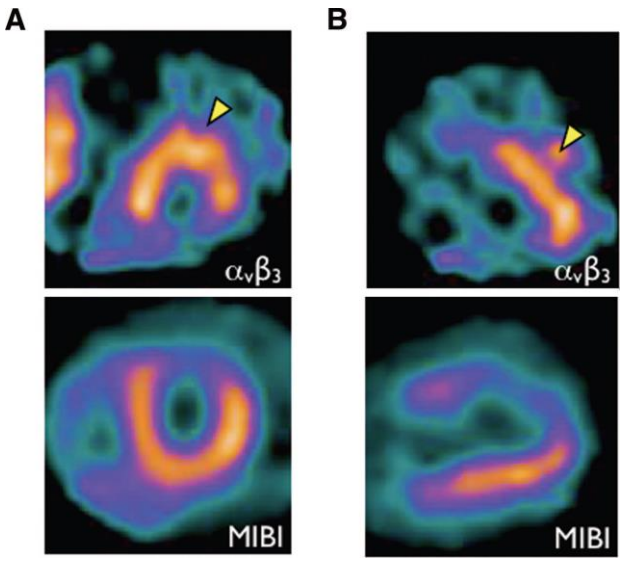

Figure 1.1-6. **Illustration of localized angiogenesis-tracer uptake (Maraciclatide:top) in a region of perfusion deficit** (MIBI: bottom). A: short axis slice; B: long axis slice. Figure was provided by courtesy of Prof. Brian Hutton.

Despite the immense progress in the field of stem cell imaging research, the pre-labeling approach for cell visualization remains challenging for now. Most of the stem cell clinical trials tend to utilize techniques for following the regenerative process (e.g. tissue growth, vascularization and functional recovery), rather than direct tracking of the injected cells (72). The use of autologous stem cell therapy for heart regeneration is of high importance for cardiomyopathy patients and is showing promising results. However, the therapeutic effect is by now mostly measured by an enhancement of the heart regional and global contractility as a cell treatment outcome (72). One other factor, often taken into consideration when testing a new approach for cardio-regeneration, is the heart perfusion efficacy. This could be measured by *i.v.* injection of [^{99m}Tc]sestamibi at rest, followed by an induction of pharmacologic stress by *i.v.* adenosine application. Successful SPECT imaging at rest and post stress suggested a trend towards improvement in cell-treated patients (73). These non-invasive approaches are able to effectively show the outcome of the therapy. Still, they do not answer the questions regarding proper homing, or viability of the injected cells.

Another possibility to assess the regeneration process is by using direct labeling of certain proteins, known to be connected to basic organ functions. This method was performed to estimate the liver self-regeneration after hepatectomy via ^{99m}Tc-labeled galactosyl-human-

serum-albumin. The liver uptake value could be calculated from SPECT/CT images of patients at different time points after surgery (74). An additional visualization possibility for the hepatic function was shown by [^{99m}Tc]phytate colloid uptake by the liver. As colloid uptake by perfused Kupffer cells is proportional to perfused hepatocyte mass, this could be used for direct quantification of perfused liver mass by quantitative SPECT in cirrhotic patients (75). Although the liver is well-known for its self-regeneration capacity, stem cell therapy seems to boost this capacity. Several studies addressed the therapeutic effect of autologous stem cells for liver regeneration (76-78). Nevertheless, none of them assessed the fate of these cells *in vivo*. Recently, the proper homing of injected autologous mesenchymal stem cells in the liver of patients with advanced cirrhosis could be illustrated, as these cells have previously been shown to have beneficial effect. The cells were labeled with [^{111}In]oxine before intravenous infusion and could be detected by SPECT/CT up to 10 days after application. Shortly after injection, accumulation of signal was observed in the lungs, and gradually shifted to the liver and spleen during the following hours to days (79). Using SPECT for evaluation of stem cell homing seems a feasible technique. However, the safety, exact mechanism of action and timing of cell delivery have to be further estimated. There is need for more essential information about the long-term benefit of stem cell therapies. Critical for the future success of SPECT is the design of new and specific tracers for the detection, localization, and staging of a disease and for monitoring of the regeneration process. In the past few decades, there is an increase in the awareness of the importance of this imaging modality, its significant impact on diagnosis and management of various diseases and successful visualization of potential treatments.

1.1.6 Conclusions and future directions

There is no perfect imaging modality for non-invasive cell tracking in clinics. The research findings of the last few decades on the arena of imaging have prompted an intense interest of many investors, who facilitated the translation of these ideas into clinics. Nevertheless, to date no state-of-the-art imaging tool is capable of delivering an all-in-one solution. Many factors have to be considered before choosing the proper visualization modality, depending on the question to be addressed. There is emerging need for versatile imaging methods capable of monitoring the autologous stem cells *in vivo*. Although developments in the field of non-invasive visualization add significant costs and have to overcome many regulatory roadblocks, it is the only way of translating the research into clinical treatments and to support future medicine by providing new tailored treatments to patients.

Despite the immense progress in the field of personalized medicine, there are still many black boxes, on which non-invasive imaging is beginning to shed light. One can observe an increased awareness of the importance of these imaging modalities and their significant impact on diagnosis and management of human disorders are being recognized. Brilliant ideas and developments in this field are catalyzing the design of new strategies every day, giving rise to possible solutions. A summary of the characteristics of the “perfect clinical imaging modality” for stem cell tracking is given in Table 1.1-2. Nevertheless, such an all-in-one technique is not available yet, but the development of hybrid imaging devices for multimodal imaging was a big step towards the ideal system.

1. Safe, non-toxic and biocompatible
2. Single-cell detection at any anatomic location
3. Limitless depth of penetration
4. High spatial and temporal resolution, excellent molecular sensitivity
5. No genetic modifications of the stem cells
6. Insignificant/no dilution with cell division
7. Possible quantification of cell number and viability
8. Serial and long term monitoring in patients up to several months/years
9. Insignificant/no uptake of tracer by non-target cells
10. Multimodality-based approach
11. Low costs

Table 1.1-2 . Requirements for the design of the “perfect clinical imaging modality” for stem cell tracking

The techniques of SPECT/CT, PET/CT and PET/MRI are the state-of-the-art modalities for successful biomedical molecular imaging. Various diseases related to metabolism, apoptosis, tumors, genetics, and stem cells have been identified by these systems (61). The same approaches are already being successfully transferred in numerous clinical studies using autologous stem cells for organ and tissue restoration. Nevertheless, the selection of a given visualization technique depends on its strengths and weaknesses with respect to the intended use. All currently developed molecular imaging techniques for stem cell tracking have inherent limitations. For imaging of delivery and short-term homing of the injected stem cells in different organs, a direct labelling approach may be the answer (iron oxide or [^{18}F]FDG), even though any potential toxicity must be taken into account. MRI offers the highest spatial resolution and near real-time image guidance for cell delivery, although with significantly lower molecular sensitivity than other modalities, such as PET or SPECT. For long-term cell monitoring, reporter gene imaging, using PET or SPECT, appears to be a better choice. Ultimately, finding the most suitable system or combination of systems for proper diagnosis and/or treatment remains the essence of health care and personalized medicine.

1.2 Stem Cell Therapies

Parts of this chapter will be published in a review "Alternative Stem Cell Sources for Muscle Tissue Engineering" by S. Salemi, D. Haralampieva, D. Keller, T. Sulser and D. Eberli

Most of the pre-clinical and clinical regenerative medicine investigations are focused on myocardium and spinal cord restoration, cartilage and muscle regeneration and diabetes. For example, there are indications that it might be possible to direct the differentiation of human embryonic stem cells towards forming insulin-producing cells for eventual transplantation in diabetic patients (80). Another research trend is concentrated in the use of bone marrow cells for rescuing a damaged heart (81, 82). However, whether these cells are able to regenerate the cardiomyocyte pool and to form new muscle tissue is under investigation. Another suggestion would be that they add to the tissue restoration by the induction of neovascularization, or help by secretion of growth factors, rather than incorporation into the heart. Advanced strategies based on different approaches offer effective treatments by combining cells, biomaterials, growth factors and biomanufacturing techniques. Nevertheless, most of the knowledge is based on promising results from pre-clinical models, serving as a basis for several human studies (83). The discrepancy between rodents and humans in terms of genetics, molecular mechanisms and functions still limits the direct translation of many successful pre-clinical therapies. Even so, many current clinical research studies are focused on identifying and refining ways for restoration of damaged or missing tissues and organs using stem cells (84) and a number of successful cases are already reality. Perhaps the most common stem cell treatment is the bone marrow transplantation, where leukaemia patients receive an infusion of stem cells from a suitable donor, allowing for generation of new, healthy, functioning blood cells. Potential stem cell treatments are applied in spinal cord injury patients, where stem cells were shown to replenish the damaged neurons. Heart diseases are among the most widely studied targets for adult stem cell therapy. Another direction of implementation of stem cells is for patients with impaired vision. After transplantation of stem cells in sheets over the damaged retina of patients, they partly restored their vision. Treatment with stem cells can heal a very broad range of medical conditions; however, more research is needed to ensure higher success rates, in order to develop a platform, from which many patients could benefit.

Similar investigations are ongoing towards finding a feasible therapy for stress urinary incontinence (SUI). SUI is a frequent condition affecting over 200 million people worldwide that can be caused by urethral sphincter muscle insufficiency and is associated with a

dramatic deterioration of the quality of life. However, the current treatment strategies are not leading to satisfactory outcomes (85).

1.2.1 Muscle Precusor Cells

Skeletal muscle is one of the few adult tissues that possess the ability to regenerate itself, and this ability resides within a population of cells, defined anatomically, as satellite cells. These cells have been simultaneously discovered by A. Mauro and B. Katz in the early 1960s and have since then been widely accepted as the resident stem cell of skeletal muscles, providing myoblasts for growth, homeostasis and repair (86). Mitotically quiescent skeletal muscle satellite cells are localized underneath the basal lamina surrounding each myofiber. Disruption of the muscle fiber integrity leads to activation of these cells. Once activated, they divide, on one hand, to supply a viable satellite-cell pool by self-renewal, and, on the other hand, to produce satellite-cell derived myoblasts that further proliferate and finally differentiate before fusing into myotubes. The end-point of differentiation is the formation of mature myofibers (87). Satellite cells are postnatal cells, committed to the formation of myotubes. Therefore, they are also referred to as muscle precursor cells (MPC) more recently (88). These cells are required throughout life for myofiber growth, repair and maintenance; therefore, a strict control is required for their proper functioning. Each of the stages (quiescence, proliferation, differentiation and self-renewal) is characterized by a combination of typical molecular markers (87, 89, 90). Satellite cells in the initial phase are shown to express high levels of the paired box transcription factor 7, Pax7, which is likely to be involved in supporting satellite cell survival. The next step of myogenesis is regulated by a family of muscle-specific transcription factors, expressed in a temporally ordered manner (myogenic differentiation factor 1 (MyoD), myogenic factor 5 (Myf5)). MyoD is highly expressed during myoblast proliferation, whereas their differentiation into myocytes is marked by myogenin upregulation. Desmin is another protein specific for differentiating myocytes and myotube formation. It is a type III intermediate filament near the Z line of sarcomeres and therefore its expression increases towards the terminal differentiation. Typical markers for this end-stage are sarcomeric alpha-actinin and myosin heavy chain 1 and 2 (MyHC). These proteins are the main tools involved in the proper functioning of sarcomeres, leading finally to muscle contraction (Fig. 1.2-1).

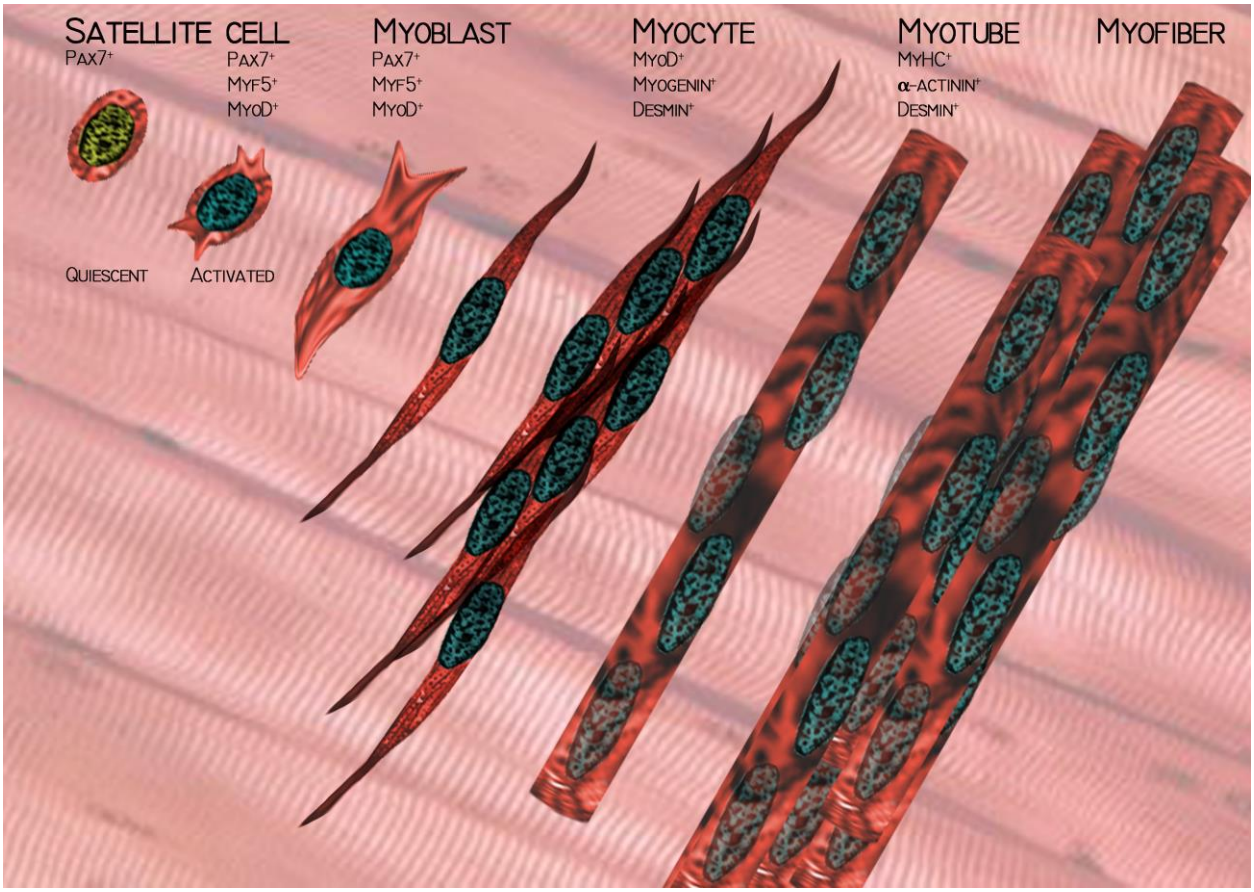

Figure 1.2-1. Differentiation of hMPCs and expression of typical protein markers

The potential use of the MPCs for therapeutic purposes is recently being discussed. After the successful implementation of this cell source in several animal studies (pigs (91-93), dogs (94), mice (95-97)), the next level to go was a clinical application. There is a broad variety of skeletal muscle diseases, awaiting potential cellular treatment. Several promising clinical trials utilizing hMPCs are ongoing, mainly aiming diseases as muscular dystrophy, faecal and urinary incontinence (84, 89). Other non-satellite cell populations have been shown to have myogenic properties (98-100). Nevertheless, numerous well-designed studies revealed inhibited skeletal muscle regeneration, in case of genetic ablation of the satellite cells (101). Therefore, MPCs are indispensable for effective skeletal muscle restoration and remain the main prerequisite for a successful cellular therapy.

1.3 PGC-1α: key factor for skeletal muscle energy metabolism

Skeletal muscles are largely dependent on their intact energy metabolism and the peroxisome proliferator-activated receptor γ (PPARγ)-coactivator (PGC-1α) has been characterized as the key master regulator of energy homeostasis by coordinating the oxidative metabolism (102). Metabolic adaptations appearing during endurance exercise have been shown to be mediated by PGC-1α, which hence represents a major factor in the exercise-triggered signalling network (103). It is a transcriptional coactivator of nuclear receptors (PPARs, HNF4α, GR and ERRα) and transcription factors (NRF-1, MEF2C, FOXO1 and YY1) (104, 105). Hence, PGC-1α activates the transcription of their target genes and its effectiveness is responsive to various stimuli including reactive oxygen species (ROS), calcium ion, thyroid hormone, estrogen, insulin, hypoxia, ATP demand, and cytokines (106, 107). Coactivation of PGC-1α not only stimulates mitochondrial DNA replication, but also regulates other crucial cellular events like mitochondrial fusion and fission (108) and antioxidant resistance (109).

In skeletal muscles PGC-1α is abundant and particularly enriched in slow twitch, oxidative muscle fibers. It has been shown, that activation of PGC-1α is associated with a switch in fiber composition towards high-endurance muscle fibers, type I and IIa slow-twitch and thus oxidative type metabolism becomes the prevailing energy source (110). The formation of a larger fraction of slow type muscle fibers requires mitochondrial biogenesis, fatty acid uptake (i.e. by CD36) and oxidation (i.e. by MCAD) in the myocytes to guarantee adequate substrate supply. All these processes are strictly coordinated by PGC-1α (111-113).

Besides being a regulator of metabolic changes within cells, PGC-1α is a controller of the neuromuscular junction program by promoting the clustering of ACHR at the motor end plate (114). Furthermore, PGC-1α has been shown to regulate a wide programme of genes involved in the coordination of neovascularization, e.g. VEGF (115). Further investigations demonstrated that the PGC-1α/ERRα/VEGF axis mediates the exercise-induced angiogenesis in skeletal muscles (116). Angiogenesis in response to hypoxia or other insults is a complex programme, requiring coordination by multiple signals (117). While PGC-1α KO mice show a remarkable failure to reconstitute blood flow in a normal manner to the limb after an ischaemic insult, transgenic expression of PGC-1α in skeletal muscle is protective (118). Taken together, these evidences strongly suggest a fundamental role of PGC-1α in the maintenance of nutrients and oxygen supply during sustained muscle contractions, thus, making PGC-1α a potential target for a development of a therapy against ischaemic diseases.

Skeletal muscle tissue shows evidence of considerable plasticity and adapts to different training regiments as well as disuse. While endurance training induces PGC-1α as described above, various experimental or pathological muscle wasting conditions like denervation-induced atrophy, statin treatment, diabetes reduce PGC-1α levels (111). Furthermore, PGC-1α KO mice display higher basal expression levels of IL-6 and TNF-α than wildtype (114, 119). Moreover, these mice appear to be viable, fertile and to retain normal mitochondrial volume in skeletal muscles, while expression of genes of oxidative phosphorylation is markedly blunted (120, 121) However, their ability to overcome stress induced conditions like cold, or ischaemia is being strikingly compromised (111, 115).

On the other hand, studies have demonstrated that ectopic expression of PGC-1α acts against atrophy *in vitro* and *in vivo* (104, 122). Recent reports from muscle-specific PGC-1α overexpression underline the benefit of PGC-1α in muscle atrophy and sarcopenia, during which PGC-1α enhanced mitochondrial biogenic pathway and reduced oxidative damage (107, 123). Moreover, transgenic mice with PGC-1α overexpression have been shown to have decreased inflammatory cytokine production and protein degradation caused by denervation (104, 124). Gain-of-function studies indicate an increased resistance to induced fatigue in isolated skeletal muscle of transgenic mice overexpressing PGC-1α (110). Similar findings were described in remobilized mice, where *in vivo* intramuscular transfection with PGC-1α led to enhanced mitochondrial biogenesis and function, increased fiber cross-sectional area and significantly decreased metabolic and redox disturbances (125). Taken together, these studies lay emphasis on the possible role of PGC-1α in not only re-establishing the metabolic balance, but also at reducing inflammation to improve muscle function and structure.

1.4 Aims of the PhD project

Aim 1. Determine the feasibility of hD2R and hPGC-1α genetically modified hMPCs for muscle tissue engineering and PET Imaging

a) Evaluate the transcription stability of hD2R and hPGC-1α transgenic hMPCs *in vitro* after adenoviral gene delivery

b) Establish whether changes on hMPCs phenotype and metabolism occur due to hD2R and hPGC-1α transduction *in vitro*

c) Establish optimal conditions for [^{18}F]Fallypride radiotracer binding to hMPC_hD2R *in vitro*

Aim 2. Investigation of the phenotypic and functional characteristics of engineered muscle tissue supplemented with hPGC-1α in two mouse models

a) Evaluate the effect of hPGC-1α expression on *ex situ* bioengineered muscle tissue *in vivo*

b) Investigate the effects of hPGC-1α delivery on muscle regeneration after hMPC transplantation into a mouse *Tibialis anterior* muscle crush injury model

Aim 3. *In vivo* PET Imaging of hMPC_hD2R with and without hPGC-1α co-expression

a) Track location, migration, distribution and survival of engineered hMPC_hD2R cells injected subcutaneously at the back of nude mice

b) Tracking of hMPC_hD2R in a *Tibialis anterior* muscle crush injury model

c) Metabolic tracking of hPGC-1α vs. GFP only control infected hMPCs in the injured/regenerating muscle tissue targeting hypoxia, neo-vascularization and glucose uptake

2 Human muscle precursor cells overexpressing PGC-1α enhance early skeletal muscle tissue formation

Deana Haralampieva[1,3,4], Souzan Salemi[1], Ivana Dinulovic[2], Tullio Sulser[1], Simon M. Ametamey[3], Christoph Handschin[2], Daniel Eberli[1,4]

[1]University Hospital Zurich and University of Zurich, Laboratory for Tissue Engineering and Stem Cell Therapy, Department of Urology, Frauenklinikstrasse 10, CH-8091 Zürich, Switzerland

[2]Biozentrum, Focal Area Growth and Development, University of Basel, Klingelbergstrasse 50-70, CH-4056 Basel, Switzerland

[3]ETH Zurich, Institute of Pharmaceutical Sciences, Vladimir-Prelog-Weg 4, CH-8093 Zürich, Switzerland

[4]Zurich Center for Integrative Human Physiology (ZIHP)

This chapter has been submitted to the Journal of Tissue Enginnering Part A

D. Haralampieva planed, performed and analyzed the *in vitro* and *in vivo* experiments and wrote the manuscript. S. Salemi supported the proper handling of the different experiments. I. Dinulovic made the PGC-1α adenoviral constructs and performed the CK assay. T. Sulser reviewed the manuscript. S. M. Ametamey, C. Handschin and D. Eberli supervised the project, read and revised the manuscript critically and approved it for publication.

2.1 Abstract

Muscle precursor cells (MPCs) are quiescent muscle cells capable of muscle fiber reconstruction. Therefore, autologous MPC transplantation is envisioned for the treatment of muscle diseases. However, the density of MPCs, as well as their proliferation and differentiation potential gradually decline with age. The goal of this research was to genetically modify human MPCs (hMPCs) to overexpress the peroxisome proliferator-activated receptor gamma coactivator (PGC-1α), a key regulator of exercise-mediated adaptation, and thereby to enhance early skeletal muscle formation and quality. We were able to confirm the sustained myogenic phenotype of the genetically modified hMPCs. While maintaining their viability and proliferation potential, PGC-1α modified hMPCs showed an enhanced fiber formation capacity *in vitro.* Engineered muscle tissues were harvested 1, 2 and 4 weeks after subcutaneous injection of cell-collagen suspensions and histological analysis confirmed the earlier myotube formation in PGC-1α modified samples, predominantly of slow twitch fibers. Increased contractile protein levels were detected by Western Blot. In summary, by genetically modifying hMPCs to overexpress PGC-1α we were able to promote early muscle fiber formation *in vitro* and *in vivo*, with an initial switch to slow type fibers. Therefore, overexpressing PGC-1α is novel strategy to further enhance skeletal muscle tissue engineering.

2.2 Introduction

Damage or loss of skeletal muscles is a major concern in many diseases. Autologous stem cell therapy is on the door step to successful clinical application and represents a novel treatment option for various muscle-related pathologies, including incontinence, vocal cord dysfunction and reflux. Muscle precursor cells (MPCs) are quiescent adult stem cells, residing underneath the basal lamina of skeletal muscle fibers. They begin to proliferate in response to tissue injury, granting sufficient progeny for tissue repair (126, 127). Due to their potential to differentiate into myoblasts and the ability to form new contractile myotubes, these cells are being investigated for muscle tissue engineering and reconstruction in the treatment of a variety of muscle disorders (128, 129).

Despite recent progress in the field of muscle tissue bioengineering, a decreased growth capacity of MPCs in the aged population remains the main shortcoming of this approach (95, 130, 131). This challenge for autologous cell therapy may be addressed by exercise and/or therapeutic regulation of gene expression, which enhances the ability of MPCs to restore muscle fibers. The transcriptional coactivator peroxisome proliferator-activated receptor γ coactivator 1α (PGC-1α) is a key player in neuromuscular activity of skeletal muscle and regulates important exercise-mediated adaptations (103, 132). The PGC-1α expression in a muscle is proportional to the amount of exercise and protects skeletal muscle cells from atrophy, thereby, being beneficial for their survival (104). It serves as a transcriptional coactivator of nuclear receptors and transcription factors, that play essential roles in the regulation of cellular differentiation, development and metabolism (carbohydrate, lipid, protein) of higher organisms (104, 105). Hence, PGC-1α is regulating the mitochondrial biogenesis and is adapting the oxidative state in muscles. The increase of PGC-1α levels goes along with a shift in the fiber composition toward high-endurance muscle fibers, that are capable of sustaining long-term contractions (110). Slow-twitch fibers mostly use oxygen as electron acceptor to generate energy (ATP), which is gradually released for sustained, long contractions, resistant to fatigue (133). Additionally, this high endurance muscle phenotype is characterized with pronounced tissue vascularization, increased mitochondria and myoglobin levels and enhanced import of glucose, lipids and lactate (133). Similar changes are observed in adaptation to exercise, a process also mediated by PGC-1α. The therapeutic potential of PGC-1α in a metabolic optimization strategy is currently being investigated and highlights the importance of novel approaches for successful muscle tissue engineering (88).

Muscle reconstruction using human MPCs (hMPCs) is a promising and feasible therapy method. However, further improvements towards engineering of larger muscles, functional

myofiber formation and increased integration into the host tissue are needed. Our project thus aimed at the generation and validation of a viral vector for ectopic expression of PGC-1α in hMPCs, in order to assess the therapeutic potential *in vivo* bioengineering of skeletal muscle tissue in a mouse model. We hypothesize that initial overexpression of PGC-1α would improve the survival, fiber formation capacity and expression of muscle-specific proteins in the hMPCs. Moreover, it would induce a fiber type switch into slow-type fibers, which are highly desirable for sphincter muscle bioengineering.

2.3 Materials and Methods

2.3.1 Isolation and expansion of hMPCs

Human muscle biopsies from the *M. rectus abdominis* were randomly collected upon ethical approval and with informed consent of hospitalized patients undergoing abdominal surgery under general anesthesia. The samples were processed according to established protocols (134). Briefly, each muscle biopsy was first minced and digested with collagenase Type I 0.2% (w/v) (Sigma) and dispase 0.4% (w/v) (Gibco). The enzymatic reaction was terminated with medium containing 10% FBS. Individual fibers were then liberated by rigorous pipetting and filtered through a strainer with a pore size of 100 µm. After centrifugation the pellet was resuspended in culture medium and the muscle fibers transferred into 35 mm dishes coated with collagen type I (1mg/ml) (BD). The culture medium consisted of DMEM/F12, 1% Penicillin/Streptomycin, 18% FBS, 10 ng/ml hEGF (Sigma), 1 ng/ml hbFGF (Sigma), 10 µg/ml human insulin (Sigma) and 0.4 µg/ml dexamethasone (Sigma) (134). After 24 h the supernatant containing non-adhered hMPCs was re-plated into dishes coated with collagen type I, in order to reduce the number of contaminating fibroblasts.

2.3.2 Adenoviral transduction

The AdEasy System was used as a tool for recombinant adenovirus generation. N-terminal HA-tagged human PGC-1α was cloned into an adenoviral vector that codes for CMV promoter-driven green fluorescent protein (GFP). The expression of PGC-1α was also under the control of a CMV promoter, thereby ensuring its robust, constitutive expression. Successful cloning was validated by sequencing, while viral infection and expression of the fluorescent reported genes was monitored by visualizing GFP (for the PGC-1α expressing adenoviral vector). As control for viral infection a GFP adenovirus was used. The viral titer was increased through additional amplification step and quantified by fluorescent and bright field microscopy. The optimal multiplicity of infection (MOI) was measured by serial titrations of the viral vectors on hMPCs and simultaneous determination of GFP expressing cells by fluorescent microscopy, cell toxicity and cell viability. Finally, the transduced hMPCs were expanded for 2 days after infection and were *s.c.* injected in nude mice.

2.3.3 Animal experimentation

All animal experiments were performed according to the animal ethics committee guidelines. A total of 24 nude mice (8 weeks old, female, Charles River) were divided in two groups (GFP and PGC-1α). For the *in vivo* experiments, the hMPCs were expanded to passage 3-4.

Each sample contained $30x10^6$ transduced hMPCs, which were gently mixed with 500 µl collagen type I carrier (final concentration: 2 mg/ml) (BD) and prepared for subcutaneous (*s.c.*) injection in the back of nude mice (135). Each animal received two bilateral *s.c.* injections and the engineered tissues were harvested after 1, 2, and 4 weeks.

2.3.4 Cell characterization

After expansion of hMPCs to passage 3 they were infected with the corresponding adenovirus and cultured for 2 days. The cells were characterized by fluorescent activated cell sorting (FACS), using the following primary antibodies: anti-Pax7 (1:100, Sigma), anti-MyoD (1:100, BD), anti-MyHC (1:1, DSHB), anti-Desmin (1:50, Sigma), anti-sarcomeric alpha-actinin (1:200, Sigma), anti-CD34 (1:100, BD) and anti-IgG Isotype control (1:100, Santa Cruise). Cy3 anti-mouse IgG (1:1000, Sigma) antibody was used as secondary antibody. A total of 50'000 events were registered by BD FACS Canto flow cytometer (BD Biosciences) immediately after labeling and the analysis was performed using FlowJo software v. 7.5 (Tree Star Inc.). All data are expressed as percentage of maximum (% Max). All measurements were performed with at least 3 different human biopsies.

Additionally, the transduced hMPCs were cultured to 70-80% confluency, fixed with 4% PFA for 10 min at room temperature, permeabilized with 0.5% TritonX-100 (Sigma) for 7 min, blocked for 30 min (5% BSA + 0.1% TritonX-100 in PBS), and finally stained with anti-Desmin (1:50, Sigma), anti-sarcomeric α-actinin (1:200, Sigma), anti-CD34 (negative control) (1:100, BD) over night at 4 ^{o}C. After washing with PBS, the cells were incubated with Cy3 anti-mouse IgG secondary antibody (1:1000, Sigma) and DAPI (1:100, Sigma) for 1h at room temperature, washed again and finally mounted (Dako). Images were acquired with Leica-Imager Type DM6000B at exposures normalized to unstained controls (secondary antibody and DAPI only).

2.3.5 Fiber formation assay

Differentiation of hMPCs into myofibers *in vitro* was performed as previously reported (fiber formation assay, FFA) (134). Briefly, hMPCs were grown to 50% confluency in culture medium and afterwards in differentiation medium (10% FBS) for 7-10 days until myofibers formed. The fibers were fixed with ice-cold methanol (7 min), stained with Giemsa (1:20, 45-60 min) and air-dried. Five high-power-fields (HPF, 10x) were obtained per condition from 4 biopsies and the results were expressed as number of fibers/HPF, number of nuclei/myofiber, and number of nuclei/HPF. The fusion rate was calculated by dividing the number of nuclei/myofiber by the number of nuclei/HPF (%). A total n=4x5HPF were analyzed. The imaging software "ImageJ for microscopy" was used for data assessment.

2.3.6 Cell viability and proliferation

In all cases, cell numbers and viability were confirmed by trypan blue staining after trypsinization. To evaluate proliferation and viability of the infected cells at different time points, hMPCs were cultured for 6 days. The cell proliferation reagent WST-1 (Roche) was used according to the manufacturer's protocol. For further confirmation of cell viability hMPCs were stained with 10 µM CellTrace Calcein Red-Orange, AM (Life Technologies) for 30 min at 37 °C. Viable cells were detected using a fluorescence microscope. All measurements were performed in duplicates of at least 3 different human biopsies.

2.3.7 Immuno-/Histological assessment

The harvested engineered muscle tissues were embedded in cryo-preservative (OCT embedding medium, Cell Path) immediately after isolation. Cryostat sections were prepared (10 µm) and further processed. Haematoxylin and eosin (H&E) (Sigma) staining was performed according to the manufacturer's protocol. For immunohistological analysis the tissues were fixed (4% PFA, 10 min), permeabilized (0.5% TritonX-100, 20 min), blocked for 30 min (5% BSA + 0.1% TritonX-100 in PBS), and finally stained with anti-sarcomeric α-actinin (1:200, Sigma) over night at 4 ^{o}C. After washing with PBS, the tissues were incubated with Cy3 anti-mouse IgG secondary antibody (1:1000, Sigma) and DAPI (1:100, Sigma) for 1 h at room temperature, washed again and finally mounted (Dako). Images were acquired with Leica-Imager Type DM6000B at exposures normalized to unstained controls (secondary antibody and DAPI only).

2.3.8 Real-time PCR

For analysis of PGC-1α downstream regulated genes (by RTPCR) and creatine kinase (CK) levels (measured using the Cobas c111 system (Roche Diagnostics) according to manufacturer's protocol), the cells were cultured for 2 days after infection and then transferred to differentiation medium for 9 h, or until day 6, respectively, and finally harvested for further assessments. For gene analysis of tissue, the harvested tissues were pulverized in liquid nitrogen and suspended in RNA lysis buffer. Total RNA was isolated for both, cells and tissues, using the SV Total RNA Isolation System kit (Promega) according to the manufacturer's protocol, which includes a DNase digestion. RNA was reverse transcribed with random primers (High-Capacity cDNA reverse transcription, Life Technologies). Pre-designed primers for human PPARGC1 (Hs01016719_m1), MYH1 (Hs00428600_m1), Desmin (Hs00157258_m1) and VEGF (Hs00900055_m1) were purchased from Life Technologies. Further primers were purchased from Microsynth: hCox5b (fwd primer: ATG GCT TCA AGG TTA CTT CGC, rev primer: CCC TTT GGG GCC AGT ACA TT), hCycS (fwd

primer: CTT TGG GCG GAA GAC AGG TC, rev primer: TTA TTG GCG GCT GTG TAA GAG), hERRα (fwd primer: AGG GTT CCT CGG AGA CAG AG, rev primer: TCA CAG GAT GCC ACA CCA TAG), hPGC-1α (fwd primer: TCT GAG TCT GTA TGG AGT GAC AT, rev primer: CCA AGT CGT TCA CAT CTA GTT CA), and hTBP (fwd primer: CCC GAA ACG CCG AAT ATA ATC C, rev primer: AAT CAG TGC CGT GGT TCG TG). 18S rRNA (4319413E) was used to normalize cDNA concentrations. For quantification, the expression of each gene was normalized to the 18S, or TBP expression in the corresponding sample. The entire experiment was repeated at least three times and samples were analyzed in triplicates.

2.3.9 Gel electrophoresis and immunoblotting

In summary, tissues were pulverized in liquid nitrogen with a mortar/pestle and suspended in lysis buffer supplemented with a protease inhibitor cocktail (Sigma). Afterwards, the samples were centrifuged for 20 min at 13,000 rpm, and the supernatant was collected for protein determination. The total protein was measured with the BCA Protein Assay Kit (Thermo Scientific) and protein lysate (30-50 µg) was loaded on a 10% or 12% gel (Bio-Rad). Western blot was performed according to the manufacturer's protocol. After the separated proteins were electro-transferred onto PVDF membrane (Immobilion-P; Millipore), the latter was incubated with a primary antibody at 4 °C overnight in TBS, 0.1% Tween-20 and 5% non-fat dry milk. The primary antibodies used were anti-MyHC1 (1:5, DSHB), anti-MyHC (1:1, DSHB), anti-Desmin (1:50, Sigma), anti-PGC-1α (1:1000, Calbiochem), anti-sarcomeric α-actinin (1:2000, Sigma), anti-GAPDH (1:2500, Sigma), and α-tubulin (1:2000, Bioconcept). Finally, the membranes were washed in TBS with 0.1% Tween-20 for 30 min and incubated with the appropriate HRP-conjugated secondary antibody (Amersham Pharmacia Biotech) for 1 h. The signals were detected by the ECL method (ECL-Kit, Amersham). The data were analyzed by Image Studio Lite (Li-Cor) software and represented as protein expression relative to GAPDH or α-tubulin.

2.3.10 Statistics

For statistical analysis IBM SPSS v22.0 (SPSS Inc,) was used and graphics were drawn with GraphPad Prism v5.04 (GraphPad Software, Inc.). All data were analyzed by Student's *t*-tests for paired samples or one-way ANOVA with Bonferroni or LSD post-hoc analysis ($p<0.05$ was considered significant). All presented data are expressed as means with corresponding standard error of the mean (±SEM).

2.4 Results

2.4.1 Generation and establishment of genetically modified hMPC

Adenoviral constructs containing hPGC-1α, or GFP only, were successfully generated and amplified for further use in hMPCs. The expression of each gene was designed to be under the control of a CMV promoter in order to assure robust expression of the transgene. The transduction efficiency was confirmed by fluorescent imaging, as both constructs contain a green fluorophore, expressed under a separate CMV promoter (Fig. 2.4-1. A, green). The constructs enabled detection of transduced cells both prior to transplantation for assessing the cell transduction efficiency, and afterwards, on engineered muscle sections. The safety of the viral infection was visualized by a cell viability assay (CaAM) (Fig. 2.4-1 A, red) and further confirmed by Trypan-blue staining for distinction of live/dead cells (Fig. 1 B), showing no significant differences between infected (GFP (90.5±1.97, n=6), PGC-1α (88.16±5.32, n=6)) and wild type (WT, 89.00±3.01, n=8) cells. The proliferation capacity of the WT, GFP- and PGC-1α-overexpressing hMPCs was determined by a cell proliferation assay (WST-1) over 6 days culturing after transduction, showing no significant variations between the different groups (Fig. 2.4-1 C, at 6 days: WT (2.77±0.18, n=6); GFP (3.12±0.19, n=9); PGC-1α (2.59±0.29, n=12)). Importantly, the designed adenoviruses did not affect the expression of specific muscle protein markers (sarcomeric α-actinin and Desmin), as detected by immunofluorescence imaging of hMPCs (Fig. 2.4-2 A) and fluorescent activated cell sorting (FACS) (Fig. 2.4-2 B). The latter also showed expression of specific well-described markers for characterization of activated hMPCs (126), as well as a significant shift in GFP expression levels in both transgenic groups, compared to uninfected WT cells (Fig. 2.4-2 C). These results confirm the successful adenoviral transduction of hMPCs and their maintained cell phenotype.

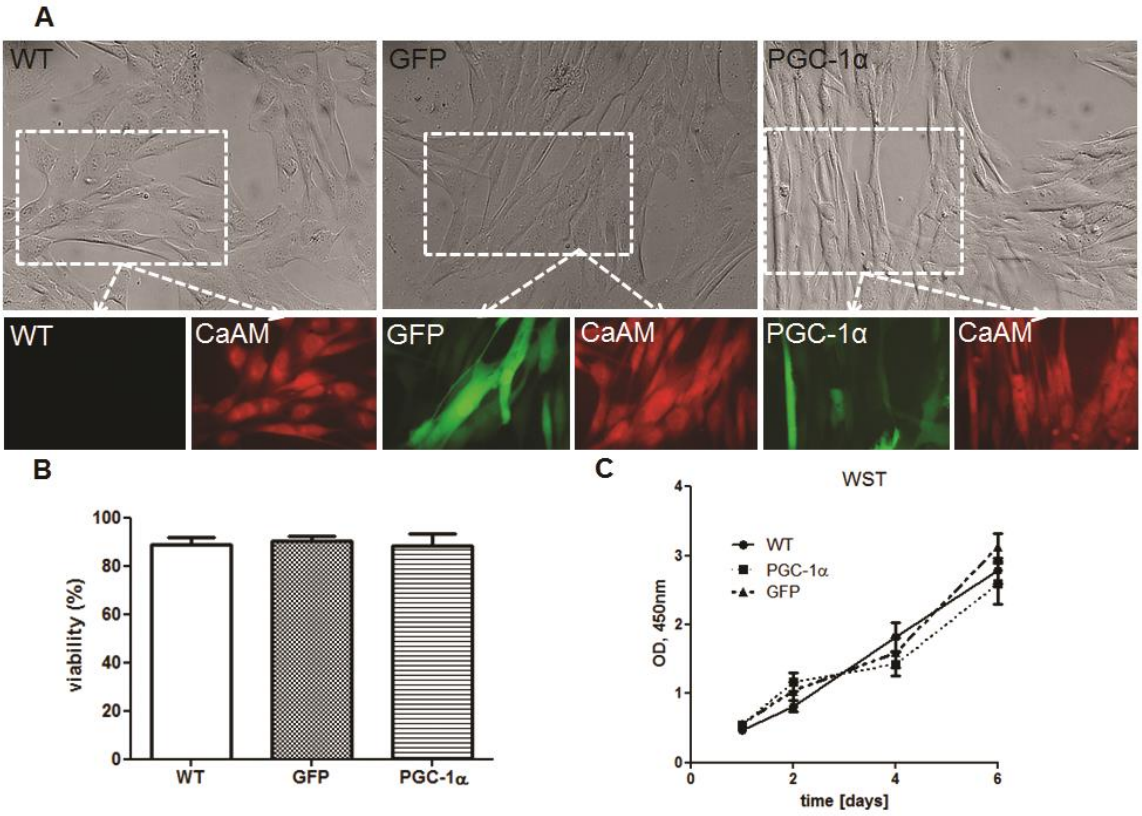

Figure 2.4-1. **PGC-1α adenoviral infection without adverse effects on hMPC.** The successful adenoviral transduction of hMPCs with GFP and PGC-1α (A, green) did not affect the cell viability, as shown by CaAM assay (A, red). This was further confirmed by Trypan Blue staining of live/dead cells (B). Proliferation rate also did not differ between the wild type (WT) non-infected cells and the infected hMPCs (C).

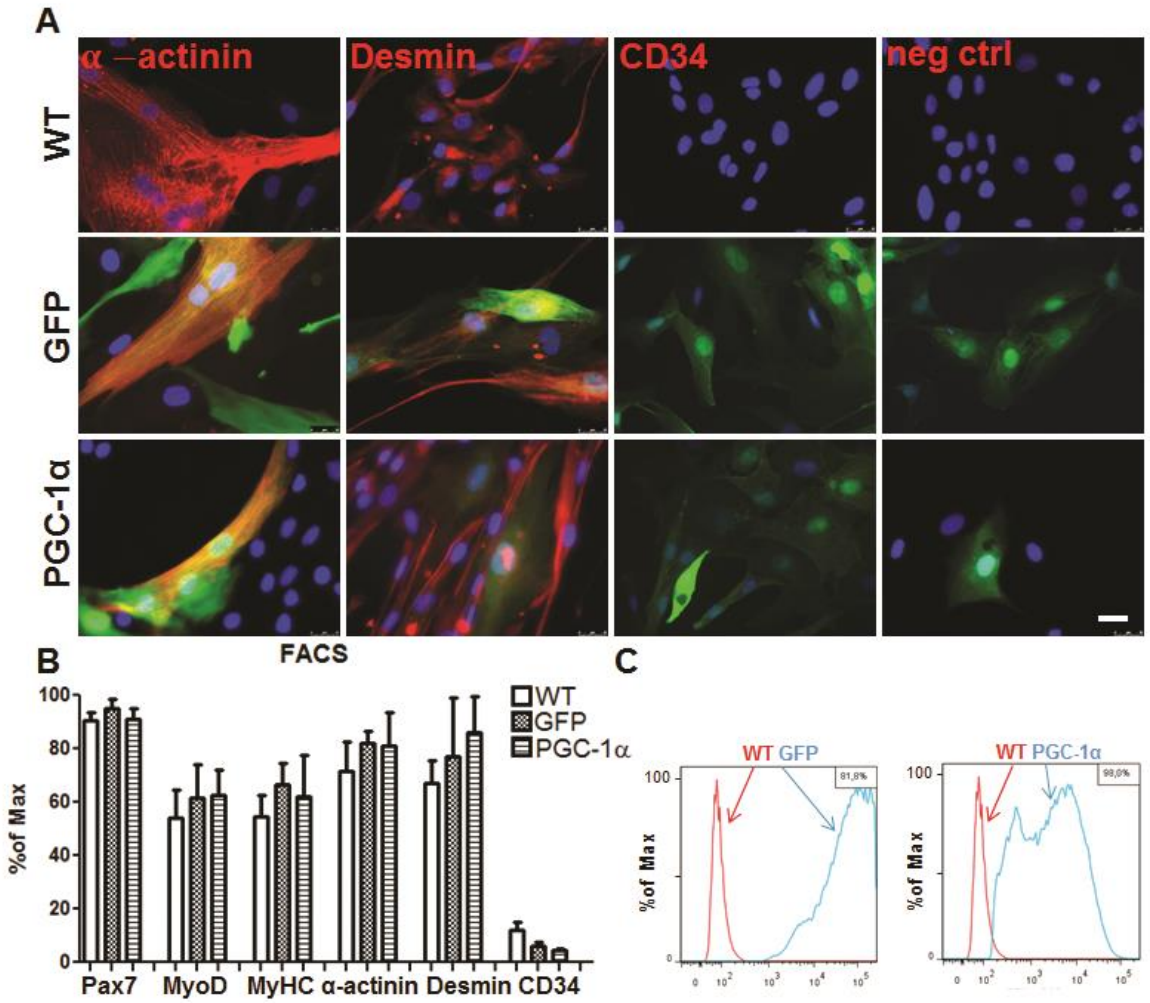

Figure 2.4-2. **Adenoviral infection did not change the hMPC phenotype.** The expression of typical muscle markers (Cy3-red) in the infected cells (green) was confirmed by Immunocytochemistry. Nuclei were stained with DAPI (blue) (A). The hMPCs were analyzed by FACS for expression of various muscle marker proteins (B) and the successful transduction was confirmed by a shift in FITC signal (C). Scale bar: 25µm

2.4.2 PGC-1α overexpression facilitates differentiation of hMPCs into myotubes *in vitro*

To directly assess the role of PGC-1α in myofiber formation, an *in vitro* hMPCs differentiation experiment was performed. A Fiber Formation Assay (FFA) with untransduced (WT), GFP- and PGC-1α-infected cells revealed an increased fusion rate in PGC-1α overexpressing myoblasts (Fig. 2.4-3 A and B, n=4x5 HPF). The participation of transduced GFP-positive cells in the myotube formation could be visualized by fluorescent microscopy (Fig. 2.4-3 A, second row, fluorescence). The facilitated initial differentiation of the PGC-1α overexpressing cells was further confirmed by Western Blot (Fig. 2.4-3 C) where elevated Desmin levels were detected already at day 2 after infection after 9h of differentiation.

The induction of differentiation goes hand in hand with an increase in metabolic activity (ATP consumption). To analyze this process, the intra- and extra-cellular creatine kinase (iCK and eCK) levels were measured 2 and 6 days after adenoviral infection and initiation of differentiation The iCK levels were significantly increased in PGC-1α infected cells at day 2 compared to GFP-infected cells ($p<0.001$) (Fig. 2.4-3 D). At day 6 an overall increase in iCK levels in all 3 groups, concomitant with the induced differentiation could be seen (Fig. 2.4-3 D). Importantly, an increase in eCK levels is often associated with muscle damage, cell death and membrane disruption (136). Our results show that the viral infection did not affect the viability and integrity of hMPCs and that the eCK levels remained low 2 and 6 days after infection (Fig. 2.4-3 E).

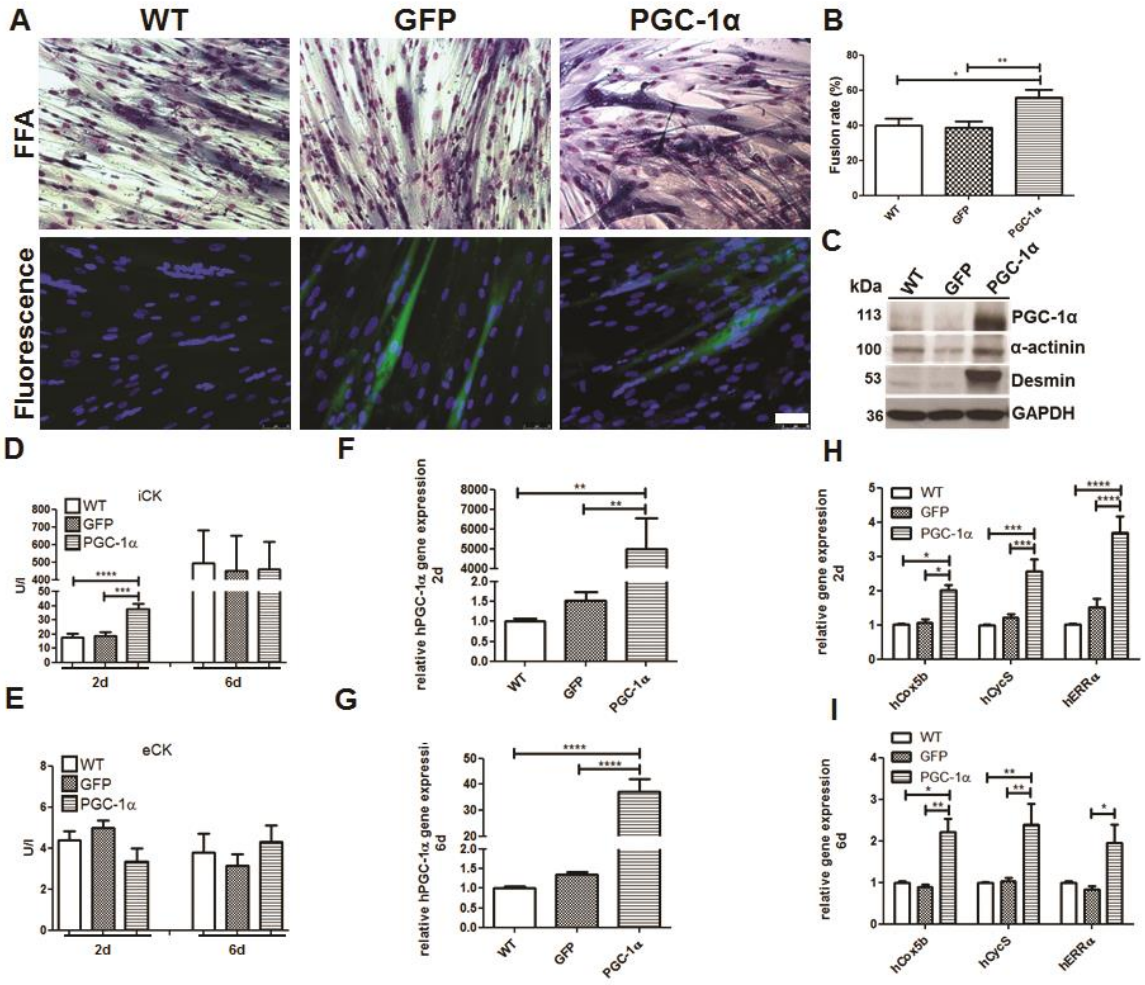

Figure 2.4-3. **PGC-1α overexpressing hMPCs differentiate faster into myotubes *in vitro*.** Fiber formation assay (FFA) and fluorescent microscopy revealed successful myotube formation in WT hMPCs and infected cells (green fluorescence) respectively (A), with an increased fusion rate in PGC-1α overexpressing cells (B). Two days after infection, PGC-1α overexpressing hMPCs displayed enhanced Desmin protein levels (C). Intracellular CK (iCK) levels were significantly increased 2 days after PGC-1α infection (D), whereas extracellular (eCK) levels remained unaffected (E). An overall increase in iCK levels was observed 6 days after inducing differentiation of the hMPCs (D) and eCK remained unchanged (E). PGC-1α gene expression levels were upregulated in hMPCs, infected with PGC-1α adenovirus after 2 (F) and 6 days (G) post infection, compared to GFP and WT controls. PGC-1α downstream genes (hCox5b; hCycS; hERRα) were upregulated in hMPCs transduced with PGC-1α, respectively (H, I). Data are presented as gene expression relative to hTBP, using the ddCt method.

2.4.3 Efficient elevation of PGC-1α and downstream regulated genes using viral vectors in hMPCs

Functionality of the expressed PGC-1α protein was validated by determination of well-described target genes of the coactivator in muscle cells. As expected, the introduction of the PGC-1α viral vector specifically elevated the corresponding gene expression level after 2 days ($p<0.01$) and 6 days ($p<0.0001$) after inducing cell differentiation (Fig. 2.4-3 F and G). The bioactivity of the construct was furthermore confirmed after 2 and 6 days, respectively, by the induction of its target genes cytochrome c oxidase subunit 5b (Cox5b) ($p<0.05$, $p<0.01$), cytochrome c (CycS) ($p<0.001$, $p<0.001$) and estrogen-related receptor α (ERR α) ($p<0.0001$, $p<0.05$), compared to the control cells infected with GFP and untransduced hMPCs (WT) (Fig. 2.4-3 H and I). These data confirm the efficiency of the presented PGC-1α adenoviral construct for genetic modification of hMPCs.

2.4.4 PGC-1α triggers early myotube formation *in vivo*

Encouraged by our *in vitro* observations, we further evaluated the capability of transduced hMPCs to form ectopic muscle tissue *in vivo*. Subcutaneously injected hMPCs (transduced with GFP or PGC-1α) were harvested after 1, 2 and 4 weeks for analysis. The weight of the collected tissues did not differ significantly between the two groups, although a tendency for visually smaller PGC-1α tissues at 1 week was observed, concomitant with the enhanced differentiation (Fig. 2.4-4 A). The constant size decrease over time due to collagen remodeling and myofiber formation has previously been reported (135). Histological assessment via H&E staining of the engineered tissue revealed earlier formation of myotubes in the PGC-1α samples (already at week 1) (Fig. 2.4-4 C, black arrows). This was further confirmed by immunohistological staining of the samples for MyHC, a marker for muscle differentiation and maturation, displaying an increased signal (Cy3, red) in the PGC-1α transduced tissues and more organized structures (myotubes) (Fig. 2.4-4 D, white arrowheads). The typical red color of slow twitch oxidative type I fibers (110) could be detected macroscopically after tissue pulverization with liquid nitrogen in the PGC-1α samples, but not in the control GFP samples after 1 week (Fig. 2.4-4 B). This was concomitant with an initial significant increase in VEGF-A gene levels ($p<0.0001$) in the harvested PGC-1α overexpressing tissues (Fig. 2.4-5 A). The PGC-1α overexpression was confirmed by RTPCR (Fig. 2.4-5 B, $p=0.009$). The earlier differentiation was further confirmed by an increase in Desmin ($p=0.047$) and MyHC1 ($p=0.024$) gene expression in the PGC-1α infected samples, while GFP-infected samples did not show expression at week 1 (Fig. 2.4-5 C and D, n=3-5). In line with this results, at protein level, PGC-1α overexpressing

engineered muscle tissue also indicated an increase in relative expression levels of Desmin (Fig. 2.4-5 E, 2.36±1.32, n=6) and MyHC1 (Fig. 2.4-5 F, 2.24±0.67, n=4) at week 1, compared to GFP samples . An increase in the expression of MyHC protein over time could be observed (Fig. 2.4-5 G, 2.5±0.96 at 4.week, n=4), leading to a suggestion for a PGC-1α-induced shift towards MyHC1 type fibers at 1 week (Fig. 2.4-5 H). Based on the findings above, PGC-1α overexpressing hMPCs hold promise for the enhanced repair of skeletal muscle tissue due to their capacity to facilitate myofiber formation, with an initial shift to oxidative type I fibers.

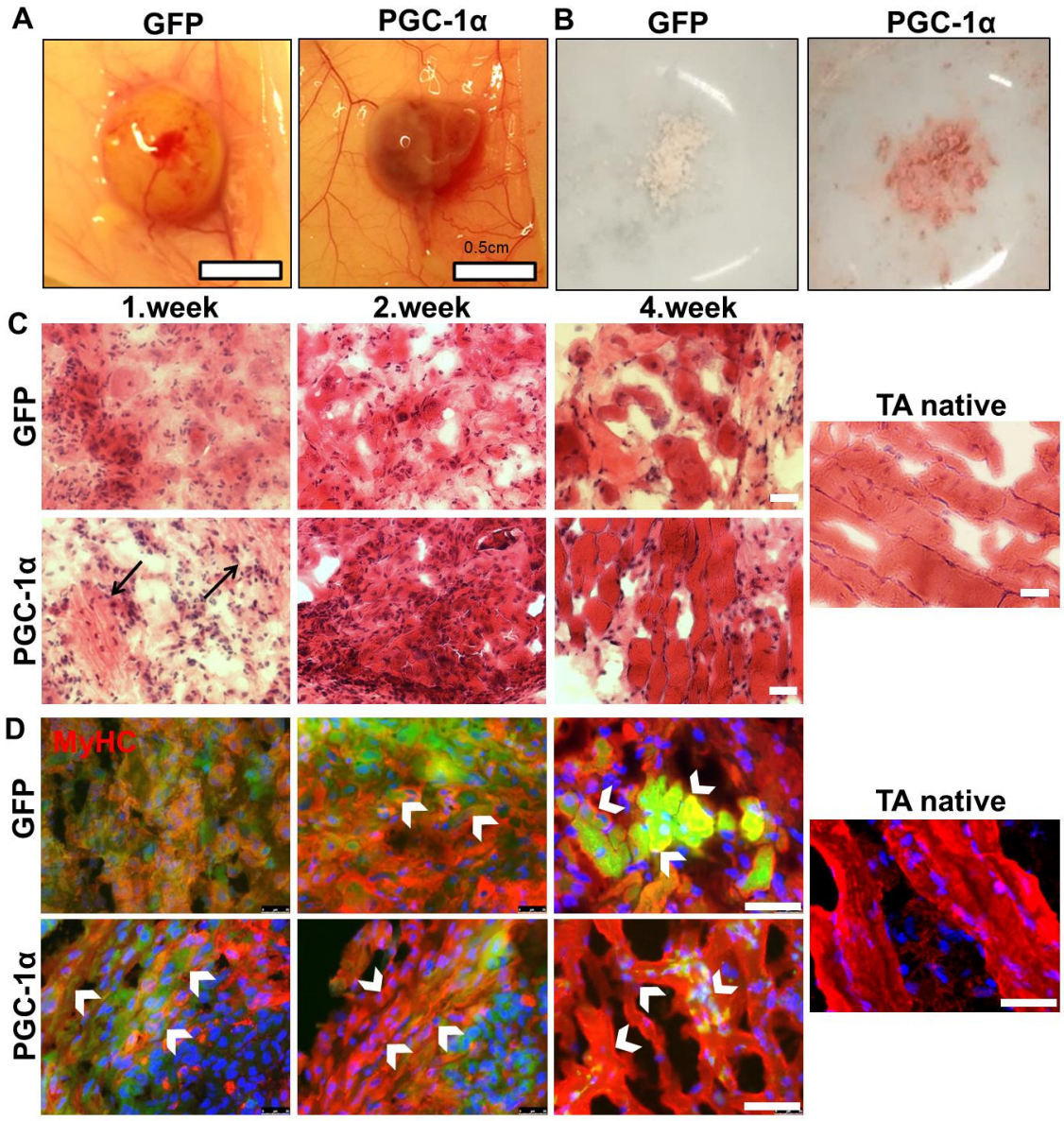

Figure 2.4-4. **Engineered muscle formation is enhanced by overexpression of PGC-1α in hMPCs.** hMPCs transduced with PGC-1α, or control GFP adenovirus were injected subcutaneously on both sides of the back of nude mice. The harvested tissue was visualized macroscopically at 1 week (A). The typical red color of oxidative type I fibers was enriched in PGC-1α samples, compared to GFP controls (samples powderized with liquid nitrogen) (B). The process of successful myofiber formation was visualized over 4 weeks with H&E staining (C), revealing an increased early myotube formation in PGC-1α overexpressing samples (black arrows). *Tibialis anterior* (TA) was used as native control for muscle fiber formation. The increased differentiation capacity of PGC-1α transgenic hMPCs at early time points (1 week) was envisioned by immunostaining for MyHC (Cy3, red) of the *ex situ* engineered muscle fibers (green) (DAPI, blue) (D). Scale bar: 50 µm

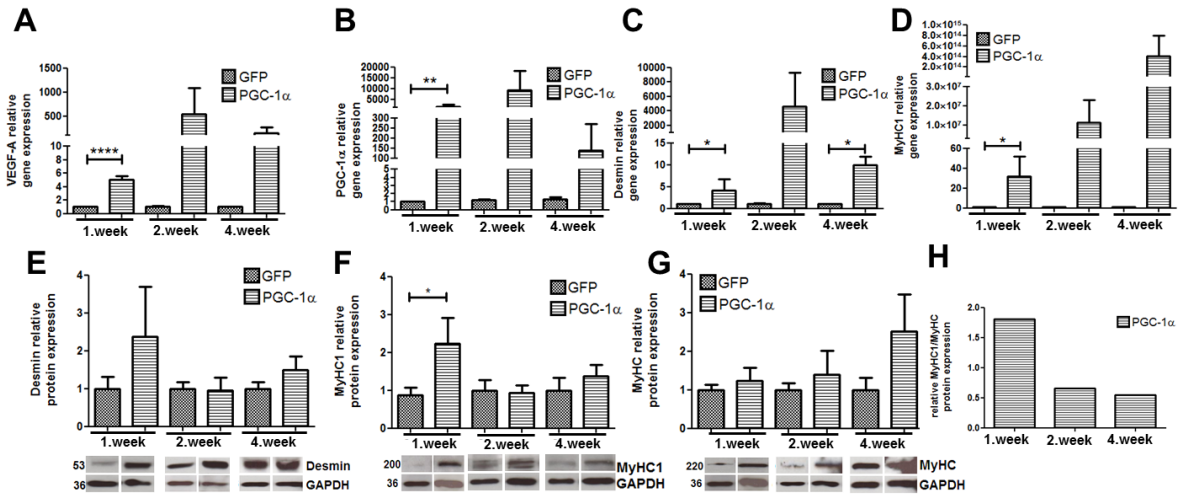

Figure 2.4-5. **Gene and protein expression in ex situ bioengineered muscle tissues, overexpressing PGC-1α**. Gradual increase of VEGF-A gene expression levels was shown by RTPCR (A). PGC-1α gene overexpression was confirmed (B). Desmin and MyHC1 gene expression levels (relative to 18S) were increased in PGC-1α overexpressing tissues (C, D). The enhanced differentiation in PGC-1α overexpressing tissues could also be shown by increased contractile protein expression levels in the corresponding bioengineered tissues (E-G). The ratio of MyHC1 to general MyHC showed an initial switch to oxidative type I fibers (H).

2.5 Discussion

Muscle tissue bioengineering has made substantial progress over the last decade, allowing us to grow functional muscle tissue (135). Nevertheless, there are still substantial limitations in size and quality of the engineered constructs. Additionally, drugs including testosterone, growth hormone, leptin, myostatin inhibitors, creatine and vitamin D have been successfully used to support muscle strength and growth (137). Yet, there are safety concerns for their long-term application and, therefore, more investigations are required in order to minimize their adverse effects. Another possible solution for rebuilding muscle tissues is cell therapy using satellite cells. The induced expression of several factors in MPCs has extensively been studied, mostly to obtain enhanced cell viability and proliferation, or to prevent apoptosis and induce angiogenesis, or to induce gap-junction formation against cardiac arrhythmias (138).

Many muscle disorders are associated with skeletal muscle inactivity and exercise is an exceptional therapeutic mediation for many disease conditions (139). Although the exact mechanisms mediating these healing effects still remain elusive, several pathways have been proposed (140). While resistance training combined with adequate nutrition remains the most effective intervention for diminishing the functional decline in muscles, there is a certain age-linked barrier to obtaining full benefits from this therapy (137).

A promising molecule controlling skeletal muscle metabolism with potential therapeutic effect has been identified (132). PGC-1α is a known and potent transcription coactivator for nuclear receptors and other transcription factors. It is expressed in skeletal muscles and is a powerful master regulator of mitochondrial biogenesis (141). Interestingly, PGC-1α has been shown to increase the expression of fiber type I fibrillar proteins by co-activating the myocyte enhancer factor 2 (Mef2) transcription factors, thereby coordinating the expression of both metabolic and contractile properties of type I myofibers (110). These findings make PGC-1α a good candidate for targeted regulation of skeletal muscle cell metabolism and plasticity in the regeneration process, and, therefore, we decided to research its applicability for the bioengineering of improved muscle tissues.

The ultimate goal in skeletal muscle tissue engineering is the construction of a functional tissue of a desired fiber type. Interested in sphincter muscle bioengineering, we aimed at improving the regenerative potential of human MPCs by inducing PGC-1α overexpression through adenoviral gene delivery. By overexpressing PGC-1α in hMPCs we targeted a major crossroad of intracellular pathways, affecting cell metabolism (mitochondrial activity upregulation) and, simultaneously, enhancing the early expression of contractile proteins (MyHC1, Desmin) and secretory factors (VEGF-A), thereby facilitating the process of skeletal

muscle bioengineering. Our data showed feasibility of viral overexpression of PGC-1α with desired phenotypic changes in the ectopic muscle but importantly without detrimental side effects on hMPC viability and differentiation.

The bioactivity of PGC-1α was confirmed by significantly enhanced expression of PGC-1α downstream targets, proving the functional efficiency of the presented construct. Some supporting evidence suggests an increased expression of mitochondrial and other metabolic genes as a plausible mechanism for rescuing a damaged muscle (139). Therefore, the demonstrated increase in PGC-1α downstream mitochondrial targets was a key milestone for further *in vitro* and *in vivo* studies.

A crucial role in the process of forming new muscle tissue is played by the capacity of myoblasts to differentiate into myotubes/myofibers and a sustained energy metabolism. Our genetically modified hMPCs showed a significantly increased fusion rate, in parallel with an enhanced energy metabolism, depicted by iCK levels and mitochondrial gene level analysis. Given the low iCK levels in myoblasts and their increase with myotube formation, our results indicate that viral overexpression of PGC-1α drives higher iCK expression, possibly due to a faster differentiation process. Moreover, elevated Desmin protein expression was detected 2 days after the adenoviral infection, showing the early appearance of sarcomeric architecture. Consistent with the observed facilitated *in vitro* differentiation, the ectopically formed skeletal muscle tissue with PGC-1α overexpression revealed myotube formation and increased expression of contractile proteins (Desmin and MyHC1) already after 1 week, indicating facilitated differentiation. Interestingly, this strong effect was reduced at later time points. However, PGC-1α modified samples expressed higher levels of general MyHC with an increase over time, when compared to GFP samples, while there was higher MyHC1 (slow twitch) protein expression at earlier time points. These data indicate a possible initial shift towards slow type fibers, which later gets reverted. Related gene-delivery studies suggest that overexpression of certain factors (e.g. VEGF) may be beneficial at the time of cell transplantation, and their transient effect may prevent the risk of malignancy formations (142, 143).

Vascularization of the bioengineered tissue is the bottle-neck of many approaches. Importantly, PGC-1α overexpressing tissues showed enhanced VEGF-A gene levels. Secretion of various effectors by the injected hMPCs may also contribute to optimization of the regenerative process (e.g. increased neovascularization) (135, 144). Moreover, PGC-1α has been demonstrated to stimulate angiogenesis in skeletal muscle by inducing the release of key factors, including VEGF, in cultured muscle cells and skeletal muscle *in vivo* (145). Furthermore, PGC-1α seems to have increased the resistance of MPCs after implantation, leading to improved cell survival at implantation and better long term survival. In line with our

in vivo observations, others have shown, that an increased VEGF release in a hypoxic environment leads to enhanced differentiation (146). This could explain the observed increase in contractile MyHC protein and myofiber formation in PGC-1α engineered tissues, when compared to the corresponding GFP samples.

The presented study does not provide information on the situation in an *in situ* model with engineered cells injected at the site of an injured muscle. Further, the use of viral gene delivery for clinical applications is still associated with several drawbacks (147). Still this model sets a significant milestone towards the possible engineering of improved muscle tissue of a desired fiber type.

3 Non-invasive Imaging and Tracking of Engineered Human Muscle Precursor Cells for Skeletal Muscle Tissue Engineering Using Positron Emission Tomography

Deana Haralampieva[1,3,4], Thomas Betzel[3], Ivana Dinulovic[2], Souzan Salemi[1], Meline Stoelting[1], Stefanie Kraemer[3], Roger Schibli[3], Tullio Sulser[1], Christoph Handschin[2], Daniel Eberli[1,4], Simon M. Ametamey[3,4]

[1]University Hospital Zurich and University of Zurich, Laboratory for Tissue Engineering and Stem Cell Therapy, Department of Urology, Frauenklinikstrasse 10, CH-8091 Zurich, Switzerland

[2]Biozentrum, Focal Area Growth and Development, University of Basel, Klingelbergstrasse 50-70, CH-4056 Basel, Switzerland

[3]ETH Zurich, Institute of Pharmaceutical Sciences, Vladimir-Prelog-Weg 4, CH-8093 Zurich, Switzerland

[4]Zurich Center for Integrative Human Physiology (ZIHP)

This chapter has been accepted for publication in the Journal of Nuclear Medicine

D. Haralampieva planed and performed the *in vitro* and *in vivo* experiments, analyzed and interpreted the data and wrote the manuscript. T. Betzel synthesized the needed radioligands and helped with the PET signal uptake evaluations. I. Dinulovic made the hD2R adenoviral construct. S. Salemi supported the proper handling of the different experiments. M. Stoelting provided preliminary data for the project. S.Kraemer helped with the data analysis and interpretation. R. Schibli and T. Sulser reviewed the manuscript. C. Handschin, D. Eberli and S. M. Ametamey supported the study conception and design, supervised the project and revised the manuscript.

3.1 Abstract

Transplantation of human muscle precursor cells (hMPCs) is envisioned for the treatment of various muscle diseases. However, a feasible non-invasive tool to monitor cell survival, migration and integration into the host tissue is still missing. **Methods**: In this study, we designed an adenoviral delivery system to genetically modify hMPCs to express a signaling-deficient form of a human dopamine D2 receptor (hD2R). The gene expression levels of the receptor were evaluated by RTPCR and infection efficiency was visualized by fluorescent microscopy. Viability, proliferation and differentiation capacity of the transduced cells were confirmed and their sustained myogenic phenotype was shown by FACS analysis and fluorescent microscopy. [^{18}F]Fallypride and [^{18}F]FMISO, two well-established PET radioligands, were successfully synthesized and evaluated for their potential to image engineered hMPCs in a mouse model. Furthermore, biodistribution studies and autoradiography were also performed to determine the extent of signal specificity. **Results**: To address the feasibility of the presented approach for tracking of hMPCs in an *in vivo* model, we first evaluated the safety of the adenoviral gene-delivery, which showed no detrimental effects on the primary human cells. Specific binding of [^{18}F]Fallypride to hD2R-hMPCs was demonstrated *in vitro*, as well as *in vivo*, by performing autoradiography, biodistribution and PET experiments, respectively. Furthermore, [^{18}F]FMISO uptake was evaluated at different time-points after cell inoculation *in vivo*, showing high signal only at the early stages. Finally, histological assessment of the harvested tissues confirmed the sustained survival of the transplanted cells at different time-points with formation of muscle tissue at the site of injection. **Conclusion**: In conclusion, we here propose a signaling-deficient human D2R as a potent reporter for *in vivo* PET tracking of hMPCs by [^{18}F]Fallypride. Or study sets a significant milestone towards potential non-invasive tracking of hMPC_hD2R cells and bioengineered muscle tissues, providing information about their exact location and metabolic read-out of their redox state.

3.2 Introduction

To date, organ transplantation is the gold standard for rescuing damaged tissues. This method comes with a number of drawbacks such as dependence on donor organs and the high morbidity of immunosuppressive therapy. Regenerative medicine using autologous stem cells may offer an alternative approach for organ and tissue replacement, overcoming the known pitfalls (148-150). Tissue engineering, one of the major components of regenerative medicine, follows the principles of cell transplantation, materials science, and engineering towards the development of biological substitutes that can restore and maintain normal function (151). Due to their regenerative capacity, muscle precursor cells (MPCs) are investigated for skeletal muscle tissue reconstruction and replacement (152). These quiescent adult stem cells reside on the periphery of muscle fibers, where they are activated after muscle injury, proliferating, differentiating into myoblasts and later fusing to form new myofibers, thereby granting sufficient progeny for repetitive tissue repair (127). The majority of MPCs are committed to the myogenic lineage and are therefore the most suitable source for muscle engineering (153). Recent preclinical studies have shown that muscle reconstruction using MPCs is a promising and feasible therapy (154), however, the fate of these cells after implantation still needs to be further investigated. In this respect, a better understanding of the engrafting process of the injected cells, their survival and metabolic changes, is critical before up-scaling to a clinical application.

Currently, these matters are addressed by histological assessment, having one major shortcoming: the invasiveness of biopsies and the destruction of the bioengineered muscle tissue. Novel non-invasive imaging technologies are therefore needed. Optimally, these imaging methods would answer many questions regarding cell fate alteration, differentiation and migration.

From a technical perspective, the chosen imaging modality should be sensitive enough to allow detection of a low number of cells and come with a high enough signal-to-background ratio to allow sufficient specificity. Additionally, the uptake of the chosen tracer should be reasonably low in non-target cells to allow high signal-to-background ratio(155, 156). Furthermore, it should not affect the specific cell morphology and allow for serial/long-term monitoring *in vivo*. An elegant way of avoiding most of the drawbacks of various imaging techniques is the utilization of a stable transfection with a reporter gene construct, which is translated into a protein interacting with an exogenous probe, resulting in a signal that can be non-invasively monitored (155-158).

Molecular imaging is an emerging field, providing essential information about heterogeneous human disorders. While bioluminescence has very poor spatial resolution and MRI lacks the high sensitivity of radionuclide-based tools, PET/CT is a system with both high resolution and high sensitivity (156). Moreover, although imaging reporter genes are available for fluorescence, bioluminescence and MRI, only radionuclide-based reporter genes are currently investigated for use in patients (159-164).

One such system is based on the imaging of dopamine 2 receptors (D2R) using positron emissions tomography (PET). Natively, the expression of D2R is largely limited to the striata nigra brain region (165). A large number of specific and high-affinity D2R PET ligands are available, some of which have found routine application in the clinic (166). Thus, the PET imaging of exogenously added hD2R in cells injected in peripheral body regions would be an attractive method to optimally track the hD2R *in vivo*. The employment of receptor-based reporter genes can be advantageous because the molecular probe does not need to cross the cell membrane for the interaction. One potential shortcoming of this approach, however, is the possible induction of undesired biological effects by gene introduction and by alteration of intracellular signalling pathways. As binding of the D2R ligand would activate G-protein-linked signalling pathway, a mutated rat receptor (D2R80A) has been reported, that uncouples ligand binding from intracellular signal transduction (167),(157). However, there are limits to the amount of signal production, as one receptor interacts with only one ligand molecule and can potentially be blocked by non-labelled endogenous ligands (155).

Skeletal muscle cells are a key target for many stem cell and gene therapy applications. With molecular PET imaging gaining increasing importance in regenerative medicine, it is high interest to study transfected MPCs as cell types that could be used to restore muscle function. In this study, we investigated the possibility of using PET/CT imaging to non-invasively monitor implanted and genetically modified hMPCs_hD2R in a mouse model. Specifically, our main aim was to study the location, level of expression and survival duration of the engineered hMPCs using hD2R as a reporter gene. The accomplishment of this goal would help to improve our understanding of the behaviour of hMPCs during *in vivo* differentiation.

3.3 Materials and Methods

3.3.1 Isolation and Expansion of hMPCs

Human muscle biopsies from the *Musculus rectus abdominis* were randomly collected with approval from the local ethics committee and after written informed consent of hospitalized patients undergoing abdominal surgery. All samples were processed according to established protocols(134). Briefly, each muscle biopsy was minced and digested with collagenase Type I 0.2% (w/v) (Sigma) and dispase 0.4% (w/v) (Gibco). The enzymatic reaction was terminated with medium containing 10% FBS. Individual fibers were then liberated by rigorous pipetting and filtered through a strainer with a pore size of 100 µm. After centrifugation the pellet was re-suspended in culture medium and the muscle fibers were transferred into 35 mm dishes coated with collagen type I (1 mg/mL) (BD). Culture medium consisted of DMEM/F12, 1% Penicillin/Streptomycin, 18% FBS, 10 ng/mL hEGF (Sigma), 1 ng/mL hbFGF (Sigma), 10 µg/mL human insulin (Sigma) and 0.4 µg/mL dexamethasone (Sigma)(134). After 24 h, the supernatant containing non-adhered hMPCs was re-plated into dishes coated with collagen type I, in order to reduce the number of contaminating fibroblasts.

3.3.2 Adenoviral Design

The AdEasy System (Stratagene (168)) was used for recombinant adenovirus construction. Briefly, we mutated phenylalanine 411 of the human D2R into alanine (F411A) to obtain a signalling-deficient human dopamine D2 receptor that still binds ligands in a normal manner but will not activate intracellular signalling upon ligand binding (169). In detail, IRAUp969E0451D vector containing hD2R (ImaGenes) and pcDNA3 plasmid containing monomer (m) RFP (Addgene) were purchased. The hD2R was subcloned into the pcDNA3.1 TOPO expressional vector (Invitrogen), which resulted in addition of C-terminal 6xHis and V5 tags. Next, the F411A pointmutation was introduced by site-directed-mutagenesis (Stratagene). The hD2R and mRFP sequences were then subcloned into the backbone of the pShuttle-CMV (cytomegalovirus) vector (Addgene), ensuring a robust, constitutive expression. The final vector thus contained hD2R and RFP sequences, both running under two separate CMV promoters. Successful cloning was validated by sequencing, while viral infection and gene expression were monitored by visualizing RFP and RTPCR, respectively. The viral titer was defined after an additional amplification step and quantified by fluorescent microscopy. The optimal multiplicity of infection (MOI) was measured by serial titrations of the viral vectors on hMPCs and simultaneous determination of RFP expressing cells by

fluorescent microscopy, cell toxicity and cell viability. Finally, the transduced cells were expanded for 2 days after infection and were subcutaneously (*s.c.*) injected into nude mice.

3.3.3 Fiber Formation Assay (FFA)

Differentiation of hMPCs into myofibers *in vitro* was performed as previously reported (fiber formation assay)(134). Briefly, hMPCs were grown to 50% confluency in culture medium and afterwards switched to differentiation medium (10% FBS) for 7-10 days until myofibers formed. The fibers were fixed with ice-cold methanol (7 min), stained with Giemsa (1:20, 45-60 min) and air-dried. Five high-power-fields (HPF, 10x) were obtained per condition and per biopsy and the results were expressed as number of fibers/HPF, number of nuclei/myofiber, and number of nuclei/HPF. The fusion rate was calculated by dividing the number of nuclei/myofiber by the number of nuclei/HPF (%). The imaging software “ImageJ for microscopy“ was used for data assessment.

3.3.4 Cell Characterization

After the expansion of hMPCs to passage 3 they were infected with the designed hD2R adenovirus and cultured for 2 days. The cells were characterized by fluorescent activated cell sorting (FACS), using the following primary antibodies: anti-Pax7 (1:100, Sigma), anti-MyoD (1:100, BD), anti-MyHC (1:1, DSHB), anti-Desmin (1:50, Sigma), anti-sarcomeric alpha-actinin (1:200, Sigma), anti-CD34 (1:100, BD) and anti-IgG Isotype control (1:100, Santa Cruise). FITC anti-mouse IgM IgG (1:200, BD) polyclonal antibody was used as secondary antibody. A total of 50’000 events were registered by BD FACS Canto flow cytometer (BD Biosciences) immediately after labeling and analysis was performed using FlowJo software v. 7.5 (Tree Star Inc.). All data are expressed as percentage of maximum (% max).

Additionally, the transduced hMPCs were cultured to 70-80% confluency, fixed with 4% PFA for 10 min at room temperature, permeabilized with 0.5% TritonX-100 (Sigma) for 7 min, blocked for 30 min (5% BSA + 0.1% TritonX-100 in PBS), and finally stained with anti-Desmin (1:50, Sigma), anti-sarcomeric α-actinin (1:200, Sigma), anti-CD34 (negative control) (1:100, BD) over night at 4 ^{o}C. After washing with PBS, the cells were incubated with FITC anti-mouse IgG IgM secondary antibody (1:500, BD) or Phalloidin (1:200, Sigma) and DAPI (1:100, Sigma) for 1 h at room temperature, washed and finally mounted (Dako). Images were acquired with Leica-Imager Type DM6000B at exposures normalized to unstained controls (secondary antibody and DAPI only).

3.3.5 Cell Viability and Proliferation

In all cases, cell numbers and viability were confirmed by trypan blue staining after trypsinization. To evaluate proliferation and viability of the infected cells at different time points, hMPCs were cultured for 6 days. The cell proliferation reagent WST-1 (Roche) was used according to manufacturer's protocol. For further confirmation of cell viability, hMPCs were stained with 10 µM CellTrace Calcein green, AM (Life Technologies) for 30 min at 37 °C. Viable cells were detected using a fluorescence microscope. All measurements were repeated at least three times and samples were analyzed in triplicates.

3.3.6 Radiosynthesis of [^{18}F]Fallypride

The synthesis of [^{18}F]Fallypride was accomplished in a one-step reaction according to a previously published procedure (170). [^{18}F]Fallypride was synthesized using an automated synthesis module. Briefly, cyclotron produced [^{18}F]fluoride was trapped on a Sep-Pak Accell Plus QMA Carbonate Plus Light cartridge (Waters) without preconditioning. The activity was eluted into the reactor by the use of a K_2CO_3/K_{222} mixture (0.33 mL H_2O, 0.77 mL MeCN, 11 mg K_{222}, 5.5 mg K_2CO_3). After azeotropic drying at 90 – 110 °C with MeCN (2×0.4 mL) under vacuum and a stream of nitrogen, the dissolved precursor (Tosyl-Fallypride, ABX Prod-No: 1550.0002, 2 mg , 3.9 µmol) in anhydrous DMSO (400 µL) was added to the dried [^{18}F]fluoride complex. The reaction was carried out at 150 °C for 20 min. After the temperature dropped below 75 °C, MeCN (0.6 mL) was added and the solution was passes through a Sep-Pak Silica Plus Light Cartridge (Waters), which was preconditioned with Et_2O (5 mL). The reaction vessel was rinsed with additional MeCN (0.5 mL) and also passed through the cartridge. The organic phase was diluted with $NaHCO_3$ solution (0.1 M, 1.5 mL) and injected on a semipreparative HPLC system (Phenomenex, Gemini, 10x250 mm, 5 µm, 110 Å), using an isocratic eluent of 55% MeCN and 45% 0.1 M $NaHCO_3$ at a flow rate of 4 mL/min. The product fraction was collected in a vessel, containing H_2O (19 mL) and the solution was transferred to a Sep-Pak tC18 Plus Light cartridge which was preconditionend with EtOH (5 mL), followed by H_2O (10 mL). The cartridge was rinsed with water for injection (8 mL) and the product was eluted with EtOH (0.5 mL) into a sterile vial, containing water for injection (9.5 mL). The radiotracer was obtained in a radiochemical purity > 95% and the specific activity ranged from 32 to 168 GBq/µmol.

3.3.7 Radiosynthesis of [^{18}F]FMISO

The radiotracer [^{18}F]FMISO was obtained in a two-step reaction in analogy to a previously published method (171). [^{18}F]FMISO was synthesized using an automated synthesis module. Briefly, cyclotron produced [^{18}F]fluoride was trapped on a Sep-Pak Accell Plus QMA

Carbonate light cartridge without preconditioning. The activity was eluted with a TBA solution (32.5 mg TBA-OH×30H_2O in 0.7 mL MeOH) into the reactor. After azeotropical drying with MeCN (2×0.4 mL) at 90 – 120 °C under vacuum and a stream of nitrogen, the dissolved precursor (NITTP, ABX Prod-No: 1400.0005, 5 mg) in a mixture of tert.-BuOH (800 µL) and MeCN (200 µL) was added and heated at 120 °C for 10 min. After the temperature dropped below 80 °C, the solvent was evaporated to a volume of 50 µL, followed by addition of HCl solution (1 M, 1 mL). The mixture was heated for 5 min at 105 °C. When the temperature dropped below 85 °C, the reaction mixture was neutralized by addition of a mixture of NaOH (1 M, 1 mL) and HPLC eluent (0.8 mL). The solution was injected onto a Whatman Partisil Magnum C18 column (500x10 mm) at a flow rate of 4 mL/min. An eluent of 0.01 M H_3PO_4/EtOH (95/5) was used. The eluting product peak was collected and per mL of product 0.25 mL 0.6 M PBS was added. Decay corrected radiochemical yield ranged from 25-37%. Radiochemical purity was higher than 95% and specific activities ranged from 34 to 190 GBq/µmol.

3.3.8 *In vitro* [^{18}F]Fallypride Uptake assay

The experiment was performed in longitudinally truncated 24-well-plates testing two AV-hD2R constructs in three concentrations (500 ng, 1 µg, 2 µg per well). Additionally, hD2R-plasmid transfection was used as a control (data not shown). Approximately 20 000 hMPCs per well were seeded and after 24 h the cells were infected with the corresponding constructs for 2 days. The modified cells were incubated with [^{18}F]Fallypride [1nM] for 15 min and scanned 26 min after start of incubation. After washing with 2x1mL ice-cold PBS the cells were imaged using VISTA eXplore, GE, Small Animal PET scanner. The scan duration was 45 min. All experiments were performed in triplicates.

3.3.9 Animal Experimentation

All animal experiments were approved by the local animal care committee. A total of 46 female, 8 week old nude mice (Charles River) were used for this study. The hMPCs were expanded to passage 3-4 for the *in vivo* experiments. Each sample contained 30x10^6 transduced hMPCs, which were gently mixed with 500 µL collagen type I carrier (final concentration: 2 mg/mL) (BD) and prepared for *s.c.* injection in the back of nude mice (135). Each animal received two bilateral *s.c.* injections (including control-collagen only injections). The engineered skeletal muscle tissues were harvested after 1, 2, and 4 weeks.

3.3.10 Tracking of Bioengineered Muscle Tissues via PET/CT Imaging

PET experiments were performed with a dedicated Small Animal PET/CT tomograph eXplore VISTA (General Electric), which uses the phoswich detector technology in a dual ring set-up (172). This system is characterized by high resolution (approximately 1 mm3), excellent sensitivity (up to 4%) and an axial field-of-view of 47 mm. For [18F]Fallypride administration, mice were restrained and injected via a lateral tail vein with 4.38-26.25 MBq (0.17-2.34 nmol) of the radioligand. For blockage experiments, Haloperidol (1mg/kg) was injected. Ten minutes after radiotracer injection, animals were anesthetized with isoflurane in an air/oxygen mixture and positioned and fixed on the bed of the camera. PET data were then acquired to yield dynamic images with sufficient count statistics. Depth of anesthesia and body temperature were monitored and controlled according to a previously published protocol (173). In addition, respiratory frequency was controlled with a 1025T monitoring system from SA Instruments (Stony Brook, NY). After the PET scan, animals recovered from anesthesia and were rescanned at a later time point with the next tracer. Raw data were reconstructed by a 2D-OSEM algorithm and the obtained image data were evaluated by visual inspection and semi-quantitative volume-of-interest (VOI) analysis using the dedicated software PMOD.

3.3.11 Biodistribution Studies

The subsequent post-mortem biodistribution assessment was performed 60 min post *i.v.* injection of [^{18}F]Fallypride. Tracer uptake in engineered muscle tissue, striatum nigra, native muscle tissue, cerebellum and injected collagen was evaluated in a gamma-counter (Cobra II Auto-gamma, Canberra Packard, Groningen, The Netherlands).

3.3.12 Autoradiography

After sacrificing the mice, the engineered and the native muscle tissues were removed and quick-frozen. Cryostat sections (20 µm) of each frozen sample were pre-incubated on ice for 12min in TRIS/HCl, 0.1% BSA, pH 7.4. Then, the slides were incubated with [^{18}F]Fallypride [0.03 nM] in the presence and absence of Haloperidol [10 µM] as blocker for 60 min. Thereafter, the slides were washed with TRIS/HCl 0.1% BSA for 5 min at 4 °C, followed by 2 x 3 min in TRIS/HCl at 4 °C and 2 x 5 s in water at 4 °C. After air-drying the tissue slices were exposed to phosphorimager plates which were analysed with a Fuji BAS-5000 phosphorimager. This allowed direct comparison of specific and unspecific [^{18}F]Fallypride binding in the various tissues.

3.3.13 Histological Assessment

The harvested engineered muscle tissues were embedded in cryo-preservative (OCT embedding medium, Cell Path) immediately after isolation. Cryostat sections were prepared (10 µm) and further processed. Haematoxylin and eosin (H&E) (Sigma) staining was performed according to the manufacturer's protocol.

3.3.14 Reverse Transcriptase Polymerase Chain Reaction (RTPCR)

The infected cells were cultured for 2 days and harvested for analysis of hD2R gene expression. For gene analysis of tissue, the harvested tissues were pulverized in liquid nitrogen and suspended in RNA lysis buffer. Total RNA was isolated for both, cells and tissues, using the SV Total RNA Isolation System kit (Promega) according to the manufacturer's protocol, which includes DNase digestion. RNA was reverse transcribed with random primers (High-Capacity cDNA reverse transcription, Life Technologies). Pre-designed primers for hD2R (Hs00241436_m1) and hVEGF-A (Hs00900055_m1) were purchased from Life Technologies. 18S rRNA (4319413E, Life Technologies) was used to normalize cDNA concentrations. For quantification, the expression of each gene was normalized to the 18S expression in the corresponding sample. The entire experiment was repeated at least three times and samples were analyzed in triplicates.

3.3.15 Gel Electrophoresis and Immunoblotting

In summary, tissues were pulverized in liquid nitrogen with a mortar/pestle and suspended in lysis buffer supplemented with a protease inhibitor cocktail (Sigma). Samples were then centrifuged for 20 min at 13,000 rpm, and the supernatant was collected for protein determination. The total protein was measured with the BCA Protein Assay Kit (Thermo Scientific) and protein lysate (30-50 µg) was loaded on a 10% or 12% gel (Bio-Rad). Western blot was performed according to the manufacturer's protocol. After the separated proteins were electro-transferred onto PVDF membrane (Immobilion-P; Millipore), the latter was incubated with a primary antibody at 4 °C overnight in TBS, 0.1% Tween-20 and 5% non-fat dry milk. The primary antibodies used were anti-MyHC (1:5, DSHB), anti-sarcomeric α-actinin (1:2000, Sigma), anti-vWf (1:500, Sigma), anti-hD2R (1:200, Santa Cruz) and anti-GAPDH (1:2500, Sigma). Finally, the membranes were washed in TBS with 0.1% Tween-20 for 30 min and incubated with the appropriate HRP-conjugated secondary antibody (1:500, Amersham Pharmacia Biotech) for 1 h. The signals were detected by the ECL method (ECL-Kit, Amersham). Data were analyzed by Image Studio Lite (Li-Cor) software and represented as protein expression relative to GAPDH.

3.3.16 Statistics

For statistical analysis IBM SPSS v22.0 (SPSS Inc,) was used and graphs were drawn with GraphPad Prism v5.04 (GraphPad Software, Inc.). All data were analysed by Student's *t*-tests or one-way ANOVA with Bonferroni or LSD post-hoc analysis ($p<0.05$ was considered significant). All presented data are expressed as means with corresponding standard error of the mean (±SEM).

3.4 Results

3.4.1 Viability, Proliferation and Differentiation Rates of Genetically Modified hMPC_hD2R

The adenoviral construct containing hD2R (F411A) was generated and amplified for further use in hMPCs. Non-toxicity of the viral infection was visualized by a cell viability assay (CaAM) (Fig. 3.4-1A, green), where no significant differences between WT and hD2R-infected cells were detected. The transduction efficiency of ~25% infected cells was confirmed by fluorescent imaging, as the designed construct contained a red fluorophore, expressed under a separate CMV promoter (Fig. 3.4-1.B, red). This construct allowed assessment of cell transduction efficiency prior to transplantation. Using a fiber formation assay (FFA), we evaluated the capability of hMPCs to form myofibers *in vitro* (Fig. 3.4-1C). Comparison between WT and hD2R-overexpressing cells did not reveal any significant difference in the number of nuclei per fiber (Fig. 3.4-1D, p=0.8629, WT: 8.325±0.6818, n=83; hD2R: 8.184±0.4635, n=87), number of nuclei per HPF (Fig. 3.4-1E, WT: 230.6±14.34, n=10; hD2R: 216.9±10.71, n=10, p=0.4539) and the number of fibers per HPF (Fig. 3.4-1F, WT: 8.3±0.8699, n=10; hD2R: 8.4±0.5812, n=10, p=0.9249). The calculated overall fusion did not differ between infected and WT cells either (Fig. 3.4-1G, WT: 30.95±3.289, n=10; hD2R: 32.40±3.085, n=10, p=0.7512). Successful transduction was also confirmed by hD2R gene expression levels in RTPCR (Fig. 3.4-1H, n=3x3, p=0.005). Furthermore, the proliferation capacity of the WT and hD2R-overexpressing hMPCs was determined by a cell proliferation assay (WST-1) over 3 days culturing following transduction, showing no significant variations between the different groups (Fig. 3.4-1 I, WT: 2.2173±0.364, n=6; hD2R: 2.0843±0314, n=6, p=0.787 at 3 days).

3.4.2 FACS and ICC Analysis of hMPC_hD2R

After confirming the stable viability, proliferation and differentiation capacity of the infected hMPCs, we further analyzed their phenotype. Both WT and infected cells were tested for expression of well-known protein markers for characterization of activated hMPCs (126). Initially, the cells were analyzed by FACS (Fig. 3.4-2A), and in parallel by immunocytochemistry (Fig. 3.4-2B) 2 days after infection, revealing a sustained muscle phenotype without any significant alterations between the groups. These results show that cell viability and differentiation remained unaffected by viral infection, and that myogenic marker protein expression was sustained.

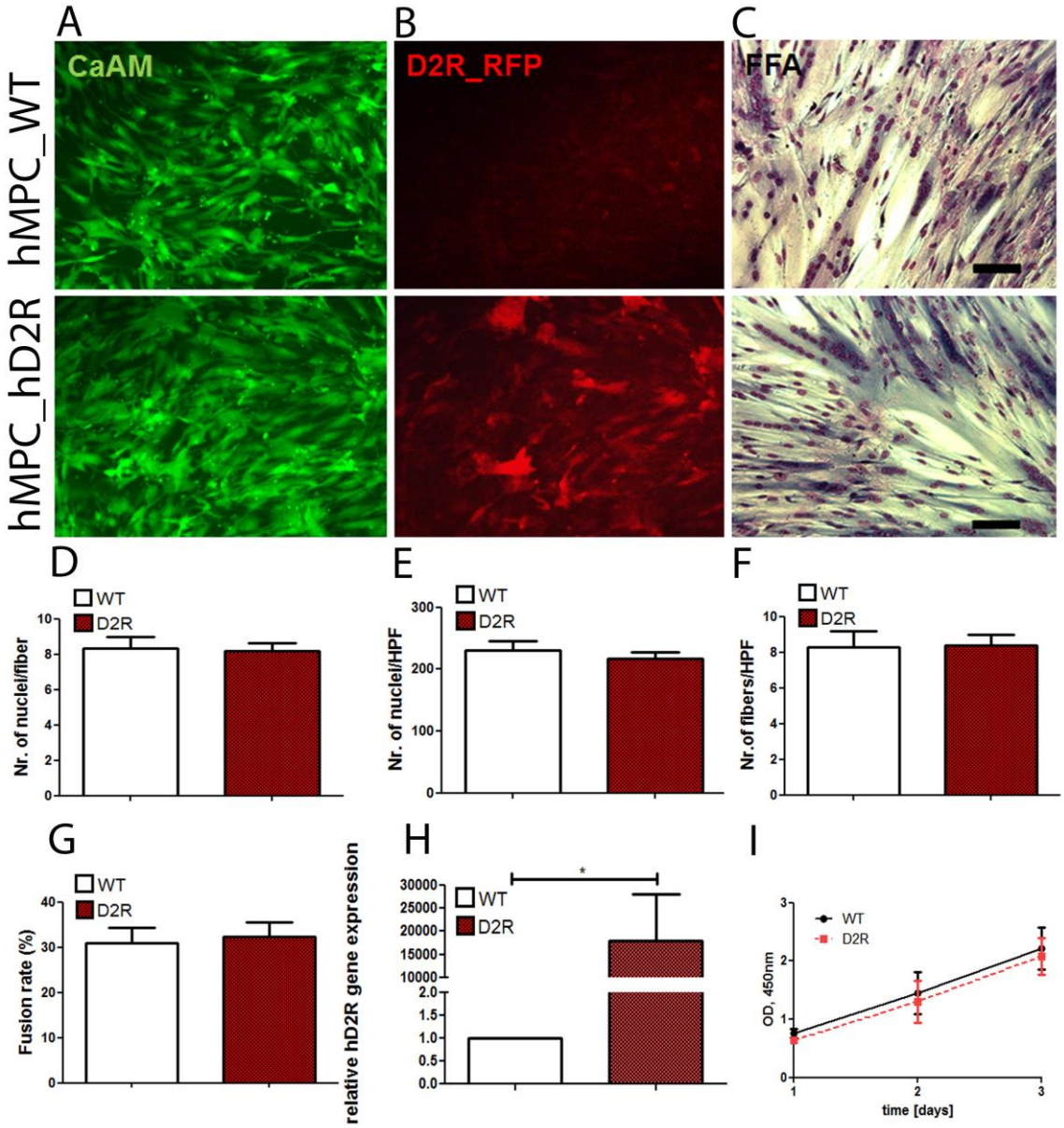

Figure 3.4-1. **hD2R adenoviral infection did not show adverse effects on hMPC.** The adenoviral transduction of hMPCs with hD2R (hMPC_hD2R) did not affect the cell viability, as shown by CaAM assay (A, green). Transduction efficiency was shown by fluorescence microscopy (B, red). The ability to form fibers (FFA) was also not affected by the viral infection (C). The number of nuclei per fiber (D), number of nuclei per HPF (H), number of fibers per HPF (F) and the resulting fusion rate (G) remained unaffected after transduction. The hD2R gene expression was evaluated by RTPCR (H). Proliferation rate also did not differ between the WT non-infected cells and the infected hMPCs (I). All measurements were performed in duplicates originating from at least 3 different human biopsies. (Student's *t*-test, *p<0.05). CaAM: calcein AM; RFP: red fluorescent protein; FFA: fiber formation assay; WT: wild type; HPF: high-power field; RTPCR: reverse transcription polymerase chain reaction

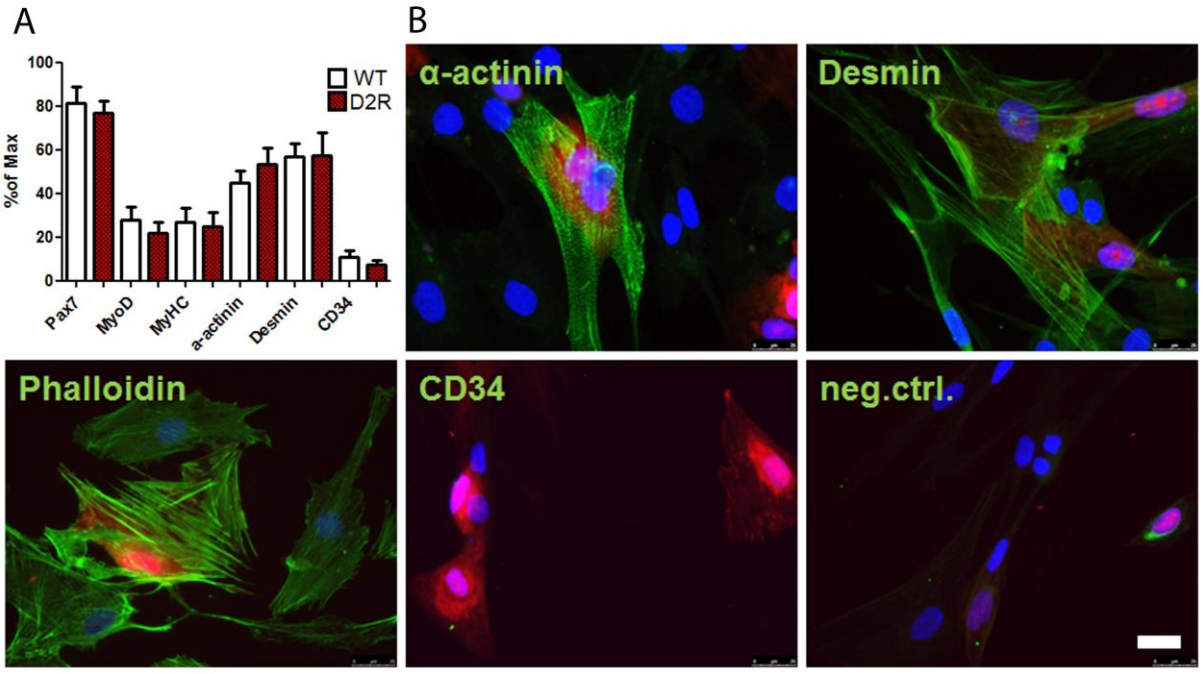

Figure 3.4-2. **Adenoviral infection with hD2R did not change the well-defined hMPC phenotype.** The hMPCs were analyzed by flow cytometry for expression of various muscle precursor cells marker proteins (A). The expression of typical muscle markers (FITC-green) in the cells expressing hD2R (red) was further confirmed by immunocytochemistry. Nuclei were stained with DAPI (blue) (B). Scale bar: 25 µm. (Student's *t*-test, *p<0.05, n=4 biopsies).

3.4.3 *In Vitro* PET/CT Imaging of hMPC_hD2R Using [^{18}F]Fallypride

Before each experiment, the infection efficiency was assessed by fluorescent microscopy and positive cells were further processed for *in vitro* or *in vivo* studies. Initially, the capacity of the transduced hMPCs_hD2R to efficiently bind [^{18}F]Fallypride was evaluated *in vitro*. When using the designed adenovirus, testing 3 different concentrations of viral particles for tracer uptake, we observed a high binding affinity (Fig. 3.4-3A). As expected, the cells infected with the highest non-toxic concentration showed the highest detectable PET signal (first row, 10x) and were thus used for further experiments. These data confirm the efficiency of the presented hD2R adenoviral construct for genetic modification of hMPCs.

3.4.4 *In Vivo* PET/CT Imaging of hMPC_hD2R Using [^{18}F]Fallypride

Encouraged by our *in vitro* results, we further evaluated the capability of transduced hMPCs to specifically bind [^{18}F]Fallypride in an established *ex situ* model for skeletal muscle tissue formation *in vivo*. hMPCs injected subcutaneously in the hip region of animals led to a high background activity of organs which hindered the quantification and detection of the signal (data not shown). Changing the injection site to the shoulder region resulted in an increased signal-to-background ratio. The hMPC_hD2R showed high standardized uptake value (SUV) after 1 week (SUV: 0.259±0.019, n=8). This signal decreased after two weeks (SUV: 0.169±0.019, n=8, p=0.005) and no significant difference to background was observed after 4 weeks (SUV: 0.134±0.014, n=6, p<0.0001) (Fig. 3.4-3B and C). Animals injected with collagen only did not show a significant radiotracer accumulation at any time (SUV: 0.115±0.011, n=10). Cerebellum brain region was used as negative control, showing negligible non-specific uptake (SUV: 0.124±0.006, n=16). This was confirmed by volume of interest (VOI) analysis, where significantly higher signal-to-background ratio of at least 2.08 at the earliest time was observed (Fig. 3.4-3 C). Biodistribution assessment also showed a significant decrease in tracer uptake in the engineered tissues over time (Fig. 3.4-3 D, n=4-16 per time point). Specificity of the signal was then demonstrated in *in vivo* PET studies using haloperidol as D2R blocking agent; the striatum region was visualized as a positive control (Fig. 3.4-3 E and F). Additionally, specificity of radioligand binding was also demonstrated in autoradiography studies, whereby hD2R-expressing tissues (including native controls) showed a reduction of radioligand uptake after incubation with haloperidol (Fig. 3.4-3 G), confirming the *in vivo* data.

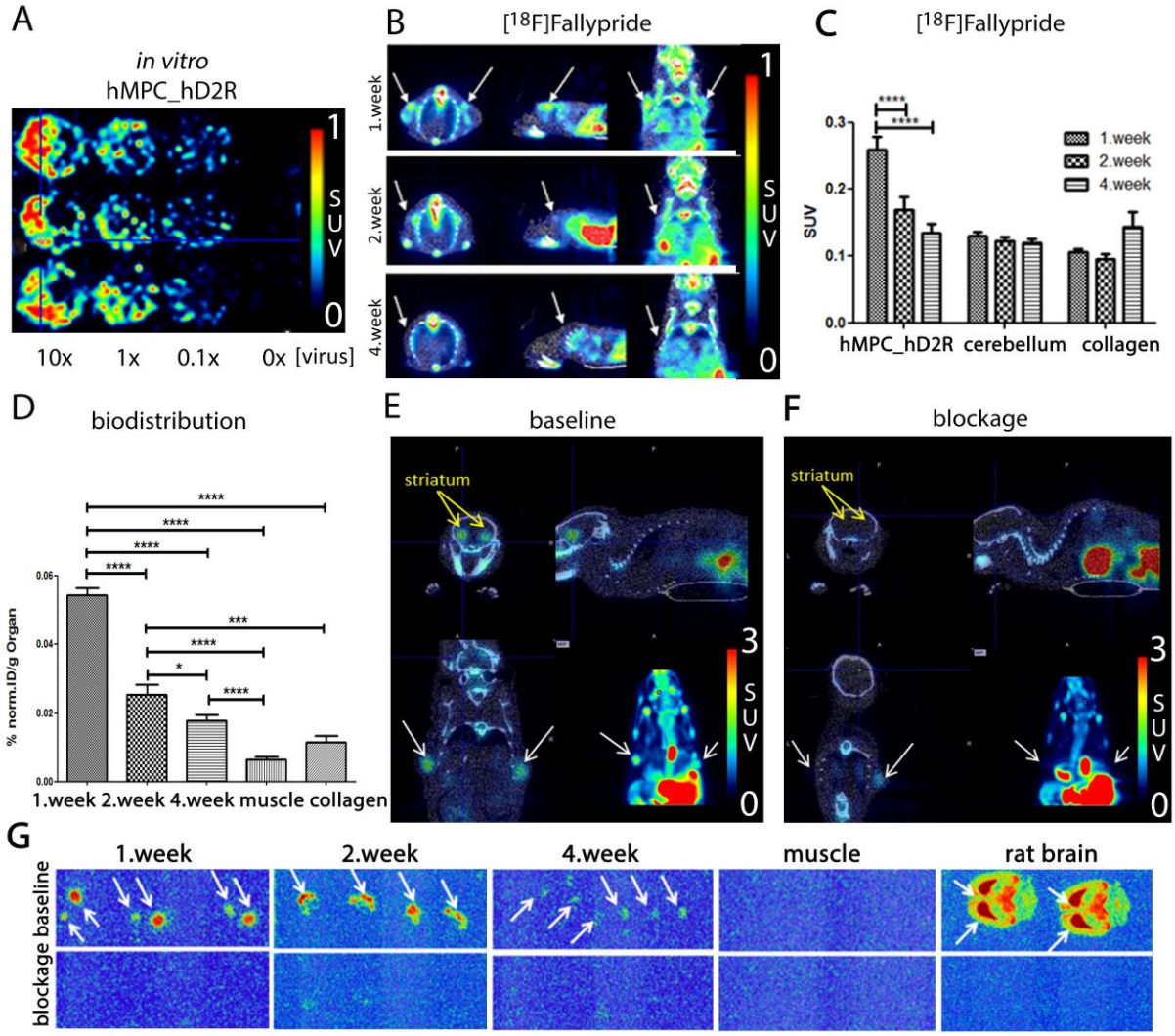

Figure 3.4-3. **Tracking of hMPCs and engineered muscle tissue via PET/CT using [^{18}F]Fallypride *in vitro* and *in vivo*.** [^{18}F]Fallypride uptake in hMPC_hD2R was detected at different adenoviral hD2R transduction levels (A). *In vivo* PET/CT imaging visualized the specific tracer uptake in the bioengineered tissues over time (B). VOI analysis illustrated the gradual decrease in signal after 1 week (C, n=6-8). Significant enhancement of [^{18}F]Fallypride uptake in engineered hMPC_hD2R tissue, compared to collagen and control muscle was observed in a biodistribution study (D, n=4-16). Tracer specificity was evaluated after blockage experiment with Haloperidol (E, F). Autoradiography of [^{18}F]Fallypride uptake on hMPC_hD2R cryosections of engineered muscle tissues showed specific tracer binding (G, lane 1). Blockage was performed with Haloperidol (lane 2) and mouse muscle and rat brain sections were used as negative and positive controls, respectively (G). Images were averaged from 60 – 120 min. Arrows indicate site of hMPCs injection. (one-way ANOVA with Bonferroni post-hoc analysis, *p<0.05), SUV: standard uptake value, VOI: volume of interest

3.4.5 PET Imaging of Hypoxia Using [^{18}F]FMISO during Formation of Bioengineered Skeletal Muscle Tissue

After successful tracking of the injected hMPC_hD2R, we were further interested in studying the oxygenation status of the cells after implantation. To address this we utilized [^{18}F]FMISO, a PET radiotracer for visualizing hypoxic regions. One week after cell inoculation, a relatively high [^{18}F]FMISO uptake was observed which decreased at later time points (Fig. 3.4-4 A). VOI analysis (Fig. 3.4-4 B) of the first week samples (SUV: 0.315±0.02, n=8) showed a mean signal change ratio of 1.6, compared to later time points (2 weeks: SUV: 0.189±0.019, n=8; 4 weeks: SUV: 0.205±0.009, n=6) and negative controls (cerebellum: SUV: 0.206±0.017, n=16; collagen: SUV: 0.251±0.003, n=10).

3.4.6 Histological Assessment, Gene and Protein Analysis of the Harvested Tissues

The relative protein expression of typical skeletal muscle protein markers (sarcomeric α-actinin, MyHC), vWf and hD2R were evaluated after tissue harvest by Western Blot (Fig. 3.4-4 C). *Tibialis anterior* (TA) and *striatum nigra* (SN) were use as controls. The protein expression levels of sarcomeric markers gradually increase in the bioengineered tissue samples (MyHC: 0.4211±0.033, n=4 (1.week); 2.1915±0.407, n=6 (2.week); 3.0734±0.72, n=8 (4.week), p=0.012, respectively; α-actinin: 0.4065±0.111, n=4 (1.week); 0.6734±0.113, n=6 (2.week); 1.2696±0.315, n=8 (1.week), p=0.043, respectively), corresponding to the expected timeline of muscle fiber formation (Fig. 3.4-4 D and E). The relative hD2R protein expression decreased steadily over time (2.4072±0.608, n=3 (1.week); 1.5881±0.25, n=6 (2.week); 1.0394±0.294, n=12 (4.week), p=0.031, respectively) (Fig. 3.4-4 F), concomitant with the observed decrease of [^{18}F]Fallypride uptake (Fig. 3.4-3 A). The decrease in [^{18}F]FMISO uptake over time coincided with an increase in vWf protein levels (endothelial cell marker, n=4) (Fig. 3.4-4 G), as well as with a rising VEGF-A gene expression (Fig. 4 H, n=9) in the bioengineered muscle tissues. Although hD2R protein levels were decreasing over time, the corresponding gene expression levels were increased (Fig. 3.4-4 I). The gradual decrease in size due to collagen remodeling and myofiber formation has previously been reported (135) (Fig. 3.4-4 J). Histological analysis revealed successful myofiber formation in the harvested tissues and could illustrate the individual cells of the samples at week 1 and the myotube formation at week 2 and 4 (Fig. 3.4-4 K).

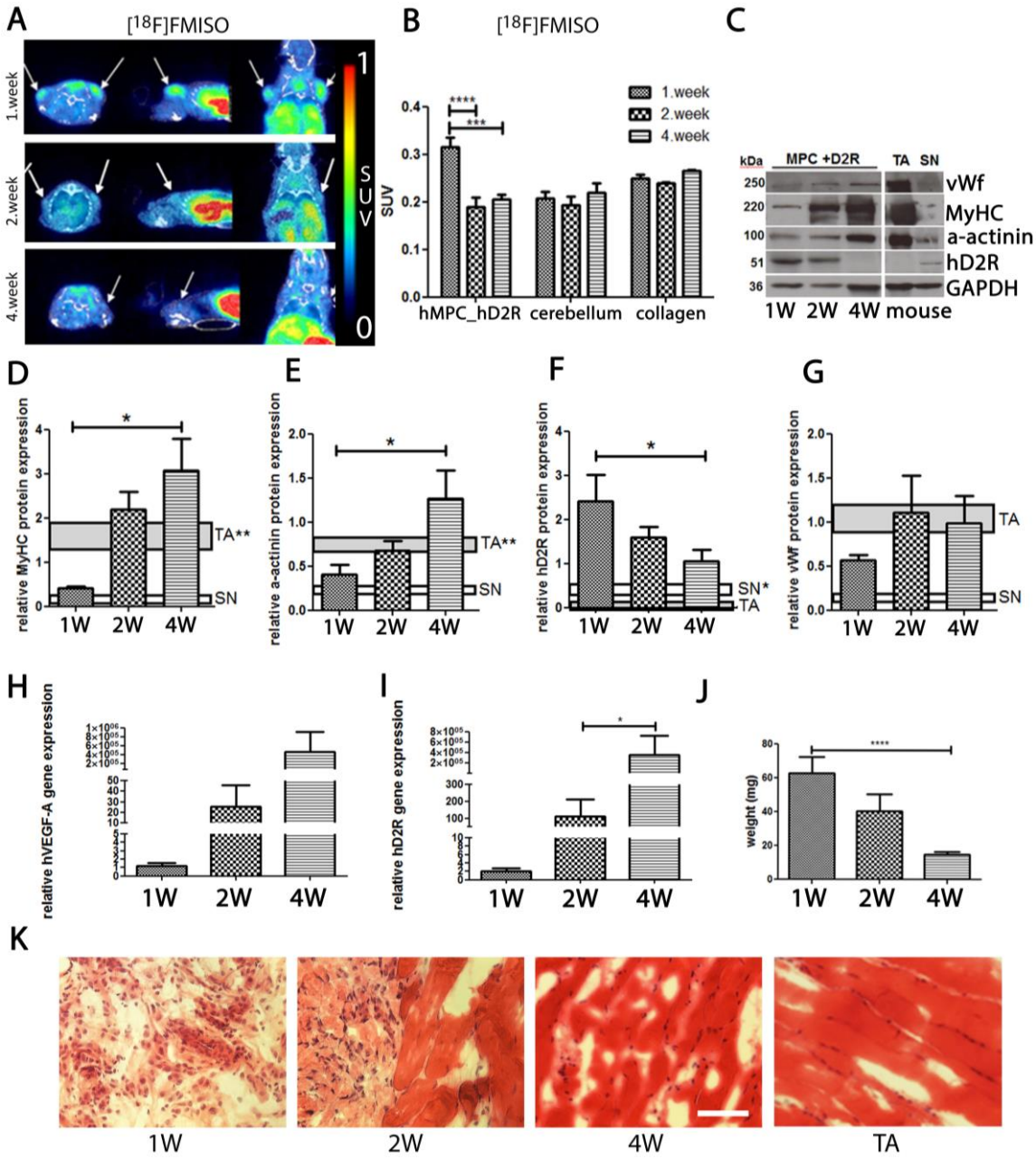

Figure 3.4-4. **Hypoxia PET/CT monitoring with [^{18}F]FMISO during formation of bioengineered muscle tissues**. The redox state of the forming tissues was illustrated with [^{18}F]FMISO [injected activity: 0.49-5.86nmol, 14.86-35.83MBq] (A) and VOIs signal was calculated for 3 different time points (B). The ex situ muscle tissues formed from 30 million genetically modified hMPCs were examined 1, 2 and 4 weeks after the injections. Protein expression levels were evaluated by Western Blot (C). MyHC (D), sarcomeric α-actinin (E), hD2R (F) and vWf (G) expression changes were visualized graphically. RTPCR analysis revealed increased VEGF-A gene expression levels over time (H). Relative hD2R gene levels were analysed by RTPCR (I). Harvested tissues decreased in weight over time (J). Histology of cryofrozen sections (H&E staining) revealed increasing fiber formation capacity over time (K). Tibialis anterior (TA) was used as a control. Images were averaged from 90 – 110 min. Arrows indicate sites of hMPCs injections. Scale bar: 100 µm (one-way ANOVA with Bonferroni or LSD post-hoc analysis, *p<0.05)

3.5 Discussion

Transplantation of MPCs has been considered as treatment option for genetic and acquired muscle disorders (135, 174, 175) and provides a prospect to reestablish damaged muscle function in patients with muscle degeneration (95, 115, 176, 177). Various research groups have been able to demonstrate the formation of muscle tissue after cellular inoculation (178). However, long-term non-invasive tracking of bioengineered muscle tissue has not been addressed so far. Therefore we sought to apply novel imaging technologies that would allow us to follow the location and oxygenation state of the implanted cells.

Molecular imaging is an emerging field, providing essential information about heterogeneous human disorders. While bioluminescence has very poor spatial resolution and MRI lacks the high sensitivity of radionuclide-based tools, PET/CT is a system with both high resolution and high sensitivity (156). Moreover, although imaging reporter genes are available for fluorescence, bioluminescence and MRI, only radionuclide-based reporter genes are currently investigated for use in patients (159-164).

Monitoring of gene therapy by PET has made enormous advances in the last years (179). Improvements in detector technologies and evolving refinements in the chemistry of molecular probe development are bringing new possibilities to non-invasive imaging. Radionuclide imaging can be widely used to characterize receptor/transporter status, enzyme activity, and biodistribution of various radiolabeled substrates (180). For these reasons, it has made the most significant progress for imaging gene therapy by monitoring gene delivery and identifying novel therapeutic strategies. Along with these developments, the recent expansion in genetic engineering is generating vectors with more robust gene transfer efficiency, bicistronic/bidirectional molecular vectors and tissue-specific amplification capacities (181).

The need to develop a system combining the use of well-established PET probes and the engineering of a novel vector for expression of the human D2R in human MPCs, has prompted our research towards non-invasive visualization of a cell therapy for application in skeletal muscle bioengineering. The generation of a vector coding for a signaling-deficient hD2R was an important milestone, as redundant cell-signaling is a major issue in gene therapies. The successful adenoviral delivery of the mutated hD2R gene into hMPCs was the next step towards clinical application of this method (157, 182). However, a more elegant way of human gene delivery, that does not employ viral particles would be ideal for clinical use.

In this study, we describe a method for metabolic imaging and tracking of hMPCs using PET/CT, thereby illustrating their exact position and the oxygenation state of the newly formed skeletal muscle tissue over time. The results of our studies indicated that: 1) the signaling-deficient hD2R could be efficiently introduced into primary hMPCs, 2) no detrimental effects on cell viability and differentiation were detected, 3) myogenic marker gene expression was unaltered, 4) the receptor was traceable with high specificity using [^{18}F]Fallypride both in cells *in vitro* as well as after injection *in vivo* and 5) receptor expression in the engineered tissues could be validated by autoradiography. We found that the capacity to track the hD2R_hMPCs is excellent in the first week and declines later on. Interestingly, while mRNA expression of hD2R remained high, its protein levels steadily declined. This indicates that the ectopically expressed hD2R is either post translationally modified and/or internalized upon constitutive expression and ultimately degraded during the process of final differentiation to myofibers. Further investigations of the exact molecular mechanism underlying hD2R degradation are needed in order to design alternative strategies that allow long-term, non-invasive tracking of bioengineered muscle tissue by PET/CT. Our data showed that by using a high-affinity PET ligand and a mutated hD2R we were able to provide important information on the localization, survival and metabolic features for the early phase after cell injection.

One essential drawback in tissue engineering is the limited size of the constructs due to restricted availability of oxygen and diffusion of nutrients. Any engineered tissue larger than 0.3 cm^3 requires rapid vascularization to guarantee survival of the cells located within the core of the construct. Vascularization of the bioengineered tissue represents the bottle-neck of many approaches. Hypoxia, which is inversely proportional to the degree of vascularization, can be analysed by invasive and non-invasive methods in tissues. The oxygenation status of cells and tissues can be determined by invasive pO2-measurements using polarographic needle electrodes or with fiber-optic probes (183-185). Non-invasive methods include the use of bio-reductive chemical markers, such as 2-nitroimidazoles (186). They form adducts under hypoxic conditions and are irreversibly bound in hypoxic cells. Several markers (EF5, NITTP, misonidazole) are available for preclinical analysis. They can be used as bio-reductive markers detectable with (immuno-) histochemical techniques. [^{18}F]FMISO is the most widely used PET radioligand for imaging hypoxia in humans (187-189).

A general problem in tissue engineering approaches is the increased oxygen demand and lack of initial vascularization during the early phases of tissue formation, leading to central necrosis (190). In our study, using [^{18}F]FMISO, we detected metabolically active bioengineered tissues with low oxygen levels, i.e. where reductive reactions dominate due to

low oxygen supply or high oxygen consumption, typical for the early stages of cell-to-myofiber formation. It has been shown that the level of oxygenation is influenced by the degree of vascularization and by the metabolic consumption of oxygen by the engineered tissue (176). Concomitant with our *in vivo* observations, an increased VEGF release in a hypoxic environment has been shown to lead to enhanced differentiation(146). Thus, additional imaging of the bioengineered muscle with PET radiotracer targeting neo-vascularization would give supplementary information. The decrease of [^{18}F]FMISO accumulation after the first week would suggest that the oxygen supply in that area has normalized. Histological analysis confirmed the cell-to-myofiber transition, correlating with normalized vascularization levels. In line with these observations, using [^{18}F]FMISO for hypoxia imaging of bioengineered constructs seems to be a feasible method. Moreover, this PET radiotracer would be a valuable tool for monitoring the changes in the hypoxic state of tissues, where neo-vascularization can be targeted by gene-therapy approaches.

3.6 Conclusion

Knowledge of the fate of the inoculated primary hMPCs is a prerequisite for the future clinical implementation of this cell therapy. To-date, most of the knowledge regarding survival, viability, localization and metabolism of the implanted cells is derived from pre-clinical models, where biopsy of the newly-built tissue/organ is the widely applied method for obtaining information about the outcome of the studied cell therapy (94). However, due to its invasiveness, this approach is not applicable for use in patients. Combining the recent developments in designing robust vectors and novel, highly-specific PET imaging probes, we were able to address the latter drawback and to offer an elegant solution, obviating the need for a destructive tissue biopsy. Our approach sets a significant milestone towards the possible non-invasive tracking of the genetically modified cells and engineered skeletal muscle tissues, providing information on their localization and metabolic read-out of their redox state.

4 Injected Human Muscle Precursor Cells Overexpressing PGC-1α Enhance Functional Muscle Regeneration after Trauma

Deana Haralampieva[1,3,4], Souzan Salemi[1], Thomas Betzel[3], Ivana Dinulovic[2], Stefanie Kraemer[3], Roger Schibli[3], Tullio Sulser[1], Christoph Handschin[2], Simon M. Ametamey[3,4], Daniel Eberli[1,4]

[1]University Hospital Zürich and University of Zürich, Laboratory for Tissue Engineering and Stem Cell Therapy, Department of Urology, Frauenklinikstrasse 10, CH-8091 Zürich, Switzerland

[2]Biozentrum, Focal Area Growth and Development, University of Basel, Klingelbergstrasse 50-70, CH-4056 Basel, Switzerland

[3]ETH Zürich, Institute for Pharmaceutical Sciences, Vladimir-Prelog-Weg 1-5/10, CH-8093 Zürich, Switzerland

[4]Zürich Center for Integrative Human Physiology (ZIHP)

This chapter will be submitted to the Journal of Tissue Enginnering Part A

D. Haralampieva planed and performed the *in vitro* and *in vivo* experiments, analyzed and interpreted the data and wrote the manuscript. S. Salemi supported the proper handling of the experiments . T. Betzel synthesized the needed radioligands and helped with the PET signal uptake evaluations. I. Dinulovic made the hD2R, hPGC-1α and GFP adenoviral constructs. S.Kraemer helped with the troubleshooting, data analysis and interpretation. R. Schibli and T. Sulser reviewed the manuscript. C. Handschin, S. M. Ametamey and D. Eberli supported the study conception and design, supervised the project and revised the manuscript.

4.1 Abstract

Muscle precursor cells (MPCs) are capable of muscle fiber reconstruction and their transplantation into damaged tissues is envisioned for the treatment of many muscle diseases. Even though many groups demonstrated the formation of new muscle tissue after injection, the capacity of MPCs to heal muscle damages in long-term is still limited. Therefore, the first goal of our project was to optimize the functional regenerative potential of hMPC by genetic modification to overexpress the peroxisome proliferator-activated receptor gamma coactivator alpha (PGC-1α), which is a key regulator of exercise-mediated adaptation. Moreover, we aimed at establishing a feasible methodology for non-invasive visualization of the implanted cells and their microenvironment in a muscle crush injury model using positron emission tomography (PET). The regenerating muscles overexpressing PGC-1α showed enhanced expression of markers, associated with myogenesis (α-actinin, myosin heavy chain 1 and 2, Desmin), vascularization (VEGF), as well as neuronal (ACHE) and mitochondrial (COXIV) activity. In line with these results, the muscles injected with hPGC-1α_hMPCs produced a significantly increased contractile force one-to-three weeks after injury. PET imaging showed distinct differences in the signal of the used radiotracers ([^{18}F]Fallypride, [^{11}C]Raclopride (both targeting dopamine 2 receptors (D2R)), [^{64}Cu]NODAGA-RGD (targeting neo-vascularization)) between injected GFP-infected control hMPCs and hMPCs_hD2R_hPGC-1α. After harvesting the regenerating muscles at different time points, we found that inflammation levels (macrophage accumulation and TNF-α secretion) were associated with the amount of radiotracer uptake, with a significantly lower uptake in the PGC-1α overexpressing samples. In summary, we were able to facilitate early functional muscle tissue regeneration, thereby introducing a novel approach to further improve skeletal muscle tissue engineering by cell therapy. Besides successful tracking of the injected cells in muscle crush injuries, we were able to show that in areas with high inflammation the specificity of the radioligands is significantly reduced, therefore, addressing a possible bottle-neck of neo-vascularization PET imaging.

4.2 Introduction

A promising treatment option for various muscle-related diseases is the use of autologous stem cells for restoration of damaged muscle fibers. Muscle precursor cells (MPCs) represent the cell population, that has been shown to be indispensable for skeletal muscle regeneration (101). Due to their potential to differentiate into myoblasts and the ability to later form new contractile myofibers, MPCs are being investigated for muscle tissue engineering and reconstruction in the treatment of a variety of muscle diseases (128, 129, 191). Still, two main concerns about their successful and safe clinical application are unsolved: the volumetric loss of the bioengineered tissues over time and the missing tools for non-invasive imaging of the fate of the implanted cells.

A major shortcoming of the implantation of hMPCs is the decreased growth capacity in the aged population (95, 130, 131). This challenge for autologous cell therapy may be addressed by exercise and/or therapeutic regulation of gene expression, which enhances the ability of MPCs to restore muscle fibers. Reduced physical activity is linked to many chronic diseases. The understanding of the molecular mechanisms behind regeneration of lost/impaired muscle tissue is vital for the development of proper treatment strategies. One key player in the regulation of important exercise-mediated adaptations and of neuromuscular activity of skeletal muscles is the transcriptional coactivator peroxisome proliferator-activated receptor (PPAR) γ coactivator 1α (PGC-1α) (103, 132). Its expression in muscle tissue is proportional to the amount of exercise and has been shown to counteract atrophy (104). Atrophy is a major limitation hindering skeletal muscle tissue bioengineering. PGC-1α plays an essential role in the regulation of cellular differentiation, development and metabolism (carbohydrate, lipid, protein) of higher organisms (104, 105). PGC-1α is further regulating the mitochondrial biogenesis and is adapting the oxidative state in muscles. In skeletal muscle, PGC-1α is abundant and particularly enriched in slow-twitch, oxidative muscle fibers, containing a large number of mitochondria. It has been shown, that increased levels of PGC-1α can promote a shift in the fiber composition toward high-endurance muscle fibers (110) (see Chapter 2). Furthermore, this muscle phenotype is characterized by pronounced tissue vascularization (116), increased myoglobin levels and enhanced import of glucose, lipids and lactate (133). In addition, PGC-1α tightly links muscle and nerve by regulating neuromuscular junction genes and by promoting clustering of acetylcholine receptors (ACHR) at the motor end plate (114). Similar changes are observed in adaptation to exercise, a process also mediated by PGC-1α. It has been proposed, that this protein controls muscle plasticity and suppresses a broad inflammatory response (139). There is further evidence suggesting that oxidative

metabolism and inflammation counteract each other in muscle tissue, outlining the central function of PGC-1 α in muscle recovery and emphasizing the possibilities that PGC-1α opens up for clinical applications (111) and novel muscle tissue engineering approaches (88).

Besides the volumetric loss of bioengineered tissues, another shortcoming in the field is the missing tools for non-invasive imaging of this cell therapy. Research towards the non-invasive imaging of autologous stem cell therapies is of high importance as both repeated biopsy and the access to many organs are not clinically feasible in many cases. Several modalities are being investigated for their applicability in cell tracking and cell metabolism read-outs (192). While MRI has lower sensitivity compared to radionuclide-based tools and bioluminescence has poor spatial resolution, PET/CT is a system with both high sensitivity and resolution (156). Additionally, although imaging reporter genes are available for fluorescence, bioluminescence and MRI, only radionuclide-based reporter genes are currently investigated for use in patients (159-164). In our previous work, we developed a feasible method for *in vivo* tracking of subcutaneously injected hMPCs using [^{18}F]Fallypride, a well-established dopamine 2 receptor (hD2R) PET ligand (see Chapter 3). After the successful generation of adenoviruses for overexpression of a signalling-deficient hD2R in human MPCs, we were able to establish an *ex situ* model for imaging of bioengineered muscle tissue (see Chapter 3). This encouraged us to concentrate our further investigations towards the applicability of these methods in an *in situ* model during skeletal muscle regeneration.

In this regard, we aimed at examining the influence of genetically modified PGC-1α overexpressing human MPCs, injected in a skeletal muscle after crush-injury, specifically investigating the effect on tissue regeneration and muscle contractility. Moreover, we used a method for non-invasive PET tracking by ectopic hD2R expression in the implanted cells (see Chapter 3) and visualization of the neo-vascularization in the regenerating muscle tissue. We hypothesize that by enhancing the PGC-1α expression in hMPCs, we can improve the regeneration capacity and contractility of the injured muscles.

4.3 Materials and Methods

4.3.1 Isolation and expansion of hMPCs

Human muscle biopsies from the *M. rectus abdominis* were collected upon ethical approval and with informed consent of 6 hospitalized patients undergoing abdominal surgery under general anesthesia. The samples were processed according to established protocols (134). Briefly, each muscle biopsy was first minced and digested with collagenase Type I 0.2% (w/v) (Sigma) and dispase 0.4% (w/v) (Gibco). The enzymatic reaction was terminated with medium containing 10% FBS. Individual fibers were then liberated by rigorous pipetting and filtered through a strainer with a pore size of 100 µm. After centrifugation the pellet was resuspended in culture medium and the muscle fibers transferred into 35 mm dishes coated with collagen type I (1mg/ml) (BD). The culture medium consisted of DMEM/F12, 1% Penicillin/Streptomycin, 18% FBS, 10 ng/ml hEGF (Sigma), 1 ng/ml hbFGF (Sigma), 10 µg/ml human insulin (Sigma) and 0.4 µg/ml dexamethasone (Sigma) (134). After 24 h a fibroblast reduction step was performed by re-plating the cells. The cultured hMPCs were characterized as published before (see Chapter 2)(134).

4.3.2 Adenoviral design and transduction

The AdEasy System was used as a tool for recombinant adenovirus generation. For the first construct, N-terminal HA-tagged human PGC-1α was cloned into an adenoviral vector that codes for CMV promoter-driven green fluorescent protein (GFP). For the second construct, phenylalanine 411 of the human D2R was mutated into alanine (F411A) to obtain a signalling-deficient human dopamine D2 receptor that still binds ligands in a normal manner but will not activate intracellular signalling upon ligand binding (169). This mutated hD2R was then joined to a C terminal histidine and V5 protein tags and cloned into an adenoviral vector that also expresses red fluorescent protein (RFP). In all cases, successful cloning was validated by sequencing, while viral infection and expression of the fluorescent reported genes was monitored by visualizing GFP/RFP (for details see Chapter 2 and 3). As control for viral infection a GFP adenovirus was used. The viral titer was increased through additional amplification steps and quantified by fluorescent microscopy. The optimal multiplicity of infection (MOI) was measured by serial titrations of the viral vectors on hMPCs and simultaneous determination of fluorescent cells, cell toxicity and cell viability and proliferation. Detailed descriptions of the performed assays were published before (see Chapter 2 and 3). Finally, the transduced hMPCs were expanded for 2 days after infection and were injected at the injured site in nude mice.

4.3.3 Animal experimentation

All animal experiments were approved by and performed according to the local commission for animal experiments. A total of 49 female 8-week-old, nude mice (Charles River, Germany) received hind limb lateral incisions on both sides (from the inferior tibiofibular joint up to the knee joint) under general anesthesia (3 % isoflurane) and aseptic conditions, according to a modified published protocol (193). Briefly, a coronal-plane beneath the *Tibialis anterior* (TA) was opened, separating the muscle from the tibia. The lower jaw of non-serrated forceps was gently inserted below the TA. Crush injury was performed by closing the forceps to its first stage for 3 seconds. The forceps was gently removed, the hMPC-collagen suspension was injected and the wound was closed. Each injection contained $6x10^6$ transduced hMPCs, which were gently mixed with 100 µl collagen type I carrier (final concentration: 2 mg/ml) (BD) prior to injection. A volume of 30 µl of the collagen-cell suspension could be injected without leakage. The muscles were harvested 8-10 days (early), 14-21 days (mid-term), or 28-35 days (late) after injection.

4.3.4 Radiosynthesis of [^{11}C]Raclopride

The radiosynthesis of [^{11}C]Raclopride was successfully accomplished using an established procedure in our lab. Briefly, cyclotron produced [^{11}C]CO_2 gas was reacted with H_2 using Ni catalyst to afford [^{11}C]CH_4, which was passed through an I_2 column to yield [^{11}C]CH_3I. [^{11}C]CH_3I was then reacted with the desmethyl precursor for 5 min at 90 °C. After HPLC purification and SPE extraction, [^{11}C]Raclopride was obtained in 99% radiochemical purity with a maximal specific activity of 239 GBq/µmol. A total of 1.09 – 1.72 GBq of [^{11}C]Raclopride was obtained in an injectable solution of 5% EtOH in 0.15 M PBS. PET scans with [^{11}C]Raclopride were acquired from 0 – 60 min *p.i.* and time frames were averaged for data analysis.

4.3.5 Radiosynthesis of [^{64}Cu]NODAGA-RGD

In order to image neo-vascularization, we used [^{64}Cu]NODAGA-RGD to target the growth factor integrin $\alpha_v\beta_{III}$. Ammonium ascorbate (0.5 M, pH 5.5) was added to [^{64}Cu]$CuCl_2$ (50 µl in 0.05 N HCl) obtained commercially or produced at Paul Scherrer Institute (PSI), followed by addition of 40 µl of NODAGA peptide (NODAGAc(RGDfk), 1mM in H_2O). Labeling was carried out at 95 °C for 15 minutes. According to analytical HPLC, 90% of ^{64}Cu-activity was chelated and only 10% [^{64}Cu]$CuCl_2$ remained unreacted. To bind this remaining fraction, 5 µl DTPA (1 g/15 ml) were added. The resulting [^{64}Cu]DTPA complex is known to be easily excreted through the renal pathway. Animals were injected with 5 – 10 MBq [^{64}Cu]NODAGA-RGD in the tail vein and were imaged 17 – 22 h p.i.

4.3.6 Immuno-/Histological assessment

The harvested TA muscles were embedded in cryo-preservative (OCT embedding medium, Cell Path) immediately after isolation. Cryostat sections were prepared (10 µm) and further processed. Haematoxylin and eosin (H&E) (Sigma) staining was performed according to the manufacturer's protocol. For immunohistological analysis the tissues were fixed (4% PFA, 10 min), permeabilized (0.5% TritonX-100, 20 min), blocked for 30 min (5% BSA + 0.1% TritonX-100 in PBS), and finally stained with anti-sarcomeric α-actinin (1:200, Sigma), F4/80 (1:100, abcam) over night at 4 ^{o}C. After washing with PBS, the tissues were incubated with Cy3 anti-mouse IgG secondary antibody (1:1000, Sigma) and DAPI (1:100, Sigma) for 1 h at room temperature, washed again and finally mounted (Dako). Images were acquired with Leica-Imager Type DM6000B at exposures normalized to unstained controls (secondary antibody and DAPI only).

4.3.7 Macrophage Staining Analysis

A computer-assisted approach was used to quantify macrophage (F4/80) immunolabeling. Longitudinal TA muscle sections were imaged using Leica-Imager Type DM6000B and the images used for analysis were captured from the crushed (central) region of the harvested muscles. For evaluation of the signal (% area) 5-20 High-Power-Fields (HPF, 20x) were analyzed by ImageJ per time point and per group.

4.3.8 Real-time PCR

For analysis of PGC-1α downstream regulated genes and skeletal contractile muscle genes in the regenerating tissue by RTPCR, the middle of the crushed region of each harvested TA muscle was excised, pulverized in liquid nitrogen and suspended in RNA lysis buffer. Total RNA was isolated using the SV Total RNA Isolation System kit (Promega) according to the manufacturer's protocol, including a DNase digestion. RNA was reverse transcribed with random primers (High-Capacity cDNA reverse transcription, Life Technologies). Pre-designed primers for human PPARGC1 (Hs01016719_m1), D2DR (dopamine 2 receptor, Hs00241436_m1), VEGF (vascular endothelial growth factor, Hs00900055_m1), MyH1 (myosin heavy chain 1, Hs00428600_m1), MyH2 (myosin heavy chain 2, Hs00430042_m1), Desmin (Hs00157258_m1), α-actinin (Hs00998100_m1), COXIV (cytochrome c oxidase subunit 4 ,Hs00971639_m1), vWf (Mm00550375_m1), TNF-α (tumor necrosis factor alpha, Mm00443258_m1) and ACHE (acetyl choline esterase, Hs00241307_m1) were purchased from Life Technologies. 18S rRNA (4319413E) was used to normalize cDNA concentrations. For quantification, the expression of each gene was normalized to the 18S, expression in the corresponding sample.

4.3.9 Organ bath (Myography)

The muscles were isolated at different time points after the lesion and the posttraumatic functional recovery was quantitatively assessed by organ bath. After harvesting, the tissues were kept under tension with constant oxygenation (95% O_2 and 5% CO_2) in Krebs solution at 25 ºC. TA muscles were fastened with vicryl into the myograph-chambers (DMT, Denmark) and allowed to equilibrate under 15 mN (1.5 g) for 20 min, adjusting the tension periodically and replacing Krebs solution every 5 min. The samples were stimulated by electrical-field stimulation (EFS) (80V, 80Hz) and 3 measurements per sample were considered for analysis. Native TA muscle was used as control. The maximum tension under tetanic contraction was registered and normalized to the sample weight (mg/mg tissue). All data were collected using a LabChart v7.0 (AD instruments, Spechbach, Germany) and expressed as mean ± S.E.M.

4.3.10 Statistics

For statistical analysis IBM SPSS v22.0 (SPSS Inc,) was used and graphics were drawn with GraphPad Prism v5.04 (GraphPad Software, Inc.). All data were analyzed by Student's *t*-tests, Mann Whitney or one-way ANOVA with Bonferroni or LSD post-hoc analysis ($p<0.05$ was considered significant). All presented data are expressed as means with corresponding standard error of the mean (±SEM).

4.4 Results

4.4.1 PGC-1α overexpressing hMPCs enhance the levels of contractile muscle markers during tissue regeneration

After successful isolation, expansion and characterization of hMPC from six patient biopsies (see Chapter 2), we evaluated the effects of PGC-1α overexpressing hMPCs in a TA crush injury model. To directly assess the role of PGC-1α in myofiber formation, immunofluorescent microscopy and RTPCR analysis of the regenerating crushed muscle tissue were performed (Fig. 4.4-1). The participation of transduced GFP-positive cells in the myotube formation (α-actinin, Cy3) over time could be visualized by fluorescent microscopy in GFP-infected samples (Fig. 4.4-1 A) and in PGC-1α-infected samples (Fig. 4.4-1 B). In line with our previous *ex situ* results (see Chapter 2), PGC-1α overexpressing engineered muscle tissue showed increased relative expression also at gene level for sarcomeric α-actinin (3.47±1.45, n=6, p=0.5476), MyHC1 (6440.64±1370.88, n=6, p=0.0238), MyHC2 (7.51±2.03, n=6, p=0.0238) and Desmin (4.78±1.76, n=6, p=0.0476) at early time points in the regenerating tissue, relative to GFP samples (Fig. 4.4-1 C).

While the Desmin and MyHC2 gene expression reached equivalent levels in PGC-1α and GFP samples over time (Fig. 4.4-1 C-E, Desmin (E):1.28±0.29, n=12, p=0.5425, MyHC2 (E) 0.55±0.18, n=18, p=0.0546), the expression of α-actinin and MyHC1 remained significantly higher in PGC-1α samples at late time points (Fig. 4.4-1 E, α-actinin: 96.15±24.43, n=15, p=0.0092, MyHC1: 312.22±132.8, n=18, p=0.015), suggesting a PGC-1α-induced shift towards slow-twitch type fibers.

4.4.2 Facilitated increased muscle contraction resulting from PGC-1α overexpressing hMPCs injection after crush injury

Encouraged by the enhanced gene expression of contractile markers in the regenerating muscles (Fig. 4.4-1) with increased PGC-1α levels, we decided to analyze the expression of further markers, known to be involved in muscle regeneration. The crushed/regenerating tissue was investigated by RTPCR for the expression of factors connected to vascularization (VEGF-A), mitochondrial activity (COXIV) and neuronal activity (ACHE). The overexpression of hD2R and hPGC-1α was sustained over time (Fig. 4.4-2 A-C). Notably, the PGC-1α “native” expression in GFP-infected samples increased at the latest time point (Fig. 4.4-2 C). Increased levels of VEGF-A in PGC-1α overexpressing samples, relative to GFP (Fig. 4.4-2

A-C) were detected at early (8-10d) (A: 2.26±0.49, n=6, p=0.0476), mid-term (14-21d) (B: 7.18±2.46, n=21, p=0.1475) and late (28-35d) (C: 204.65±49.7, n=18, p=0.0124) time points. Similarly, the PGC-1α downstream-regulated mitochondrial activity was enhanced (COXIV) (A: 4.32±1.02, n=6, p=0.0238; B: 88.87±38.06, n=21, p=0.1475; C: 1595.35±547.55, n=18, p=0.003). Finally, the gene expression levels of ACHE illustrated the expected increase in the PGC-1α modified regenerating tissues (A: 3.96±1.04, n=6, p=0.0238; B: 10.52±3.51, n=18, p=0.0012; C: 9.99±2.89, n=12, p=0.0032). In line with the enhanced gene expression of markers for contractility, vascularization and neurons, we observed an increased muscle contraction in PGC-1α overexpressing muscles. Organ bath measurement at 80V and 80Hz revealed significantly elevated contraction force at early (PGC-1α: 43.75±5.27, n=6; GFP: 28.36±2.89, n=13, p=0.0337) and mid-term (PGC-1α: 89.49±6.14, n=33; GFP: 69.85±7.12, n=18, p=0.0435) time points in PGC-1α treated muscles (Fig. 4.4-2 D). At late time points both, PGC-1α and GFP overexpressing muscles contracted at similar levels (PGC-1α: 82.33±3.73, n=21; GFP: 70.52±5.17, n=9, p=0.0830) as TA native control.

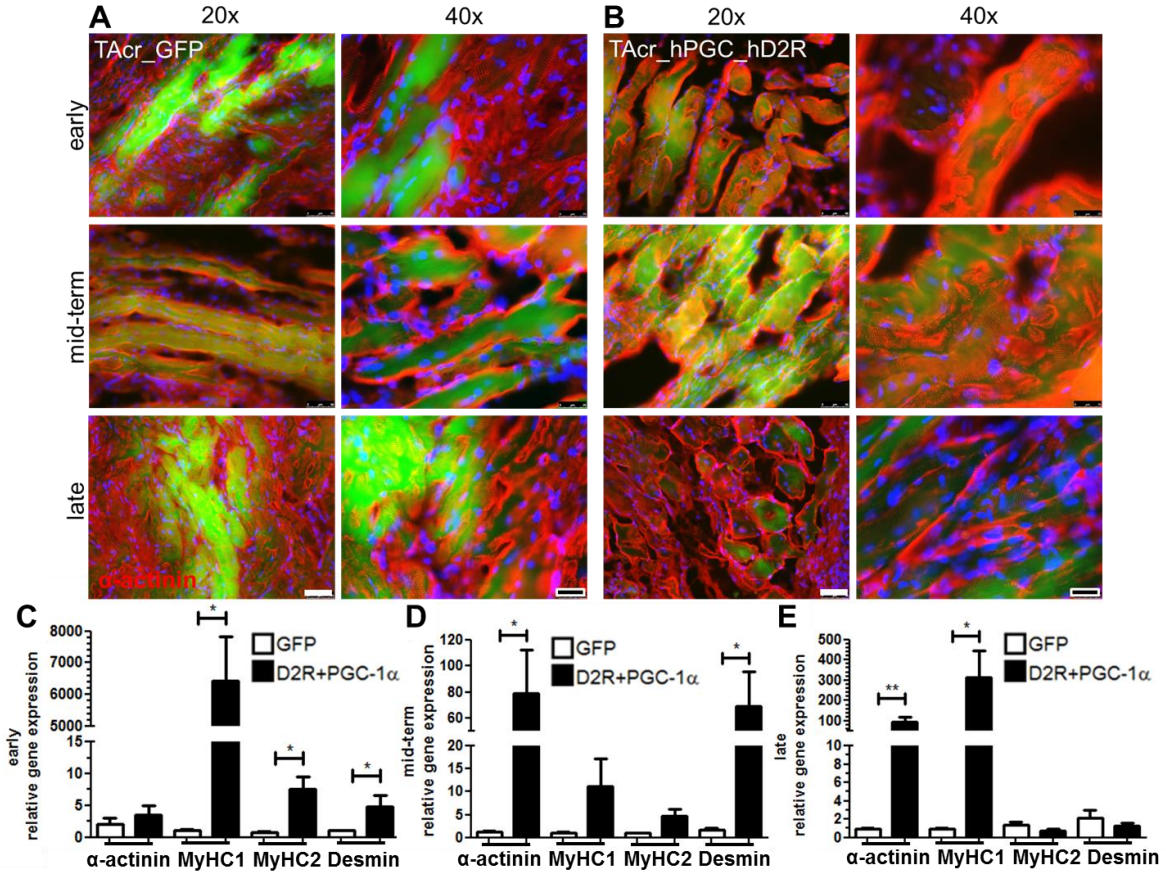

Figure 4.4-1. **PGC-1α induces upregulation of the expression of contractile genes in the regenerating muscle**. Immunohistological assessment of newly-build muscle fibers (green), stained with sarcomeric α-actinin antibody (Cy3, red) over time (A: GFP, B: PGC-1α). RTPCR analysis showed enhanced α-actinin, MyHC1, MyHC2 and Desmin gene expression when PGC-1α was overexpressed at (C) early (8-10d), (D) mid-term (14-21d) and (E) late (28-35d) time points after the TA crush injury. TAcr: crushed *Tibialis anterior*

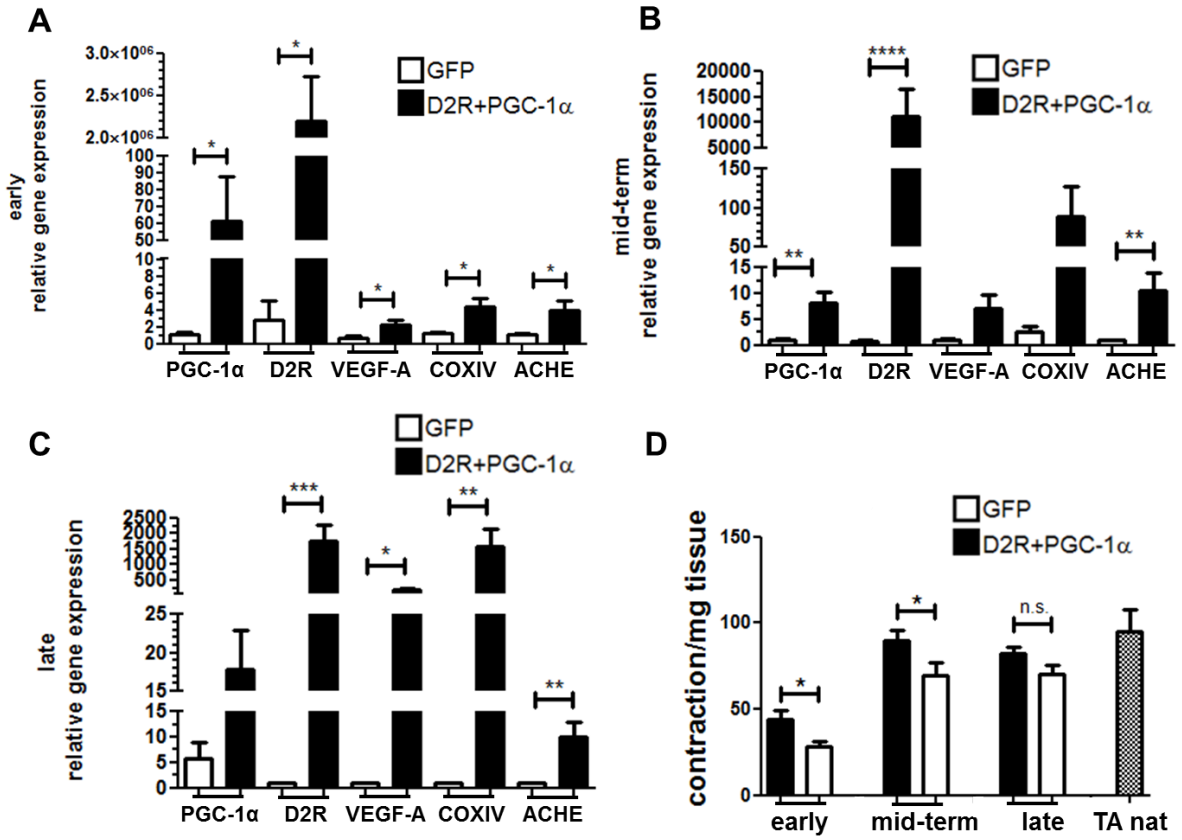

Figure 4.4-2. **PGC-1α_hMPCs induce expression of genes related to vascularization, mitochondrial and neuronal activation, and enhance the contractility at early and mid-term time points after TA crush injury during regeneration**. RTPCR analysis confirmed the sustained overexpression of hPGC-1α and the signalling-deficient hD2R genes at the crush injury site over time. Relative VEGF-A, COXIV and ACHE gene levels were enhanced in the corresponding samples, compared to control GFP_hMPCs at (A) early, (B) mid-term and (C) late time points of regeneration. (D) PGC-1α overexpression led to increased TA contractile force at early and mid-term time points. VEGF-A: vascular endothelial growth factor-a, COXIV: Cytochrome c oxidase subunit 4, ACHE: acetylcholine esterase

4.4.3 Tracking of hMPC in a TA muscle crush injury

A crush injury was introduced to the TA muscle of nude mice (Fig. 4.4-3 A). The injected hD2R_hMPCs were successfully tracked in the crush injury region using the specific D2R radiotracer [^{18}F]Fallypride (early time-point), resulting in a virus-dose-dependent signal (Fig. 4.4-3 B). The injection of 50% hD2R-positive cells in the damaged tissue led to an increased radiotracer uptake, compared to the injection of 25% positive cells. No signal could be detected in the crush only controls. To exclude signal contamination from [^{18}F]-fluoride in the tibial bone, [^{11}C]Raclopride was used as an alternative high-affinity D2R ligand for further experiments. For these experiments a viral combination of hD2R and hPGC-1α, compared to GFP-control infected cells was used (Fig. 4.4-3 C and D). Uptake of [^{11}C]Raclopride could be detected in hD2R_hPGC-1α_hMPCs at early time points only (Fig. 4.4-3 C). Further studies revealed an unspecific radiotracer uptake at the site of injury when GFP_hMPCs were used (Fig. 4.4-3 D).

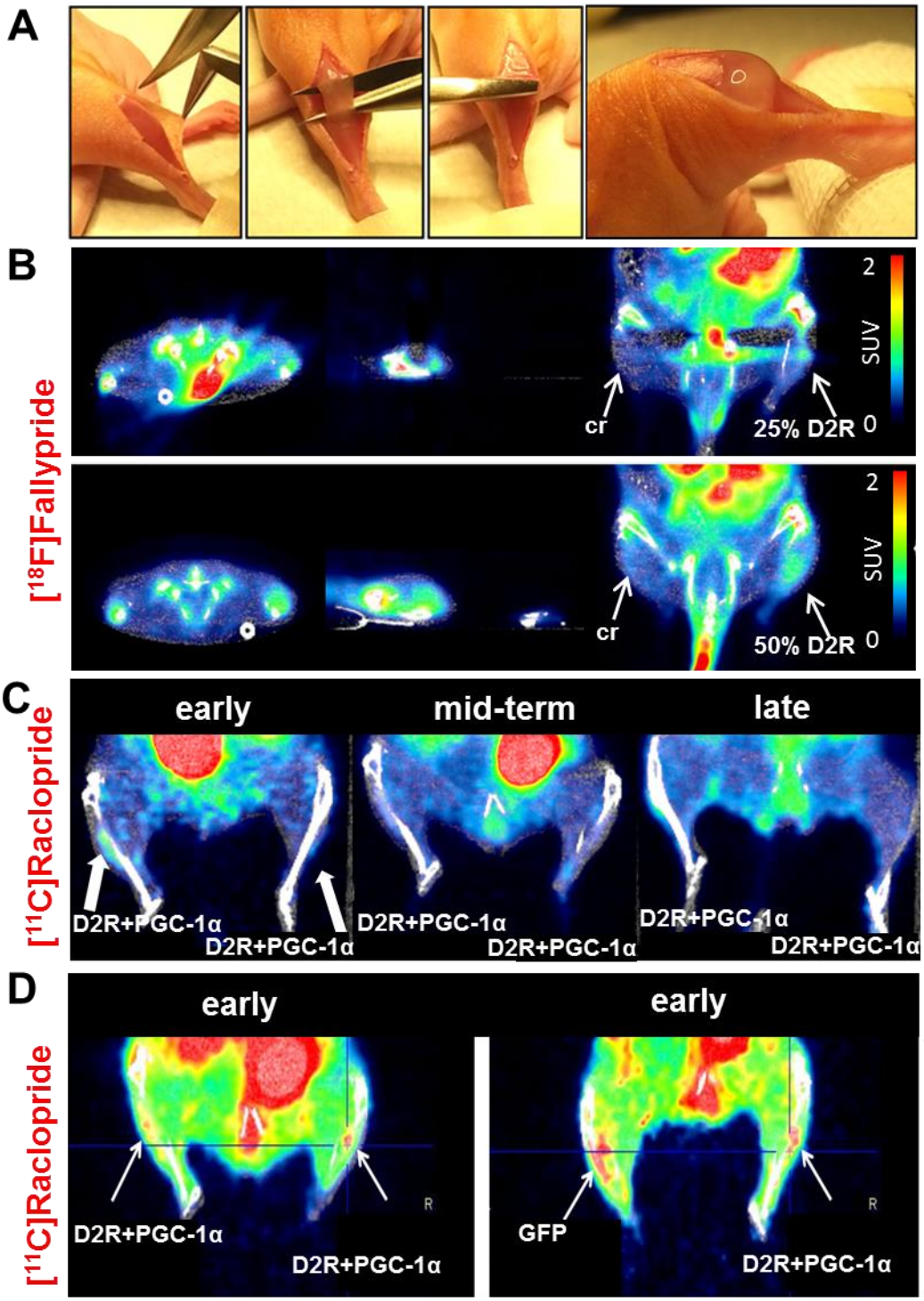

Figure 4.4-3. **PET/CT tracking of hD2R_hMPCs in a TA crush injury model**. (A) Nude mice were subjected to a TA crush injury, followed by injection of cell-collagen suspension. (B) Feasible tracking of hD2R_hMPCs with [^{18}F]Fallypride in a virus-dose-dependent manner (25% vs. 50% hD2R-positive cells). No tracer uptake in the crush only (cr) TA. (C) [^{11}C]Raclopride accumulation in hD2R_hPGC-1α_hMPCs at early time-points, but not at mid-term and late. (D) Enhanced accumulation of [^{11}C]Raclopride at GFP_hMPCs injection site, compared to hD2R_hPGC-1α_hMPCs. SUV: standard uptake value, cr: crush only.

4.4.4 PGC-1α overexpressing hMPCs reduce the pro-inflammatory response after muscle crush injury

Initially aiming at imaging of neo-angiogenesis with the specific $\alpha_v\beta_{III}$ radiotracer [^{64}Cu]NODAGA-RGD, we observed a highly increased accumulation of the tracer in TA crush only in the early periods after injury, when compared to native TA and to the crushed muscles with injected hMPCs (Fig. 4.4-4 A, first and second lane). At later time points no PET signal was detectable (Fig. 4.4-4 A, mid-term and late). Furthermore, immunohistological analysis of harvested muscles with a macrophage expression marker (F4/80, Cy3) demonstrated 1) a highly increased macrophage accumulation in crushed TA compared to native (Fig. 4.4-4 B and C, first line); 2) a decreased signal in the hD2R_hPGC_hMPCs compared to GFP_hMPCs (Fig. 4.4-4 B and C, second line). The latter effect was observed also at later time points (Fig. 4.4-4 B and C, mid-term and late). RTPCR analysis of the pro-inflammatory cytokine TNF-α in the crushed/regenerating tissue confirmed the highly increased signal in TA crush versus TA native (Fig. 4.4-4 D first line, 44.73±4.52, n=3, 0.57±0.19, n=6, $p<0.0001$) and the decreased expression in PGC-1α overexpressing tissues compared to GFP (Fig. 4.4-4 D second line, 0.443±0.11, n=3, 0.98±0.07, n=3, $p=0.0177$). The PGC-1α-related reduction of inflammation was sustained also at mid-term (Fig. 4.4-4 D, 0.23±0.03, n=15, 1.35±0.30, n=3, $p<0.0001$), and late time points (Fig. 4.4-4 D, 0.15±0.02, n=9, 0.84±0.24, n=3, $p=0.0005$).

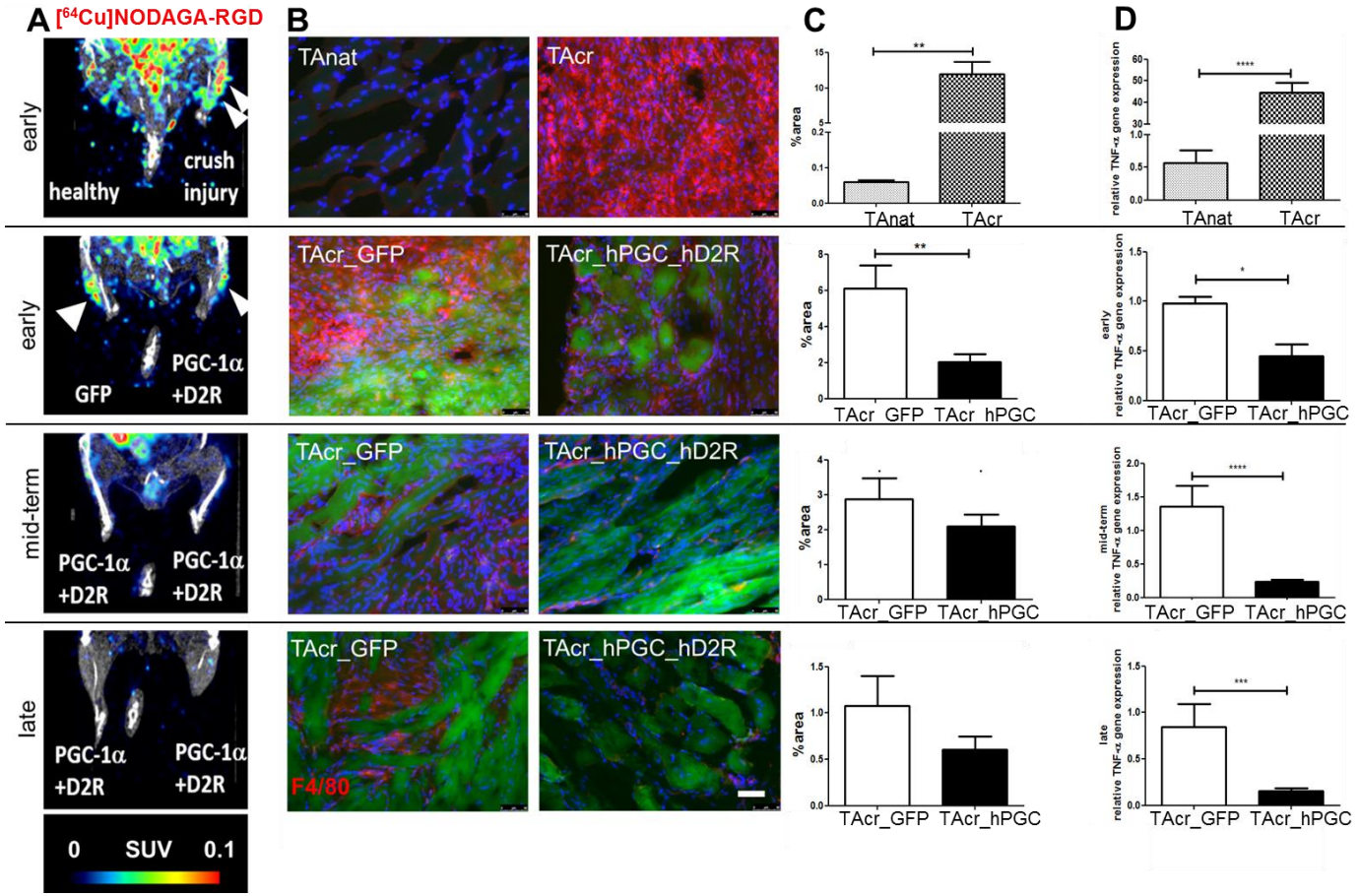

Figure 4.4-4 **PGC-1α overexpression in hMPCs reduces the inflammatory response in the crush injury.** (A) Unspecific accumulation of neo-vascularization radiotracer [^{64}Cu]NODAGA-RGD in the early time-points after the injury. (B) Immunohistological assessment of macrophage (F4/80, red) invasion in the injured region with and without hMPCs (green). (C) Evaluation of the fluorescent intensity showed increased F4/80 signal in TA crush only, compared to TA native (first line) and reduced signal at the site of injection of hD2R_hPGC-1α infected cells, compared to GFP (second line). The latter trend was visible also at later time points (third and fourth lines). (D) RTPCR analysis of the relative TNF-α gene expression in the crushed tissue could further confirm the anti-inflammatory effect of PGC-1α overexpressing hMPCs, sustained over time. SUV: standard uptake value, TAnat: native *Tibialis anterior*, TAcr: crushed only *Tibialis anterior*

4.5 Discussion

Muscle precursor cells, or activated satellite cells, are responsible for the regeneration in postnatal skeletal muscles. In the past decades, these cells have been investigated for muscle tissue bioengineering approaches, allowing the growth of new myofibers (128, 129, 135, 194). However, there are certain limitations in quality of the de-novo engineered constructs. The process of proliferation and differentiation of these cells is largely driven by growth factors, and altered by tissue injury or exercise (195, 196). To address this matter we designed a model for facilitated muscle regeneration after injury, by inducing overexpression of hPGC-1α in the injected hMPCs.

Intensive research has shown that the natural process after muscle injury follows a highly conserved sequence of steps, leading to the restoration of tissue architecture, and importantly also function (197). A crucial step in the process of forming new muscle tissue is the capacity of MPCs to differentiate into myotubes. Consistent with the previously reported facilitated *in vitro* and *in vivo ex situ* differentiation of PGC-1α_hMPCs (see Chapter 2), the regenerating TA muscles with PGC-1α overexpression demonstrated earlier myotube formation *in situ*. The injection of hMPC_hPGC-1α in the crush injury also significantly increased the expression of contractile proteins at all time points after the injury, indicating facilitated restoration compared to GFP infected controls. Furthermore, PGC-1α seems to have increased the resistance of MPCs after implantation, leading to improved cell survival at implantation and better long term survival. In line with our *in vivo* observations, others have shown, that an increased VEGF release in a hypoxic environment leads to enhanced differentiation of muscle cells (146). It has been demonstrated that secretion of various effectors by the injected hMPCs contributes to optimization of the regenerative process (e.g. neovascularization) (135, 144, 198). The PGC-1α-related regeneration enhancement was further promoted by an increase in factors for mitochondrial (COXIV) and neuromuscular (ACHE) activity, which are known to be vital for successful muscle tissue bioengineering. Further supporting evidence suggested an increased expression of mitochondrial and other metabolic genes as a plausible mechanism for rescuing a damaged muscle (139). All these evidences support the observed enhanced contraction force production by the regenerating muscles injected with hMPC_hPCG-1α.

While resistance training combined with adequate nutrition remains the most effective intervention to diminish the functional decline in muscles, there is a certain age-linked barrier

to obtaining full benefits from this therapy (137). PGC-1α would be a promising "exercise molecule", which controls skeletal muscle metabolism and has potential therapeutic effects. Therefore, we believe that by inducing PGC-1α overexpression in the injected hMPCs, we are able to mediate muscle healing effects for structural, metabolic and functional restoration, irrespective of physical status and age of the patient.

Besides improving the quality of the engineered skeletal tissues, we aimed at establishing a method to non-invasively image the cell fate after implantation. Molecular imaging with PET is gaining increasing importance in regenerative medicine due to the possibility for non-invasive metabolic read-outs. A recent study described the feasibility of imaging human Na/I symporter (NIS) expression in two mouse models of muscular dystrophy and vascular disease by bioluminescence and PET imaging (199). This study demonstrated that luciferase - and NIS - engineered skeletal muscle could successfully be imaged. In our present study, we presented a method for non-invasive visualization of the implanted cells in the TA crush injury using PET/CT imaging of hD2R. Tracking of hMPCs via ectopic expression of a signalling-deficient hD2R was previously reported in an *ex situ* muscle tissue formation model (see Chapter 3). We were able to visualize the cells in a viral dose-dependent manner in the injured TA muscles of the animals using the highly-specific hD2R radiotracer [^{18}F]Fallypride. Nevertheless, the proximity of the muscle injury to the tibial bone led to unspecific signal uptake due to possible defluorination of the radiotracer. To circumvent this problem, we used [^{11}C]Raclopride as an alternative hD2R PET imaging agent.

Interestingly, animals injected with GFP-only hMPCs showed a higher [^{11}C]Raclopride uptake, compared to the regenerating muscles with injected hD2R_hPGC-1α_hMPCs. This was also true for other tracers used in the study (data not shown). Additionally, while aiming at visualizing neo-vascularization using [^{64}Cu]NODAGA-RGD, a relatively high amount of radioactivity was detected in the TA crushed only, where no cells were injected. These observations led to the assumption that the recorded signals were rather related to inflammation, than to vascularization or specific hD2R detection. Immunohistological analysis with macrophage marker F4/80 and the TNF-α gene expression levels in the harvested samples correlated with [^{64}Cu]NODAGA-RGD tracer uptake in the injury region. In line with our observations, another study revealed that in addition to neo-vessels and myofibroblasts, macrophages have also been shown to express $\alpha_v\beta_{III}$ integrin (200). However, the relative amounts of integrin in these cell types have not been followed over time. Importantly, we were able to show, that PGC-1α overexpression in the hMPCs could significantly reduce pro-inflammatory cytokine expression (TNF-α), therefore enhancing the healing process. A

relation between PGC-1α and suppression of the broad inflammatory response has previously been reported (139).

Based on the findings above, PGC-1α overexpressing hMPCs hold promise for the enhanced repair of skeletal muscle tissue. They demonstrated capacities to amplify the expression of contractile markers, to facilitate the contraction force generation in the regenerating muscles and to decrease the inflammatory response after crush injury. Additionally, we were able to track the implanted cells in the crushed muscles using PET radioligands. Nonetheless, several challenges remain which need to be overcome in order to establish a feasible method for metabolic imaging of this cellular therapy.

5 Conclusions and Future Perspectives

To date, donated organs and tissues are often used for replacement of damaged or missing tissues, but the need for donors far outweighs the available supply. Regenerative medicine offers an elegant alternative, using autologous stem cell therapy. Cellular insufficiency or deficiency, due to dysfunction or degeneration, respectively, is the cause of illnesses such as heart failure, neurodegenerative disorders, diabetes, bone marrow failure, and spinal cord injury. For decades, therapeutic approaches have been limited to the surgical removal of damaged tissues or treatment with pharmacological therapies to ameliorate symptoms and fight infection. Therefore, the vision of exchanging impaired or missing cells with new functional cells has shifted the therapeutic paradigm towards restoring tissue function (201).

Treatment with stem cells can heal a very broad range of medical conditions; however, more research is needed to ensure higher success rates, in order to develop a platform, from which many patients could benefit. Thorough investigations are ongoing towards finding a feasible therapy for stress urinary incontinence (SUI). SUI is a frequent condition affecting over 200 million people worldwide that can be caused by urethral sphincter insufficiency and is associated with a dramatic deterioration of the quality of life. However, the current treatment strategies are not leading to satisfactory outcomes (85). Since the discovery of MPCs, many studies have examined their properties and highlighted their indispensable role in the process of muscle regeneration (202, 203). Skeletal muscle tissue engineering approaches showed that these cells are the most suitable cell source for skeletal muscle restoration (129, 204, 205). Considering the recent advances of using a cell therapy, we aimed at overcoming some of the major pitfalls of the available techniques. To get one step closer towards the successful clinical application of autologous stem cell therapy for SUI, we considered improvements in two directions: 1) the insufficient systematic analysis for overexpression of certain factors, supporting muscle regeneration by influencing cell differentiation, immune response, vascularization, neuron formation and functionality of the newly engineered skeletal muscle tissues. 2) the missing tools for non-invasive monitoring of the applied cell-based therapy.

A more complete understanding of the genetic and molecular patterns of the regeneration processes may yield valuable information towards new strategies for therapy. Therefore, we first examined the effect of peroxisome proliferator-activated receptor-γ coactivator (PGC-1α) overexpression in hMPCs and later aimed at visualizing the benefits from this genetic manipulation by PET imaging. PGC-1α is a key regulator of energy metabolism and is known

to control muscle plasticity, mitochondrial biogenesis and neuromuscular junction formation (114). We have been able to prove the supporting effect of PGC-1α overexpression in hMPCs towards enhanced and facilitated *ex situ* muscle formation and *in situ* muscle regeneration. However, with a future perspective of applying this therapy in patients, several issues have to be considered. Although viral gene delivery has some advantages such as high transduction efficiency and long-term gene expression, this method has several drawbacks, i.e. immunogenicity, mutagenicity, toxicity, low target-cell specificity and high production costs, leading to concerns for its clinical application. Therefore, the evaluation of a new therapeutic strategy based on non-viral gene delivery technique would allow for an increase in relative safety, introduction of large size genes, decrease in toxicity and, importantly, these vectors could be modified with ligands for tissue/cell-specific targeting. Another future perspective would be the use of clustered regularly interspaced short palindromic repeat (CRISPR) technology for genetic manipulation. Cas9 has already been utilized to carry synthetic transcription factors for activation of specific human genes. Some of the affected genes were related to human diseases involved in muscle differentiation, inflammation and cancer (206).

An elegant way of omitting the genetic manipulation would be to learn from gene therapy and to develop new drugs accordingly. For instance, chemical modulation of the PGC-1α pathway in skeletal muscles could have a substantial impact in the clinic (139). This approach would allow for more controlled timing for the upregulation of this factor, thereby promoting its effect depending on the patient's needs. Furthermore, a tissue-specific action is of high importance, in order to assure the stimulation of the proper cells. One published therapeutic approach is the combination of alpha-lipoic acid with coenzyme Q10 (207), which has been shown to increase PGC-1α levels in cultured myoblasts, providing a convenient drug target to facilitate muscle regeneration in these patients.

An alternative approach for enhancing the regenerative process could be the utilization of different growth factors and engineering matrices/biomaterials. For example, a recent publication presented a method where C2C12 myoblasts were seeded on a special hydrogel, creating a cell sheet, and later on transfected with VEGF-A plasmids using nanoparticles (208). After implantation of these sheets to ischemic areas in mice, an enhanced angiogenic paracrine effect could be observed. More and more research is being concentrated on the combination of specifically engineered biomaterials, together with the use of various factors, which are either released from the matrices themselves, or by the seeded cells. Efforts in this direction would provide more effective and optimized treatment options for cell-based therapies in future.

In order to utilize this autologous cell therapy in the clinic, a non-invasive method for visualization of the location, viability and metabolism of the injected cells over time is of great importance, as continuous tissue biopsies are unfavourable (209). In this thesis, efforts were undertaken to non-invasively follow human MPCs that were genetically modified to overexpress a signalling-deficient hD2R, allowing us to use [^{18}F]Fallypride for PET cell-tracking in an *ex situ* muscle bioengineering model, combined with [^{18}F]FMISO for imaging the hypoxic environment. After successful establishment of the conditions for *in vivo* cell tracking, we further used PET imaging for visualization of the hMPC-based regeneration in a *Tibialis anterior* crush injury mouse model using [^{18}F]Fallypride and [^{11}C]Raclopride for hD2R tracking and [^{64}Cu]NODAGA-RGD for imaging neo-vascularization.

One major issue in the field of skeletal muscle tissue engineering is the insufficient vascularization at the initial time points after implantation of the constructs, often leading to central necrosis in the newly-built tissues (190). In order to visualize the hypoxia state of the injected constructs, we used [^{18}F]FMISO, which showed a rapid decrease in signal after the first week. This correlated with the expected neovascularisation of the bioengineered tissues, suggested by the increase in vWf protein and VEGF-A gene expression levels in the harvested tissues over time. Ideally, one would compare the [^{18}F]FMISO uptake with a signal from a radiotracer targeting the formation of new blood vessels, i.e. [^{64}Cu]NODAGA-RGD. This combination would allow for an elegant non-invasive proof of the applicability of the suggested cell-therapy, optimally showing the exact time of simultaneous disappearance of hypoxia and appearance of neovascularisation. Ideally, this would give further information regarding the possible application of drugs with narrow therapeutic windows for facilitating the initial formation of blood vessels.

Aiming at imaging neovascularization of the newly grown muscle tissue, another method might be more applicable, as the currently available PET radiotracer are all based on the RGD sequence for targeting the $\alpha_V ß_{III}$ integrin (210, 211), that is known to be also expressed by macrophages (212). An alternative would be the implementation of gadolinium-enhanced MRI. This technique may be useful in developing pro-angiogenic strategies to improve the transplantation outcome in experimental and clinical settings (213). Moreover, considering the generally low [^{18}F]FMISO uptake in the injured muscles, suggesting that the muscles are regenerating quite fast without being hypoxic, earlier time points for imaging should be considered. Furthermore, to reduce the effect of fast regeneration, a mouse model, lacking satellite cells would be an option. Such a transgenic model has been established, allowing for endogenous Pax7 expression while permitting specific deletion of satellite cells by tamoxifen-inducible Cre recombinase (Jackson Laboratory). In this case, the only source for

regeneration would be the injected hMPCs, thus making the evaluation of their regenerative potential more prominent.

In addition to the observed decrease in [^{18}F]FMISO signal, we detected a significant reduction in [^{18}F]Fallypride PET signal over time. We were able to prove the survival of the constructs by histology after harvesting of the bioengineered muscle tissues. Additionally, gene and protein analysis, confirmed the successful cell-to-myofiber transition and, ultimately, muscle tissue formation. Alternatively, to non-invasively resolve this matter, [^{18}F]FDG could be used to investigate cell viability by monitoring glucose metabolism (214). A sustained [^{18}F]FDG signal over time would give a non-invasive proof of the viability of the injected cells, suggesting that the loss of signal is not related to cell death.

In this thesis, a reliable model for enhancement and imaging of skeletal muscle bioengineering was successfully established. However, further investigations towards imaging of stem cell-based therapies are needed before up-scaling to clinical application.

6 References

1. Piscaglia, A.C. Stem cells, a two-edged sword: risks and potentials of regenerative medicine. World J Gastroenterol **14**, 4273, 2008.

2. Health, U.S.N.I.o. www.clinicaltrials.gov.

3. Kraitchman, D.L., andBulte, J.W. Imaging of stem cells using MRI. Basic research in cardiology **103**, 105, 2008.

4. Srinivas, M., Aarntzen, E.H., Bulte, J.W., Oyen, W.J., Heerschap, A., de Vries, I.J., andFigdor, C.G. Imaging of cellular therapies. Advanced drug delivery reviews **62**, 1080, 2010.

5. Ametamey, S.M., Honer, M., andSchubiger, P.A. Molecular imaging with PET. Chem Rev **108**, 1501, 2008.

6. Dominietto, M., andRudin, M. Could magnetic resonance provide histology? Front Genet **4**, 298, 2014.

7. Collins, S.A., Hiraoka, K., Inagaki, A., Kasahara, N., andTangney, M. PET imaging for gene & cell therapy. Curr Gene Ther **12**, 20, 2012.

8. Sutton, E.J., Henning, T.D., Pichler, B.J., Bremer, C., andDaldrup-Link, H.E. Cell tracking with optical imaging. Eur Radiol **18**, 2021, 2008.

9. Rinck, P.A. Magnetic Resonance Imaging – How It All Began. http://www.rinckside.org/Rinckside%20Columns/1990%20MRI%20How%20it%20all%20began.htm2003.

10. Nuclear Magnetic Resonance http://www.imaios.com/de/e-Courses/e-MRI/NMR.

11. Corti, R. SWiss Multicenter Intracoronary Stem Cells Study in Acute Myocardial Infarction (SWISS-AMI).

12. W.M.Bulte, J. 19F Hot Spot MRI of Human Adipose-derived Stem Cells for Breast Reconstruction (CS-1000).

13. Evaluation of Autologous Mesenchymal Stem Cell Transplantation (Effects and Side Effects) in Multiple Sclerosis http://clinicaltrials.gov/ct2/show/NCT01377870?term=stem+cells+MRI&rank=47.

14. Safety and Efficacy Study of Autologus Bone Marrow Mesenchymal Stem Cells in Multiple Sclerosis.

15. Treatment of Knee Osteoarthritis by Intra-articular Injection of Bone Marrow Mesenchymal Stem Cells http://clinicaltrials.gov/ct2/show/NCT02123368?term=stem+cells+MRI&rank=13.

16. Jo, C.H., Lee, Y.G., Shin, W.H., Kim, H., Chai, J.W., Jeong, E.C., Kim, J.E., Shim, H., Shin, J.S., Shin, I.S., Ra, J.C., Oh, S., andYoon, K.S. Intra-articular injection of mesenchymal stem cells for the treatment of osteoarthritis of the knee: a proof-of-concept clinical trial. Stem Cells **32**, 1254, 2014.

17. Safety and Effect of Adipose Tissue Derived Mesenchymal Stem Cell Implantation in Patients With Spinal Cord Injury.

18. Safety and Efficacy of Autologous Bone Marrow Stem Cells in Treating Spinal Cord Injury (ABMST-SCI).

19. Park, J.H., Kim, D.Y., Sung, I.Y., Choi, G.H., Jeon, M.H., Kim, K.K., andJeon, S.R. Long-term results of spinal cord injury therapy using mesenchymal stem cells derived from bone marrow in humans. Neurosurgery **70**, 1238, 2012.

20. Guenoun, J., Ruggiero, A., Doeswijk, G., Janssens, R.C., Koning, G.A., Kotek, G., Krestin, G.P., andBernsen, M.R. In vivo quantitative assessment of cell viability of gadolinium or iron-labeled cells using MRI and bioluminescence imaging. Contrast media & molecular imaging **8**, 165, 2013.

21. Modo, M., Mellodew, K., Cash, D., Fraser, S.E., Meade, T.J., Price, J., andWilliams, S.C. Mapping transplanted stem cell migration after a stroke: a serial, in vivo magnetic resonance imaging study. Neuroimage **21**, 311, 2004.

22. GUERBET Press releases: FDA approves Dotarem.

23. Varnas, K., Varrone, A., andFarde, L. Modeling of PET data in CNS drug discovery and development. Journal of pharmacokinetics and pharmacodynamics **40**, 267, 2013.

24. Phelps, M.E., Hoffman, E.J., Mullani, N.A., andTer-Pogossian, M.M. Application of annihilation coincidence detection to transaxial reconstruction tomography. J Nucl Med **16**, 210, 1975.

25. Hill, D.L., Batchelor, P.G., Holden, M., andHawkes, D.J. Medical image registration. Physics in medicine and biology **46**, R1, 2001.

26. Segers, V.F., andLee, R.T. Stem-cell therapy for cardiac disease. Nature **451**, 937, 2008.

27. Zhang, Y., Ruel, M., Beanlands, R.S., deKemp, R.A., Suuronen, E.J., andDaSilva, J.N. Tracking stem cell therapy in the myocardium: applications of positron emission tomography. Curr Pharm Des **14**, 3835, 2008.

28. Doyle, B., Kemp, B.J., Chareonthaitawee, P., Reed, C., Schmeckpeper, J., Sorajja, P., Russell, S., Araoz, P., Riederer, S.J., andCaplice, N.M. Dynamic tracking during intracoronary injection of 18F-FDG-labeled progenitor cell therapy for acute myocardial infarction. J Nucl Med **48**, 1708, 2007.

29. Ahmad, N., Welch, I., Grange, R., Hadway, J., Dhanvantari, S., Hill, D., Lee, T.Y., andHoffman, L.M. Use of imaging biomarkers to assess perfusion and glucose metabolism in the skeletal muscle of dystrophic mice. BMC Musculoskelet Disord **12**, 127, 2011.

30. Goncalves, M.D., Alavi, A., andTorigian, D.A. FDG-PET/CT assessment of differential chemotherapy effects upon skeletal muscle metabolism in patients with melanoma. Ann Nucl Med **28**, 386, 2014.

31. Colombo, A., Castellani, M., Piccaluga, E., Pusineri, E., Palatresi, S., Longari, V., Canzi, C., Sacchi, E., Rossi, E., Rech, R., Gerundini, P., Viecca, M., Deliliers, G.L., Rebulla, P., Soligo, D., andGiordano, R. Myocardial blood flow and infarct size after CD133+ cell injection in large myocardial infarction with good recanalization and poor reperfusion: results from a randomized controlled trial. Journal of cardiovascular medicine **12**, 239, 2011.

32. Yang, J.J., Liu, Z.Q., Zhang, J.M., Wang, H.B., Hu, S.Y., Liu, J.F., Wang, C.Y., andChen, Y.D. Real-time tracking of adipose tissue-derived stem cells with injectable scaffolds in the infarcted heart. Heart Vessels **28**, 385, 2013.

33. Chen, I.Y., andWu, J.C. Molecular imaging: the key to advancing cardiac stem cell therapy. Trends Cardiovasc Med **23**, 201, 2013.

34. Schwaiger, M., andBengel, F.M. From thallium scan to molecular imaging. Molecular imaging and biology : MIB : the official publication of the Academy of Molecular Imaging **4**, 387, 2002.

35. Pei, Z., Lan, X., Cheng, Z., Qin, C., Wang, P., He, Y., Yen, T.C., Tian, Y., Mghanga, F.P., andZhang, Y. A multimodality reporter gene for monitoring transplanted stem cells. Nuclear medicine and biology **39**, 813, 2012.

36. Roelants, V., Labar, D., de Meester, C., Havaux, X., Tabilio, A., Gambhir, S.S., Di Ianni, M., Bol, A., Bertrand, L., andVanoverschelde, J.L. Comparison between adenoviral and retroviral vectors for the transduction of the thymidine kinase PET reporter gene in rat mesenchymal stem cells. J Nucl Med **49**, 1836, 2008.

37. Gyongyosi, M., Blanco, J., Marian, T., Tron, L., Petnehazy, O., Petrasi, Z., Hemetsberger, R., Rodriguez, J., Font, G., Pavo, I.J., Kertesz, I., Balkay, L., Pavo, N., Posa, A., Emri, M., Galuska, L., Kraitchman, D.L., Wojta, J., Huber, K., andGlogar, D. Serial noninvasive in vivo positron emission tomographic tracking of percutaneously intramyocardially injected autologous porcine mesenchymal stem cells modified for transgene reporter gene expression. Circulation Cardiovascular imaging **1**, 94, 2008.

38. Willmann, J.K., Paulmurugan, R., Rodriguez-Porcel, M., Stein, W., Brinton, T.J., Connolly, A.J., Nielsen, C.H., Lutz, A.M., Lyons, J., Ikeno, F., Suzuki, Y., Rosenberg, J., Chen, I.Y., Wu, J.C., Yeung, A.C., Yock, P., Robbins, R.C., andGambhir, S.S. Imaging gene expression in human mesenchymal stem cells: from small to large animals. Radiology **252**, 117, 2009.

39. Zhang, W.Y., Ebert, A.D., Narula, J., andWu, J.C. Imaging cardiac stem cell therapy: translations to human clinical studies. J Cardiovasc Transl Res **4**, 514, 2011.

40. Schoder, H., Erdi, Y.E., Larson, S.M., andYeung, H.W. PET/CT: a new imaging technology in nuclear medicine. European journal of nuclear medicine and molecular imaging **30**, 1419, 2003.

41. Krause, B.J., Schwarzenbock, S., andSouvatzoglou, M. FDG PET and PET/CT. Recent Results Cancer Res **187**, 351, 2013.

42. Chiotellis, A., Mu, L., Muller, A., Selivanova, S.V., Keller, C., Schibli, R., Kramer, S.D., andAmetamey, S.M. Synthesis and biological evaluation of (1)(8)F-labeled fluoropropyl tryptophan analogs as potential PET probes for tumor imaging. European journal of medicinal chemistry **70**, 768, 2013.

43. Campanile, C., Arlt, M.J., Kramer, S.D., Honer, M., Gvozdenovic, A., Brennecke, P., Fischer, C.R., Sabile, A.A., Muller, A., Ametamey, S.M., Born, W., Schibli, R., andFuchs, B. Characterization of different osteosarcoma phenotypes by PET imaging in preclinical animal models. J Nucl Med **54**, 1362, 2013.

44. Lundgren, K. Bone Reconstruction of the Skull Using a Metal Ceramic Implant After Previously Failed Reconstruction.

45. Garcia-Orta, R., Mahia-Casado, P., Gomez de Diego, J.J., Barba-Cosials, J., Rodriguez-Palomares, J.F., Aguade-Bruix, S., andCandell-Riera, J. Update on Cardiac Imaging Techniques 2013. Rev Esp Cardiol 2014.

46. Mignone, J.L., Kreutziger, K.L., Paige, S.L., andMurry, C.E. Cardiogenesis from human embryonic stem cells. Circulation journal : official journal of the Japanese Circulation Society **74**, 2517, 2010.

47. Schuster, M.D., Kocher, A.A., Seki, T., Martens, T.P., Xiang, G., Homma, S., andItescu, S. Myocardial neovascularization by bone marrow angioblasts results in cardiomyocyte regeneration. Am J Physiol Heart Circ Physiol **287**, H525, 2004.

48. Li, Z., Lee, A., Huang, M., Chun, H., Chung, J., Chu, P., Hoyt, G., Yang, P., Rosenberg, J., Robbins, R.C., andWu, J.C. Imaging survival and function of transplanted cardiac resident stem cells. Journal of the American College of Cardiology **53**, 1229, 2009.

49. Gong, Z., andNiklason, L.E. Use of human mesenchymal stem cells as alternative source of smooth muscle cells in vessel engineering. Methods in molecular biology **698**, 279, 2011.

50. Reiman, E.M., andJagust, W.J. Brain imaging in the study of Alzheimer's disease. Neuroimage **61**, 505, 2012.

51. Varrone, A., andHalldin, C. New developments of dopaminergic imaging in Parkinson's disease. The quarterly journal of nuclear medicine and molecular imaging : official publication of the Italian Association of Nuclear Medicine **56**, 68, 2012.

52. Song, F., Tian, M., andZhang, H. Molecular imaging in stem cell therapy for spinal cord injury. BioMed research international **2014**, 759514, 2014.

53. Bai JZ, L.Z., Ding WM, Xu GH, Shen L, Wang F, Tian JH. Tracking neural progenitor cells transplanted into rabbit spinal cord by detection of dopamine receptor 2 with positron emission computed tomography. Zhonghua Yi Xue Za Zhi **86**, 2060, 2006.

54. : clinical trials.

55. von Schulthess, G.K., Kuhn, F.P., Kaufmann, P., andVeit-Haibach, P. Clinical positron emission tomography/magnetic resonance imaging applications. Seminars in nuclear medicine **43**, 3, 2013.

56. Herzog, H. PET/MRI: challenges, solutions and perspectives. Zeitschrift fur medizinische Physik **22**, 281, 2012.

57. Schlemmer, H.P., Pichler, B.J., Schmand, M., Burbar, Z., Michel, C., Ladebeck, R., Jattke, K., Townsend, D., Nahmias, C., Jacob, P.K., Heiss, W.D., andClaussen, C.D. Simultaneous MR/PET imaging of the human brain: feasibility study. Radiology **248**, 1028, 2008.

58. Herzog, H., Langen, K.J., Weirich, C., Rota Kops, E., Kaffanke, J., Tellmann, L., Scheins, J., Neuner, I., Stoffels, G., Fischer, K., Caldeira, L., Coenen, H.H., andShah, N.J. High resolution BrainPET combined with simultaneous MRI. Nuklearmedizin **50**, 74, 2011.

59. Pace, L., Nicolai, E., Luongo, A., Aiello, M., Catalano, O.A., Soricelli, A., andSalvatore, M. Comparison of whole-body PET/CT and PET/MRI in breast cancer patients: lesion detection and

quantitation of 18F-deoxyglucose uptake in lesions and in normal organ tissues. Eur J Radiol **83**, 289, 2014.

60. History of Nuclear Medicine.

61. Saha, G.B. Fundamentals of Nuclear Pharmacy. 6th ed: Springer; 2010.

62. Muller, C., andSchibli, R. Single photon emission computed tomography tracer. Recent Results Cancer Res **187**, 65, 2013.

63. Vrtovec, B., Poglajen, G., Lezaic, L., Sever, M., Socan, A., Domanovic, D., Cernelc, P., Torre-Amione, G., Haddad, F., andWu, J.C. Comparison of transendocardial and intracoronary CD34+ cell transplantation in patients with nonischemic dilated cardiomyopathy. Circulation **128**, S42, 2013.

64. Silva, S.A., Sousa, A.L., Haddad, A.F., Azevedo, J.C., Soares, V.E., Peixoto, C.M., Soares, A.J., Issa, A.F., Felipe, L.R., Branco, R.V., Addad, J.A., Moreira, R.C., Tuche, F.A., Mesquita, C.T., Drumond, C.C., Junior, A.O., Rochitte, C.E., Luz, J.H., Rabischoffisky, A., Nogueira, F.B., Vieira, R.B., Junior, H.S., Borojevic, R., andDohmann, H.F. Autologous bone-marrow mononuclear cell transplantation after acute myocardial infarction: comparison of two delivery techniques. Cell Transplant **18**, 343, 2009.

65. Goussetis, E., Manginas, A., Koutelou, M., Peristeri, I., Theodosaki, M., Kollaros, N., Leontiadis, E., Theodorakos, A., Paterakis, G., Karatasakis, G., Cokkinos, D.V., andGraphakos, S. Intracoronary infusion of CD133+ and CD133-CD34+ selected autologous bone marrow progenitor cells in patients with chronic ischemic cardiomyopathy: cell isolation, adherence to the infarcted area, and body distribution. Stem Cells **24**, 2279, 2006.

66. Barbosa da Fonseca, L.M., Xavier, S.S., Rosado de Castro, P.H., Lima, R.S., Gutfilen, B., Goldenberg, R.C., Maiolino, A., Chagas, C.L., Pedrosa, R.C., andCampos de Carvalho, A.C. Biodistribution of bone marrow mononuclear cells in chronic chagasic cardiomyopathy after intracoronary injection. International journal of cardiology **149**, 310, 2011.

67. Kurpisz, M., Czepczynski, R., Grygielska, B., Majewski, M., Fiszer, D., Jerzykowska, O., Sowinski, J., andSiminiak, T. Bone marrow stem cell imaging after intracoronary administration. International journal of cardiology **121**, 194, 2007.

68. Hofmann, M., Wollert, K.C., Meyer, G.P., Menke, A., Arseniev, L., Hertenstein, B., Ganser, A., Knapp, W.H., andDrexler, H. Monitoring of bone marrow cell homing into the infarcted human myocardium. Circulation **111**, 2198, 2005.

69. Schachinger, V., Aicher, A., Dobert, N., Rover, R., Diener, J., Fichtlscherer, S., Assmus, B., Seeger, F.H., Menzel, C., Brenner, W., Dimmeler, S., andZeiher, A.M. Pilot trial on determinants of progenitor cell recruitment to the infarcted human myocardium. Circulation **118**, 1425, 2008.

70. Verjans, J., Wolters, S., Laufer, W., Schellings, M., Lax, M., Lovhaug, D., Boersma, H., Kemerink, G., Schalla, S., Gordon, P., Teule, J., Narula, J., andHofstra, L. Early molecular imaging of interstitial changes in patients after myocardial infarction: comparison with delayed contrast-enhanced magnetic resonance imaging. Journal of nuclear cardiology : official publication of the American Society of Nuclear Cardiology **17**, 1065, 2010.

71. Mozid, A.M., Holstensson, M., Choudhury, T., Ben-Haim, S., Allie, R., Martin, J., Sinusas, A.J., Hutton, B.F., andMathur, A. Clinical feasibility study to detect angiogenesis following bone marrow stem cell transplantation in chronic ischaemic heart failure. Nuclear medicine communications **35**, 839, 2014.

72. Dimmeler, S., andZeiher, A.M. Cell therapy of acute myocardial infarction: open questions. Cardiology **113**, 155, 2009.

73. Perin, E.C., Silva, G.V., Henry, T.D., Cabreira-Hansen, M.G., Moore, W.H., Coulter, S.A., Herlihy, J.P., Fernandes, M.R., Cheong, B.Y., Flamm, S.D., Traverse, J.H., Zheng, Y., Smith, D., Shaw, S., Westbrook, L., Olson, R., Patel, D., Gahremanpour, A., Canales, J., Vaughn, W.K., andWillerson, J.T. A randomized study of transendocardial injection of autologous bone marrow mononuclear cells and cell function analysis in ischemic heart failure (FOCUS-HF). American heart journal **161**, 1078, 2011.

74. Yoshida, M., Shiraishi, S., Sakamoto, F., Beppu, T., Utsunomiya, D., Okabe, H., Tomiguchi, S., Baba, H., andYamashita, Y. Assessment of hepatic functional regeneration after hepatectomy using Tc-GSA SPECT/CT fused imaging. Ann Nucl Med 2014.

75. Zuckerman, E., Slobodin, G., Sabo, E., Yeshurun, D., Naschitz, J.E., andGroshar, D. Quantitative liver-spleen scan using single photon emission computerized tomography (SPECT) for assessment of hepatic function in cirrhotic patients. Journal of hepatology **39**, 326, 2003.

76. Mohamadnejad, M., Namiri, M., Bagheri, M., Hashemi, S.M., Ghanaati, H., Zare Mehrjardi, N., Kazemi Ashtiani, S., Malekzadeh, R., andBaharvand, H. Phase 1 human trial of autologous bone marrow-hematopoietic stem cell transplantation in patients with decompensated cirrhosis. World J Gastroenterol **13**, 3359, 2007.

77. Levicar, N., Pai, M., Habib, N.A., Tait, P., Jiao, L.R., Marley, S.B., Davis, J., Dazzi, F., Smadja, C., Jensen, S.L., Nicholls, J.P., Apperley, J.F., andGordon, M.Y. Long-term clinical results of autologous infusion of mobilized adult bone marrow derived CD34+ cells in patients with chronic liver disease. Cell proliferation **41 Suppl 1**, 115, 2008.

78. Pan, X.N., Shen, J.K., Zhuang, Y.P., Chen, X.L., Li, Y.X., Chen, L.J., andYang, H. [Autologous bone marrow stem cell transplantation for treatment terminal liver diseases]. Nan fang yi ke da xue xue bao = Journal of Southern Medical University **28**, 1207, 2008.

79. Gholamrezanezhad, A., Mirpour, S., Bagheri, M., Mohamadnejad, M., Alimoghaddam, K., Abdolahzadeh, L., Saghari, M., andMalekzadeh, R. In vivo tracking of 111In-oxine labeled mesenchymal stem cells following infusion in patients with advanced cirrhosis. Nuclear medicine and biology **38**, 961, 2011.

80. Segev, H., Fishman, B., Ziskind, A., Shulman, M., andItskovitz-Eldor, J. Differentiation of human embryonic stem cells into insulin-producing clusters. Stem Cells **22**, 265, 2004.

81. Kim, H., Kim, S.W., Nam, D., Kim, S., andYoon, Y.S. Cell therapy with bone marrow cells for myocardial regeneration. Antioxid Redox Signal **11**, 1897, 2009.

82. Melo, L.G., Pachori, A.S., Kong, D., Gnecchi, M., Wang, K., Pratt, R.E., andDzau, V.J. Molecular and cell-based therapies for protection, rescue, and repair of ischemic myocardium: reasons for cautious optimism. Circulation **109**, 2386, 2004.

83. Bethesda, M. What are the potential uses of human stem cells and the obstacles that must be overcome before these potential uses will be realized? Stem Cell Information National Institutes of Health, U.S. Department of Health and Human Services; 2015.

84. https://www.clinicaltrials.gov/ct2/results?term=stem+cells&Search=Search. www.clinicaltrials.gov.

85. Holroyd-Leduc, J.M., andStraus, S.E. Management of urinary incontinence in women: scientific review. JAMA **291**, 986, 2004.

86. Scharner, J., andZammit, P.S. The muscle satellite cell at 50: the formative years. Skeletal muscle **1**, 28, 2011.

87. Zammit, P.S., Partridge, T.A., andYablonka-Reuveni, Z. The skeletal muscle satellite cell: the stem cell that came in from the cold. The journal of histochemistry and cytochemistry : official journal of the Histochemistry Society **54**, 1177, 2006.

88. Handschin, C., Mortezavi, A., Plock, J., andEberli, D. External physical and biochemical stimulation to enhance skeletal muscle bioengineering. Advanced drug delivery reviews 2014.

89. Fahd Azzabi Zouraq, M.S.a.D.E. Skeletal Muscle Regeneration for Clinical Application. In: Andrades P.J.A., ed. Regenerative Medicine and Tissue Engineering: InTech; 2013.

90. Yablonka-Reuveni, Z., Day, K., Vine, A., andShefer, G. Defining the transcriptional signature of skeletal muscle stem cells. Journal of animal science **86**, E207, 2008.

91. Laumonier, T., Holzer, N., Bernheim, L., Hoffmeyer, P., Bader, C.R., andMenetrey, J. Myogenic precursor cell transplantation in pigs: a step towards a clinical use for muscle regeneration? Swiss medical weekly **137 Suppl 155**, 44S, 2007.

92. Riviere, C., Lecoeur, C., Wilhelm, C., Pechoux, C., Combrisson, H., Yiou, R., andGazeau, F. The MRI assessment of intraurethrally--delivered muscle precursor cells using anionic magnetic nanoparticles. Biomaterials **30**, 6920, 2009.

93. Holzer, N., Hogendoorn, S., Zurcher, L., Garavaglia, G., Yang, S., Konig, S., Laumonier, T., andMenetrey, J. Autologous transplantation of porcine myogenic precursor cells in skeletal muscle. Neuromuscular disorders : NMD **15**, 237, 2005.

94. Eberli, D., Andersson, K.E., Yoo, J.J., andAtala, A. A canine model of irreversible urethral sphincter insufficiency. BJU Int **103**, 248, 2009.

95. Stolting, M.N., Hefermehl, L.J., Tremp, M., Azzabi, F., Sulser, T., andEberli, D. The role of donor age and gender in the success of human muscle precursor cell transplantation. Journal of tissue engineering and regenerative medicine 2014.

96. Azzabi, F., Rottmar, M., Jovaisaite, V., Rudin, M., Sulser, T., Boss, A., andEberli, D. Viability, differentiation capacity, and detectability of super-paramagnetic iron oxide-labeled muscle precursor cells for magnetic-resonance imaging. Tissue Eng Part C Methods **21**, 182, 2015.

97. Chuck, N.C., Azzabi Zouraq, F., Rottmar, M., Eberli, D., andBoss, A. MR imaging relaxometry allows noninvasive characterization of in vivo differentiation of muscle precursor cells. Radiology **274**, 800, 2015.

98. Peault, B., Rudnicki, M., Torrente, Y., Cossu, G., Tremblay, J.P., Partridge, T., Gussoni, E., Kunkel, L.M., andHuard, J. Stem and progenitor cells in skeletal muscle development, maintenance, and therapy. Mol Ther **15**, 867, 2007.

99. Dellavalle, A., Maroli, G., Covarello, D., Azzoni, E., Innocenzi, A., Perani, L., Antonini, S., Sambasivan, R., Brunelli, S., Tajbakhsh, S., andCossu, G. Pericytes resident in postnatal skeletal muscle differentiate into muscle fibres and generate satellite cells. Nat Commun **2**, 499, 2011.

100. Tedesco, F.S., Dellavalle, A., Diaz-Manera, J., Messina, G., andCossu, G. Repairing skeletal muscle: regenerative potential of skeletal muscle stem cells. The Journal of clinical investigation **120**, 11, 2010.

101. Relaix, F., andZammit, P.S. Satellite cells are essential for skeletal muscle regeneration: the cell on the edge returns centre stage. Development **139**, 2845, 2012.

102. Liang, H., andWard, W.F. PGC-1alpha: a key regulator of energy metabolism. Adv Physiol Educ **30**, 145, 2006.

103. Pilegaard, H., Saltin, B., andNeufer, P.D. Exercise induces transient transcriptional activation of the PGC-1alpha gene in human skeletal muscle. J Physiol **546**, 851, 2003.

104. Sandri, M., Lin, J., Handschin, C., Yang, W., Arany, Z.P., Lecker, S.H., Goldberg, A.L., andSpiegelman, B.M. PGC-1alpha protects skeletal muscle from atrophy by suppressing FoxO3 action and atrophy-specific gene transcription. Proc Natl Acad Sci U S A **103**, 16260, 2006.

105. Rodgers, J.T., Lerin, C., Gerhart-Hines, Z., andPuigserver, P. Metabolic adaptations through the PGC-1 alpha and SIRT1 pathways. FEBS Lett **582**, 46, 2008.

106. Puigserver, P., andSpiegelman, B.M. Peroxisome proliferator-activated receptor-gamma coactivator 1 alpha (PGC-1 alpha): transcriptional coactivator and metabolic regulator. Endocr Rev **24**, 78, 2003.

107. Kang, C., andLi Ji, L. Role of PGC-1alpha signaling in skeletal muscle health and disease. Ann N Y Acad Sci **1271**, 110, 2012.

108. Chan, D.C. Dissecting mitochondrial fusion. Dev Cell **11**, 592, 2006.

109. St-Pierre, J., Drori, S., Uldry, M., Silvaggi, J.M., Rhee, J., Jager, S., Handschin, C., Zheng, K., Lin, J., Yang, W., Simon, D.K., Bachoo, R., andSpiegelman, B.M. Suppression of reactive oxygen species and neurodegeneration by the PGC-1 transcriptional coactivators. Cell **127**, 397, 2006.

110. Lin, J., Wu, H., Tarr, P.T., Zhang, C.Y., Wu, Z., Boss, O., Michael, L.F., Puigserver, P., Isotani, E., Olson, E.N., Lowell, B.B., Bassel-Duby, R., andSpiegelman, B.M. Transcriptional co-activator PGC-1 alpha drives the formation of slow-twitch muscle fibres. Nature **418**, 797, 2002.

111. Eisele, P.S., andHandschin, C. Functional crosstalk of PGC-1 coactivators and inflammation in skeletal muscle pathophysiology. Semin Immunopathol **36**, 27, 2014.

112. Little, J.P., Safdar, A., Benton, C.R., andWright, D.C. Skeletal muscle and beyond: the role of exercise as a mediator of systemic mitochondrial biogenesis. Appl Physiol Nutr Metab **36**, 598, 2011.

113. Wende, A.R., Schaeffer, P.J., Parker, G.J., Zechner, C., Han, D.H., Chen, M.M., Hancock, C.R., Lehman, J.J., Huss, J.M., McClain, D.A., Holloszy, J.O., andKelly, D.P. A role for the transcriptional coactivator PGC-1alpha in muscle refueling. J Biol Chem **282**, 36642, 2007.

114. Handschin, C., Kobayashi, Y.M., Chin, S., Seale, P., Campbell, K.P., andSpiegelman, B.M. PGC-1alpha regulates the neuromuscular junction program and ameliorates Duchenne muscular dystrophy. Genes Dev **21**, 770, 2007.

115. Arany, Z., Foo, S.Y., Ma, Y., Ruas, J.L., Bommi-Reddy, A., Girnun, G., Cooper, M., Laznik, D., Chinsomboon, J., Rangwala, S.M., Baek, K.H., Rosenzweig, A., andSpiegelman, B.M. HIF-independent regulation of VEGF and angiogenesis by the transcriptional coactivator PGC-1alpha. Nature **451**, 1008, 2008.

116. Chinsomboon, J., Ruas, J., Gupta, R.K., Thom, R., Shoag, J., Rowe, G.C., Sawada, N., Raghuram, S., andArany, Z. The transcriptional coactivator PGC-1alpha mediates exercise-induced angiogenesis in skeletal muscle. Proc Natl Acad Sci U S A **106**, 21401, 2009.

117. Jain, R.K. Molecular regulation of vessel maturation. Nat Med **9**, 685, 2003.

118. Arany, Z., Lebrasseur, N., Morris, C., Smith, E., Yang, W., Ma, Y., Chin, S., andSpiegelman, B.M. The transcriptional coactivator PGC-1beta drives the formation of oxidative type IIX fibers in skeletal muscle. Cell metabolism **5**, 35, 2007.

119. Valle, I., Alvarez-Barrientos, A., Arza, E., Lamas, S., andMonsalve, M. PGC-1alpha regulates the mitochondrial antioxidant defense system in vascular endothelial cells. Cardiovasc Res **66**, 562, 2005.

120. Arany, Z., He, H., Lin, J., Hoyer, K., Handschin, C., Toka, O., Ahmad, F., Matsui, T., Chin, S., Wu, P.H., Rybkin, II, Shelton, J.M., Manieri, M., Cinti, S., Schoen, F.J., Bassel-Duby, R., Rosenzweig, A., Ingwall, J.S., andSpiegelman, B.M. Transcriptional coactivator PGC-1 alpha controls the energy state and contractile function of cardiac muscle. Cell metabolism **1**, 259, 2005.

121. Lin, J., Wu, P.H., Tarr, P.T., Lindenberg, K.S., St-Pierre, J., Zhang, C.Y., Mootha, V.K., Jager, S., Vianna, C.R., Reznick, R.M., Cui, L., Manieri, M., Donovan, M.X., Wu, Z., Cooper, M.P., Fan, M.C., Rohas, L.M., Zavacki, A.M., Cinti, S., Shulman, G.I., Lowell, B.B., Krainc, D., andSpiegelman, B.M. Defects in adaptive energy metabolism with CNS-linked hyperactivity in PGC-1alpha null mice. Cell **119**, 121, 2004.

122. Brault, J.J., Jespersen, J.G., andGoldberg, A.L. Peroxisome proliferator-activated receptor gamma coactivator 1alpha or 1beta overexpression inhibits muscle protein degradation, induction of ubiquitin ligases, and disuse atrophy. J Biol Chem **285**, 19460, 2010.

123. Ji, L.L., andKang, C. Role of PGC-1alpha in sarcopenia: etiology and potential intervention - a mini-review. Gerontology **61**, 139, 2015.

124. Wenz, T., Rossi, S.G., Rotundo, R.L., Spiegelman, B.M., andMoraes, C.T. Increased muscle PGC-1alpha expression protects from sarcopenia and metabolic disease during aging. Proc Natl Acad Sci U S A **106**, 20405, 2009.

125. Kang, C., Goodman, C.A., Hornberger, T.A., andJi, L.L. PGC-1alpha overexpression by in vivo transfection attenuates mitochondrial deterioration of skeletal muscle caused by immobilization. FASEB J **29**, 4092, 2015.

126. Hawke, T.J., andGarry, D.J. Myogenic satellite cells: physiology to molecular biology. Journal of applied physiology **91**, 534, 2001.

127. Hill, M., Wernig, A., andGoldspink, G. Muscle satellite (stem) cell activation during local tissue injury and repair. Journal of anatomy **203**, 89, 2003.

128. Gussoni, E., Soneoka, Y., Strickland, C.D., Buzney, E.A., Khan, M.K., Flint, A.F., Kunkel, L.M., andMulligan, R.C. Dystrophin expression in the mdx mouse restored by stem cell transplantation. Nature **401**, 390, 1999.

129. Yiou, R., Yoo, J.J., andAtala, A. Restoration of functional motor units in a rat model of sphincter injury by muscle precursor cell autografts. Transplantation **76**, 1053, 2003.

130. Schultz, E., andLipton, B.H. Skeletal muscle satellite cells: changes in proliferation potential as a function of age. Mechanisms of ageing and development **20**, 377, 1982.

131. Rando, T.A. Stem cells, ageing and the quest for immortality. Nature **441**, 1080, 2006.

132. Handschin, C. The biology of PGC-1alpha and its therapeutic potential. Trends Pharmacol Sci **30**, 322, 2009.

133. Schiaffino, S., andReggiani, C. Fiber types in mammalian skeletal muscles. Physiological reviews **91**, 1447, 2011.

134. Eberli, D., Soker, S., Atala, A., andYoo, J.J. Optimization of human skeletal muscle precursor cell culture and myofiber formation in vitro. Methods **47**, 98, 2009.

135. Delo, D.M., Eberli, D., Williams, J.K., Andersson, K.E., Atala, A., andSoker, S. Angiogenic gene modification of skeletal muscle cells to compensate for ageing-induced decline in bioengineered functional muscle tissue. BJU Int **102**, 878, 2008.

136. Baird, M.F., Graham, S.M., Baker, J.S., andBickerstaff, G.F. Creatine-kinase- and exercise-related muscle damage implications for muscle performance and recovery. Journal of nutrition and metabolism **2012**, 960363, 2012.

137. Rolland, Y., Onder, G., Morley, J.E., Gillette-Guyonet, S., Abellan van Kan, G., andVellas, B. Current and future pharmacologic treatment of sarcopenia. Clinics in geriatric medicine **27**, 423, 2011.

138. Ciecierska, A., Chodkowska, K., Motyl, T., andSadkowski, T. Myogenic cells applications in regeneration of post-infarction cardiac tissue. Journal of physiology and pharmacology : an official journal of the Polish Physiological Society **64**, 401, 2013.

139. Handschin, C., andSpiegelman, B.M. The role of exercise and PGC1alpha in inflammation and chronic disease. Nature **454**, 463, 2008.

140. Egan, B., andZierath, J.R. Exercise metabolism and the molecular regulation of skeletal muscle adaptation. Cell metabolism **17**, 162, 2013.

141. Wu, Z., Puigserver, P., Andersson, U., Zhang, C., Adelmant, G., Mootha, V., Troy, A., Cinti, S., Lowell, B., Scarpulla, R.C., andSpiegelman, B.M. Mechanisms controlling mitochondrial biogenesis and respiration through the thermogenic coactivator PGC-1. Cell **98**, 115, 1999.

142. Lee, R.J., Springer, M.L., Blanco-Bose, W.E., Shaw, R., Ursell, P.C., andBlau, H.M. VEGF gene delivery to myocardium: deleterious effects of unregulated expression. Circulation **102**, 898, 2000.

143. Ozawa, C.R., Banfi, A., Glazer, N.L., Thurston, G., Springer, M.L., Kraft, P.E., McDonald, D.M., andBlau, H.M. Microenvironmental VEGF concentration, not total dose, determines a threshold between normal and aberrant angiogenesis. The Journal of clinical investigation **113**, 516, 2004.

144. Zimna, A., Janeczek, A., Rozwadowska, N., Fraczek, M., Kucharzewska, P., Rucinski, M., Mietkiewski, T., andKurpisz, M. Biological properties of human skeletal myoblasts genetically modified to simultaneously overexpress the pro-angiogenic factors vascular endothelial growth factor-A and fibroblast growth factor-4. Journal of physiology and pharmacology : an official journal of the Polish Physiological Society **65**, 193, 2014.

145. Thom, R., Rowe, G.C., Jang, C., Safdar, A., White, J.P., andArany, Z. Hypoxic induction of vascular endothelial growth factor (VEGF) and angiogenesis in muscle by N terminus peroxisome proliferator-associated receptor gamma coactivator (NT-PGC)-1alpha. J Biol Chem **290**, 19543, 2015.

146. Bryan, B.A., Walshe, T.E., Mitchell, D.C., Havumaki, J.S., Saint-Geniez, M., Maharaj, A.S., Maldonado, A.E., andD'Amore, P.A. Coordinated vascular endothelial growth factor expression and signaling during skeletal myogenic differentiation. Molecular biology of the cell **19**, 994, 2008.

147. Kay, M.A. State-of-the-art gene-based therapies: the road ahead. Nat Rev Genet **12**, 316, 2011.

148. Chun, S.Y., Cho, D.H., Chae, S.Y., Choi, K.H., Lim, H.J., Yoon, G.S., Kim, B.S., Kim, B.W., Yoo, J.J., andKwon, T.G. Human amniotic fluid stem cell-derived muscle progenitor cell therapy for stress urinary incontinence. Journal of Korean medical science **27**, 1300, 2012.

149. Nikolavasky, D., Stangel-Wojcikiewicz, K., Stec, M., andChancellor, M.B. Stem cell therapy: a future treatment of stress urinary incontinence. Seminars in reproductive medicine **29**, 61, 2011.

150. Aref-Adib, M., Lamb, B.W., Lee, H.B., Akinnawo, E., Raza, M.M., Hughes, A., Mehta, V.S., Odonde, R.I., andYoong, W. Stem cell therapy for stress urinary incontinence: a systematic review in human subjects. Archives of gynecology and obstetrics **288**, 1213, 2013.

151. Olson, J.L., Atala, A., andYoo, J.J. Tissue engineering: current strategies and future directions. Chonnam Med J **47**, 1, 2011.

152. Smaldone, M.C., andChancellor, M.B. Muscle derived stem cell therapy for stress urinary incontinence. World J Urol **26**, 327, 2008.

153. Benchaouir, R., Rameau, P., Decraene, C., Dreyfus, P., Israeli, D., Pietu, G., Danos, O., andGarcia, L. Evidence for a resident subset of cells with SP phenotype in the C2C12 myogenic line: a tool to explore muscle stem cell biology. ExpCell Res **294**, 254, 2004.

154. Eberli, D., Aboushwareb, T., Soker, S., Yoo, J.J., andAtala, A. Muscle Precursor Cells for the Restoration of Irreversibly Damaged Sphincter Function. Cell Transplant 2012.

155. Rodriguez-Porcel, M. In vivo imaging and monitoring of transplanted stem cells: clinical applications. Current cardiology reports **12**, 51, 2010.

156. Deana G. Haralampieva, S.M.A., Tullio Sulser, Daniel Eberli. Non-Invasive Imaging Modalities for Clinical Investigation in Regenerative Medicine Cells and Biomaterials in Regenerative Medicine: InTech; 2014.

157. Schonitzer, V., Haasters, F., Kasbauer, S., Ulrich, V., Mille, E., Gildehaus, F.J., Carlsen, J., Pape, M., Beck, R., Delker, A., Boning, G., Mutschler, W., Bocker, W., Schieker, M., andBartenstein, P. In Vivo Mesenchymal Stem Cell Tracking with PET Using the Dopamine Type 2 Receptor and 18F-Fallypride. J Nucl Med **55**, 1342, 2014.

158. Massoud, T.F., andGambhir, S.S. Molecular imaging in living subjects: seeing fundamental biological processes in a new light. Genes Dev **17**, 545, 2003.

159. Yaghoubi, S.S., Jensen, M.C., Satyamurthy, N., Budhiraja, S., Paik, D., Czernin, J., andGambhir, S.S. Noninvasive detection of therapeutic cytolytic T cells with 18F-FHBG PET in a patient with glioma. Nature clinical practice Oncology **6**, 53, 2009.

160. Penuelas, I., Mazzolini, G., Boan, J.F., Sangro, B., Marti-Climent, J., Ruiz, M., Ruiz, J., Satyamurthy, N., Qian, C., Barrio, J.R., Phelps, M.E., Richter, J.A., Gambhir, S.S., andPrieto, J. Positron emission tomography imaging of adenoviral-mediated transgene expression in liver cancer patients. Gastroenterology **128**, 1787, 2005.

161. Penuelas, I., Haberkorn, U., Yaghoubi, S., andGambhir, S.S. Gene therapy imaging in patients for oncological applications. European journal of nuclear medicine and molecular imaging **32 Suppl 2**, S384, 2005.

162. Dempsey, M.F., Wyper, D., Owens, J., Pimlott, S., Papanastassiou, V., Patterson, J., Hadley, D.M., Nicol, A., Rampling, R., andBrown, S.M. Assessment of 123I-FIAU imaging of herpes simplex viral gene expression in the treatment of glioma. Nuclear medicine communications **27**, 611, 2006.

163. Jacobs, A., Voges, J., Reszka, R., Lercher, M., Gossmann, A., Kracht, L., Kaestle, C., Wagner, R., Wienhard, K., andHeiss, W.D. Positron-emission tomography of vector-mediated gene expression in gene therapy for gliomas. Lancet **358**, 727, 2001.

164. Barton, K.N., Stricker, H., Brown, S.L., Elshaikh, M., Aref, I., Lu, M., Pegg, J., Zhang, Y., Karvelis, K.C., Siddiqui, F., Kim, J.H., Freytag, S.O., andMovsas, B. Phase I study of noninvasive imaging of adenovirus-mediated gene expression in the human prostate. Mol Ther **16**, 1761, 2008.

165. MacLaren, D.C., Gambhir, S.S., Satyamurthy, N., Barrio, J.R., Sharfstein, S., Toyokuni, T., Wu, L., Berk, A.J., Cherry, S.R., Phelps, M.E., andHerschman, H.R. Repetitive, non-invasive imaging of the dopamine D2 receptor as a reporter gene in living animals. Gene therapy **6**, 785, 1999.

166. Siessmeier, T., Zhou, Y., Buchholz, H.G., Landvogt, C., Vernaleken, I., Piel, M., Schirrmacher, R., Rosch, F., Schreckenberger, M., Wong, D.F., Cumming, P., Grunder, G., andBartenstein, P. Parametric mapping of binding in human brain of D2 receptor ligands of different affinities. J Nucl Med **46**, 964, 2005.

167. Liang, Q., Satyamurthy, N., Barrio, J.R., Toyokuni, T., Phelps, M.P., Gambhir, S.S., andHerschman, H.R. Noninvasive, quantitative imaging in living animals of a mutant dopamine D2 receptor reporter gene in which ligand binding is uncoupled from signal transduction. Gene therapy **8**, 1490, 2001.

168. Luo, J., Deng, Z.L., Luo, X., Tang, N., Song, W.X., Chen, J., Sharff, K.A., Luu, H.H., Haydon, R.C., Kinzler, K.W., Vogelstein, B., andHe, T.C. A protocol for rapid generation of recombinant adenoviruses using the AdEasy system. Nature protocols **2**, 1236, 2007.

169. Cho, W., Taylor, L.P., Mansour, A., andAkil, H. Hydrophobic residues of the D2 dopamine receptor are important for binding and signal transduction. J Neurochem **65**, 2105, 1995.

170. Mukherjee, J., Yang, Z.Y., Das, M.K., andBrown, T. Fluorinated benzamide neuroleptics--III. Development of (S)-N-[(1-allyl-2-pyrrolidinyl)methyl]-5-(3-[18F]fluoropropyl)-2, 3-dimethoxybenzamide as an improved dopamine D-2 receptor tracer. Nuclear medicine and biology **22**, 283, 1995.

171. Lim, J.L., andBerridge, M.S. An efficient radiosynthesis of [18F]fluoromisonidazole. Appl Radiat Isot **44**, 1085, 1993.

172. Wang, Y., Seidel, J., Tsui, B.M., Vaquero, J.J., andPomper, M.G. Performance evaluation of the GE healthcare eXplore VISTA dual-ring small-animal PET scanner. J Nucl Med **47**, 1891, 2006.

173. Honer, M., Bruhlmeier, M., Missimer, J., Schubiger, A.P., andAmetamey, S.M. Dynamic imaging of striatal D2 receptors in mice using quad-HIDAC PET. J Nucl Med **45**, 464, 2004.

174. Benchaouir, R., Rameau, P., Decraene, C., Dreyfus, P., Israeli, D., Pietu, G., Danos, O., andGarcia, L. Evidence for a resident subset of cells with SP phenotype in the C2C12 myogenic line: a tool to explore muscle stem cell biology. Experimental cell research **294**, 254, 2004.

175. Mitchell, P.O., andPavlath, G.K. Skeletal muscle atrophy leads to loss and dysfunction of muscle precursor cells. American journal of physiology Cell physiology **287**, C1753, 2004.

176. Phelps, E.A., andGarcia, A.J. Update on therapeutic vascularization strategies. Regenerative medicine **4**, 65, 2009.

177. Kadi, F., Charifi, N., Denis, C., andLexell, J. Satellite cells and myonuclei in young and elderly women and men. Muscle Nerve **29**, 120, 2004.

178. Putman, C.T., Sultan, K.R., Wassmer, T., Bamford, J.A., Skorjanc, D., andPette, D. Fiber-type transitions and satellite cell activation in low-frequency-stimulated muscles of young and aging rats. The journals of gerontology Series A, Biological sciences and medical sciences **56**, B510, 2001.

179. Yaghoubi, S.S., Campbell, D.O., Radu, C.G., andCzernin, J. Positron emission tomography reporter genes and reporter probes: gene and cell therapy applications. Theranostics **2**, 374, 2012.

180. Nichol, C., andKim, E.E. Molecular imaging and gene therapy. J Nucl Med **42**, 1368, 2001.

181. Min, J.J., andGambhir, S.S. Gene therapy progress and prospects: noninvasive imaging of gene therapy in living subjects. Gene therapy **11**, 115, 2004.

182. Serganova, I., Ponomarev, V., andBlasberg, R. Human reporter genes: potential use in clinical studies. Nuclear medicine and biology **34**, 791, 2007.

183. Hockel, M., Schlenger, K., Aral, B., Mitze, M., Schaffer, U., andVaupel, P. Association between tumor hypoxia and malignant progression in advanced cancer of the uterine cervix. Cancer research **56**, 4509, 1996.

184. Nordsmark, M., Overgaard, M., andOvergaard, J. Pretreatment oxygenation predicts radiation response in advanced squamous cell carcinoma of the head and neck. Radiotherapy and oncology : journal of the European Society for Therapeutic Radiology and Oncology **41**, 31, 1996.

185. Nordsmark, M., Alsner, J., Keller, J., Nielsen, O.S., Jensen, O.M., Horsman, M.R., andOvergaard, J. Hypoxia in human soft tissue sarcomas: adverse impact on survival and no association with p53 mutations. British journal of cancer **84**, 1070, 2001.

186. Machulla, H.-J. Imaging of Hypoxia: Tracer Developments: Springer-Science+Business Media, B.V.; 1999.

187. Bruehlmeier, M., Roelcke, U., Schubiger, P.A., andAmetamey, S.M. Assessment of hypoxia and perfusion in human brain tumors using PET with 18F-fluoromisonidazole and 15O-H2O. J Nucl Med **45**, 1851, 2004.

188. Kawai, N., Lin, W., Cao, W.D., Ogawa, D., Miyake, K., Haba, R., Maeda, Y., Yamamoto, Y., Nishiyama, Y., andTamiya, T. Correlation between (1)(8)F-fluoromisonidazole PET and expression of HIF-1alpha and VEGF in newly diagnosed and recurrent malignant gliomas. European journal of nuclear medicine and molecular imaging **41**, 1870, 2014.

189. Muzi, M., Peterson, L.M., O'Sullivan, J.N., Fink, J.R., Rajendran, J.G., McLaughlin, L.J., Muzi, J.P., Mankoff, D.A., andKrohn, K.A. 18F-Fluoromisonidazole Quantification of Hypoxia in Human Cancer Patients Using Image-Derived Blood Surrogate Tissue Reference Regions. J Nucl Med **56**, 1223, 2015.

190. Lovett, M., Lee, K., Edwards, A., andKaplan, D.L. Vascularization strategies for tissue engineering. Tissue Eng Part B Rev **15**, 353, 2009.

191. Blaganje, M., andLukanovic, A. Intrasphincteric autologous myoblast injections with electrical stimulation for stress urinary incontinence. Int J Gynaecol Obstet **117**, 164, 2012.

192. Deana G. Haralampieva, S.M.A., Tullio Sulser and Daniel Eberli Non-Invasive Imaging Modalities for Clinical Investigation in Regenerative Medicine. In: Eberli D.D., ed. Cells and Biomaterials in Regenerative Medicine: InTech; 2014.

193. Grounds, M.D., andMcGeachie, J.K. Reutilisation of tritiated thymidine in studies of regenerating skeletal muscle. Cell Tissue Res **250**, 141, 1987.

194. Seidel, M., Borczynska, A., Rozwadowska, N., andKurpisz, M. Cell-based therapy for heart failure: skeletal myoblasts. Cell Transplant **18**, 695, 2009.

195. Allen, R.E., andBoxhorn, L.K. Regulation of skeletal muscle satellite cell proliferation and differentiation by transforming growth factor-beta, insulin-like growth factor I, and fibroblast growth factor. J Cell Physiol **138**, 311, 1989.

196. Bischoff, R. A satellite cell mitogen from crushed adult muscle. Dev Biol **115**, 140, 1986.

197. Moyer, A.L., andWagner, K.R. Regeneration versus fibrosis in skeletal muscle. Curr Opin Rheumatol **23**, 568, 2011.

198. Shvartsman, D., Storrie-White, H., Lee, K., Kearney, C., Brudno, Y., Ho, N., Cezar, C., McCann, C., Anderson, E., Koullias, J., Tapia, J.C., Vandenburgh, H., Lichtman, J.W., andMooney, D.J. Sustained delivery of VEGF maintains innervation and promotes reperfusion in ischemic skeletal muscles via NGF/GDNF signaling. Mol Ther **22**, 1243, 2014.

199. Watanabe, Y., Horie, S., Funaki, Y., Kikuchi, Y., Yamazaki, H., Ishii, K., Mori, S., Vassaux, G., andKodama, T. Delivery of Na/I symporter gene into skeletal muscle using nanobubbles and ultrasound: visualization of gene expression by PET. J Nucl Med **51**, 951, 2010.

200. Savill, J., Dransfield, I., Hogg, N., andHaslett, C. Vitronectin receptor-mediated phagocytosis of cells undergoing apoptosis. Nature **343**, 170, 1990.

201. Tissue Engineering in Regenerative Medicine: Springer; 2011.

202. Yin, H., Price, F., andRudnicki, M.A. Satellite cells and the muscle stem cell niche. Physiological reviews **93**, 23, 2013.

203. Boonen, K.J., andPost, M.J. The muscle stem cell niche: regulation of satellite cells during regeneration. Tissue Eng Part B Rev **14**, 419, 2008.

204. Chancellor, M.B., Yokoyama, T., Tirney, S., Mattes, C.E., Ozawa, H., Yoshimura, N., de Groat, W.C., andHuard, J. Preliminary results of myoblast injection into the urethra and bladder wall: a possible method for the treatment of stress urinary incontinence and impaired detrusor contractility. Neurourol Urodyn **19**, 279, 2000.

205. Eberli, D., Aboushwareb, T., Soker, S., Yoo, J.J., andAtala, A. Muscle precursor cells for the restoration of irreversibly damaged sphincter function. Cell Transplant **21**, 2089, 2012.

206. Pennisi, E. The CRISPR craze. Science **341**, 833, 2013.

207. Wagner, A.E., Ernst, I.M., Birringer, M., Sancak, O., Barella, L., andRimbach, G. A combination of lipoic acid plus coenzyme Q10 induces PGC1alpha, a master switch of energy metabolism, improves stress response, and increases cellular glutathione levels in cultured C2C12 skeletal muscle cells. Oxid Med Cell Longev **2012**, 835970, 2012.

208. Lee, J., Jun, I., Park, H.J., Kang, T.J., Shin, H., andCho, S.W. Genetically engineered myoblast sheet for therapeutic angiogenesis. Biomacromolecules **15**, 361, 2014.

209. Haralampieva, D.A., S.M. ; Sulser, T. ; Eberli, D. . Non-Invasive Imaging Modalities for Clinical Investigation in Regenerative Medicine. In: D.Eberli, ed. Cells and Biomaterials in Regenerative Medicine: InTech; 2014.

210. Haubner, R. Alphavbeta3-integrin imaging: a new approach to characterise angiogenesis? European journal of nuclear medicine and molecular imaging **33 Suppl 1**, 54, 2006.

211. Shi, J., Jin, Z., Liu, X., Fan, D., Sun, Y., Zhao, H., Zhu, Z., Liu, Z., Jia, B., andWang, F. PET imaging of neovascularization with (68)Ga-3PRGD2 for assessing tumor early response to Endostar antiangiogenic therapy. Mol Pharm **11**, 3915, 2014.

212. Antonov, A.S., Antonova, G.N., Munn, D.H., Mivechi, N., Lucas, R., Catravas, J.D., andVerin, A.D. alphaVbeta3 integrin regulates macrophage inflammatory responses via PI3 kinase/Akt-dependent NF-kappaB activation. J Cell Physiol **226**, 469, 2011.

213. Hathout, E., Sowers, L., Wang, R., Tan, A., Mace, J., Peverini, R., Chinnock, R., andObenaus, A. In vivo magnetic resonance imaging of vascularization in islet transplantation. Transpl Int **20**, 1059, 2007.

214. Wolfs, E., Struys, T., Notelaers, T., Roberts, S.J., Sohni, A., Bormans, G., Van Laere, K., Luyten, F.P., Gheysens, O., Lambrichts, I., Verfaillie, C.M., andDeroose, C.M. 18F-FDG labeling of mesenchymal stem cells and multipotent adult progenitor cells for PET imaging: effects on ultrastructure and differentiation capacity. J Nucl Med **54**, 447, 2013.

7 Curriculum Vitae

Deana G. Haralampieva, M.Sc.

deana.haralampieva@usz.ch

Personal Profile

Date of birth	20th of February 1986
Nationality	Bulgaria, Germany

Education

2012-2015	PhD candidate at ImMed program LSZGS and ZIHP: ETH Zürich, Institute for Pharmaceutical Sciences, Switzerland University Hospital Zürich, Dept. Urology, Laboratory for Tissue Engineering and Stem cell Therapy, Switzerland
2009 – 2011	M.Sc. (Cellular and Molecular Biology), University of Konstanz, Germany,
2006 – 2009	B.Sc. (Biological Sciences), University of Konstanz, Germany
2000 – 2005	Second English Language High School 'T. Jefferson', Sofia, Bulgaria

Experience

04.2014, 04.2015	Assistant Biopharmacy, Institute of Pharmaceutical Sciences, ETHZ, Switzerland
10.2011-12.2011	Research Associate, Chair of Developmental Neurobiology, University of Konstanz, Germany
2007-2011	Student Tutor in general and inorganic Chemistry, Dept. Chemistry, University of Konstanz, Germany
01.2010-03.2010	Student Tutor in Chemical Operations for Biologists, University of Konstanz
09.2010-12.2010	Laboratory Assistant, Chair of Developmental Neurobiology, University of Konstanz, Germany
2006-2011	Event coordinator and service, Konzil Konstanz, Germany
03.2009-04.2009 03.2008-04.2008	Research Internship, National Center of Infectious and Parasitic Diseases, Sofia, Bulgaria
09.2008-10.2008	Research Internship, University Hospital Freiburg, Dept. Internal Medicine, Hematology and Oncology
2002-2005	Agent for Cosmetics Sales and Consulting, AVON, Sofia, Bulgaria

Publications

D Haralampieva, T Betzel, I Dinulovic, S Salemi, MNL Stoelting, S Kraemer, R Schibli, T Sulser, C Handschin, D Eberli, S M Ametamey: **Non-invasive Imaging and Tracking of Engineered Human Muscle Precursor Cells for Skeletal Muscle Tissue Engineering Using Positron Emission Tomography** (accepted, Journal of Nuclear Medicine)

M Rottmar, **D Haralampieva**, S Salemi, C Eberhardt, M Wurnig, A Boss*, D Eberli*: **Magnetization transfer MRI to monitor muscle tissue formation during myogenic *in vivo* differentiation of muscle precursor cells** (accepted, Journal of Radiology)

MNL Stoelting; A S Arnold; **D Haralampieva**; C Handschin; T Sulser; D Eberli: **Magnetic stimulation supports muscle and nerve regeneration after trauma in mice,** *Muscle Nerve* (2015), doi: 10.1002/mus.24780

D G Haralampieva, S M Ametamey, T Sulser and D Eberli (2014). **Non-Invasive Imaging Modalities for Clinical Investigation in Regenerative Medicine**, Cells and Biomaterials in Regenerative Medicine, ISBN: 978-953-51-1731-5, InTech, DOI: 10.5772/59356. Available from: http://www.intechopen.com/books/cells-and-biomaterials-in-regenerative-medicine/non-invasive-imaging-modalities-for-clinical-investigation-in-regenerative-medicine

J C Koch; P Lingor; U Michel; A Shypitsyna; G P Solis; M Bähr; V Bodrikov; **D Haralampieva**; L Tönges; C A O Stuermer : **Upregulation of reggie-1/flotillin-2 promotes axon regeneration in the rat optic nerve *in vivo* and neurite growth *in vitro*.** *Neurobiology of Disease* (2012), doi: 10.1016/j.nbd.2012.11.007

Abstracts/ Posters/ Presentations/ Conference contributions

Metabolic tracking of muscle precursor cells for skeletal muscle tissue engineering using PET/CT; TERMIS World conference 2015, Boston, USA (oral presentation)

Genetically modified human muscle precursor cells overexpressing PGC-1α support early myofiber formation in bioengineered muscle tissue; TERMIS World conference 2015, Boston, USA (poster)

Adipose Derived Stem Cell therapy for skeletal muscle regeneration TERMIS World conference 2015, Boston, USA (poster)

Genetically modified human muscle precursor cells overexpressing PGC-1α support early myofiber formation in bioengineered muscle tissue; 71st Annual Meeting 2015 of the Swiss Society for Urology 2015, St. Gallen, Switzerland (oral presentation/poster)

Genetically modified human muscle precursor cells overexpressing PGC-1α support early myofiber formation in bioengineered muscle tissue; 11th Symposium of the ZIHP 2015, Zürich, Switzerland (poster)

Metabolic Tracking of Muscle Precursor Cells for Skeletal Muscle Tissue Engineering using PET/CT; Summer school of Translation Biology EPFL-ETHZ, Interlaken, Switzerland, July 2015 (poster and flash talk)

Metabolic Tracking of Muscle Precursor Cells for Muscle Tissue Engineering; 14th clinical research day 2015, USZ, Zürich, Switzerland (poster)

Non-Invasive Tracking of Muscle Precursor Cells for Muscle Tissue Engineering Using PET; TERMIS-AM conference 2014, Washington DC, USA (poster)

Non-Invasive Tracking of Muscle Precursor Cells for Muscle Tissue Engineering Using PET, Doctoral Student Day at ETH Hoenggerberg, September 2014, Zürich (oral presentation)

Non-Invasive Tracking of Muscle Precursor Cells for Muscle Tissue Engineering Using PET; Pharmacology and Toxicology Poster Day 2014, University of Zürich Irchel, Switzerland (poster)

Non-Invasive Tracking of Muscle Precursor Cells for Sphincter Muscle Engineering; 70th Annual Meeting 2014 of the Swiss Society for Urology 2014, Montreux, Switzerland (oral presentation)

Non-Invasive Tracking of Muscle Precursor Cells for Muscle Tissue Engineering; 10th Symposium of the ZIHP 2014, Zürich, Switzerland (poster)

Non-Invasive Tracking of Muscle Precursor Cells for Muscle Tissue Engineering Using PET; Audit Session at ETHZ and PSI 2014, Zürich and Villigen, Switzerland (poster)

Non-invasive tracking of engineered muscle tissue, Bioengineering seminar at USZ, May 2014, Zürich, Switzerland (oral presentation)

Non-Invasive Tracking of Muscle Precursor Cells for Muscle Tissue Engineering; 13th clinical research day 2014, USZ, Zürich, Switzerland (poster)

Non-Invasive Tracking of Muscle Precursor Cells for Muscle Tissue Engineering; Swiss Stem Cell Meeting 2014, Geneva, Switzerland (poster)

Non-Invasive Tracking of Muscle Precursor Cells for Sphincter Muscle Engineering; The Journal of Urology, American Urological Association (AUA) 2014, Orlando, USA (poster)

Non-Invasive Tracking of Muscle Precursor Cells for Sphincter Muscle Engineering; European Association of Urology (EAU) 2014, Stockholm, Sweden (poster)

Remodeling and optimization of bladder smooth muscle cells for functional bladder engineering in children with neuropathic disorders, TERMIS-AP conference 2013, Shanghai, China (poster)

The Role of Autophagy in the Differentiation of Adipose Derived Stem Cells to Functional Smooth Muscle Bioengineering, TERMIS-AP conference 2013, Shanghai, China (oral presentation)

Age and Gender Limitations For The Bioengineering Of Contractile Muscle Tissue For Human Muscle Precursor Cells (MPC); TERMIS-AP conference 2013, Shanghai, China (poster)

Non-Invasive Tracking Of Muscle Precursor Cells For Muscle Tissue Engineering; TERMIS-AP conference 2013, Shanghai, China (poster)

The impact of PGC-1α and VEGF-A on engineered muscle tissue and the use of PET-Scan for cell tracking and functional analyses, Seminar day Radiopharmacy at Paul Scherer Institute (PSI), June 2013, Villigen, Switzerland (oral presentation)

The impact of PGC-1α and VEGF-A on engineered muscle tissue and the use of PET-Scan for cell tracking and functional analyses, research colloquium at the Division of Surgical Research 2013, USZ, Zürich, Switzerland (oral presentation)

Non-Invasive Tracking of Muscle Precursor Cells for Muscle Tissue Engineering; 9th Symposium of the ZIHP, 2013, Zürich, Switzerland (poster)

Volume limitations in cell therapy for muscle engineering, 12th clinical research day 2013, USZ, Zürich, CH (poster)

Age and Gender Limitations for the Bioengineering of Contractile Muscle Tissue for Human Muscle Precursor Cells (MPC); 3rd TERMIS World conference 2012, Vienna, Austria (poster)

Grants/Honors/ Awards/ Licenses/ Certification

06.2015	Good Clinical Practice certificates 1+2+3
09.2014	Poster Jury committee at 10th Symposium of the ZIHP, 29th of August 2014, Zürich
10.2012	Research Grant - Novartis foundation for medical-biological research, Switzerland
09.2012	Research Grant – Promedica/UBS, Switzerland
08.2012	Internal Grant Matching Funds, University Hospital Zurich, Switzerland
06.2012	Animal Management System (iRATS) License

10.2010	License for care and use of laboratory animals (LTK-Module1), FELASA
06.2005	High School Diploma with Honors (grade: excellent 1.0) Second English Language High School 'T. Jefferson', Sofia, Bulgaria
07.2004	"Zentrale Oberstufenprüfung" (ZOP), Goethe Institut, Sofia, Bulgaria
06.2004	"TOEFL", Sofia, Bulgaria

Further Education

10.2015	Patent and Spin-off workshop, Unitectra, Switzerland
07.2015	EPFL+ETHZ Summer School Translational Biology, Interlaken, Switzerland
03.2014	Voice training and presentation skills in the Sciences and Medicine, Switzerland
07.2013	Radiopharmaceutical Sciences lectures+oral exam, ETHZ, Switzerland
01.2013	Advanced Microscopy Winterschool at ZMB, LSZGS, UZH+ETHZ, Switzerland
01.2013	Flow Cytometry graduate course, LSZGS, UZH+ETHZ, Switzerland
11.2012	Applying statistical methods in biosciences, LSZGS, UZH+ETHZ, Switzerland
10.2012	Project management for early stage researchers, LSZGS, UZH+ETHZ, Switzerland
10.2012	Scientific writing in the Sciences and Medicine, LSZGS, UZH+ETHZ, Switzerland
08.2012	Advances in Tissue Engineering, Summer School, Houston Rice University, USA

Skills

Languages	Bulgarian (native proficiency); English (full professional proficiency);German (full professional proficiency); Spanish (basic knowledge)
IT	Microsoft Office, Adobe Photoshop, Image J, Axio Vision, LSM Image Browser, ZEN (Zeiss), FlowJo, GraphPad Prism, Imaris, LabChart, SPSS, Endnote, PMOD